



2011

CHARACTERIZATION OF VIRAL AND HOST PROTEINS AND RNA ELEMENTS IN TOMBUSVIRUS REPLICATION

Kunj Bihari Pathak

University of Kentucky, kunj.pathak@gmail.com

[Right click to open a feedback form in a new tab to let us know how this document benefits you.](#)

Recommended Citation

Pathak, Kunj Bihari, "CHARACTERIZATION OF VIRAL AND HOST PROTEINS AND RNA ELEMENTS IN TOMBUSVIRUS REPLICATION" (2011). *Theses and Dissertations--Plant Pathology*. 1.
https://uknowledge.uky.edu/plantpath_etds/1

This Doctoral Dissertation is brought to you for free and open access by the Plant Pathology at UKnowledge. It has been accepted for inclusion in Theses and Dissertations--Plant Pathology by an authorized administrator of UKnowledge. For more information, please contact UKnowledge@lsv.uky.edu.

STUDENT AGREEMENT:

I represent that my thesis or dissertation and abstract are my original work. Proper attribution has been given to all outside sources. I understand that I am solely responsible for obtaining any needed copyright permissions. I have obtained and attached hereto needed written permission statements(s) from the owner(s) of each third-party copyrighted matter to be included in my work, allowing electronic distribution (if such use is not permitted by the fair use doctrine).

I hereby grant to The University of Kentucky and its agents the non-exclusive license to archive and make accessible my work in whole or in part in all forms of media, now or hereafter known. I agree that the document mentioned above may be made available immediately for worldwide access unless a preapproved embargo applies.

I retain all other ownership rights to the copyright of my work. I also retain the right to use in future works (such as articles or books) all or part of my work. I understand that I am free to register the copyright to my work.

REVIEW, APPROVAL AND ACCEPTANCE

The document mentioned above has been reviewed and accepted by the student's advisor, on behalf of the advisory committee, and by the Director of Graduate Studies (DGS), on behalf of the program; we verify that this is the final, approved version of the student's dissertation including all changes required by the advisory committee. The undersigned agree to abide by the statements above.

Kunj Bihari Pathak, Student

Dr. Peter Nagy, Major Professor

Dr. Lisa Vaillancourt, Director of Graduate Studies

CHARACTERIZATION
OF VIRAL AND HOST PROTEINS
AND RNA ELEMENTS IN TOMBUSVIRUS REPLICATION

DISSERTATION

A dissertation submitted in partial fulfillment of the
requirements for the degree of Doctor of Philosophy in the
College of Agriculture at the University of Kentucky

By
Kunj Bihari Pathak

Lexington, Kentucky

Director: Dr. Peter Nagy, Professor
Department of Plant Pathology
Lexington, Kentucky
2011

Copyright © Kunj Bihari Pathak 2011

ABSTRACT OF DISSERTATION

CHARACTERIZATION OF VIRAL AND HOST PROTEINS AND RNA ELEMENTS IN TOMBUSVIRUS REPLICATION

Two thirds of plant viruses are positive-strand RNA viruses including the family Tombusviridae. One of the best-studied members of this family is *Tomato bushy stunt virus* (TBSV). Like many other viruses, TBSV has much fewer genes when compared to its hosts' genome. Nevertheless, TBSV utilizes its genome very judiciously. To compensate for a lack of many proteins of its own, it codes for multi-functional replication protein p33 and also co-opts host factors to facilitate its replication.

By using recombinant replication proteins p33 and p92 containing single amino acid changes in protein-protein interaction domains (S1 and S2), I demonstrated that the replication proteins are required in sequential steps during virus replication. The *in vitro* cell-free extract (CFE) based TBSV replication assays revealed that mutations in S1 and S2 domains affected RNA template selection, recruitment and assembly of replicase complex. TBSV replicates on the cytosolic surface of peroxisomal membranes.

To identify the host factor involved in this process of transporting viral replication proteins to peroxisome, I tested the peroxisomal transporter proteins for their ability to bind to p33 *in vitro*, which led to the discovery of Pex19p. Pull-down and co-purification experiments revealed transient nature of p33-Pex19p binding as expected from a transporter. When pex19p was retargeted to mitochondria, a large fraction of p33 was also re-distributed to the mitochondria validating the importance of Pex19p in p33 localization.

TBSV also utilizes its genomic RNA for non-template activities during its replication. Accordingly, TBSV RNA serves as a platform for the assembly of replicase complex. To further characterize the regulatory cis-elements involved in this process, I utilized CFE and different TBSV RNA mutants together with recombinant p33 and p92 *in vitro* replication assays. These experiments revealed the role of RNA recruitment element [RIISL(+)] and 3' non-coding regions as minimal cis-elements required to assemble functional replicase complex. The experiments also indicated that the RIISL(+) and 3' non coding regions could be physically separated on two different RNA molecules to assemble TBSV replicase, suggesting insights into viral evolution.

KEYWORDS: Virus, RNA replication, replicase complex, protein interaction, host-factors.

Kunj Bihari Pathak

Student's Signature

November 17, 2011

Date

CHARACTERIZATION
OF VIRAL AND HOST PROTEINS
AND RNA ELEMENTS IN TOMBUSVIRUS REPLICATION

By

Kunj Bihari Pathak

Dr. Peter D Nagy

Director of Dissertation

Dr. Lisa Vaillancourt

Director of Graduate Studies

November, 2011

ACKNOWLEDGEMENTS

Many people should be thanked for helping me during the entire duration of my graduate school, but I will single out a few for particular mention. I am very grateful to all the present and past members of my lab who provided valuable advice, guidance and feedback. I am also grateful to my teachers, dissertation committee members, Director graduate studies and external examiner for valuable suggestions. The person who should perhaps receive most thanks is my advisor Dr. Peter Nagy. Finishing a dissertation like this would not be rewarding task it is without his support, and often blunt criticisms. Finally, I would like to thank my family for respecting my harping on the same old phrase, 'I have to go back to the lab and I'll be late'. It's OK now Niharika and Monika; I've broken the harp, at least temporarily.

TABLE OF CONTENTS

Acknowledgements.....	iii
List of figures.....	vii
List of files.....	ix
Chapter 1. Introduction.....	1
THE EXPERIMENTAL SYSTEM.....	1
TOMBUSVIRUS GENOME STRUCTURE.....	1
DEFECTIVE INTERFERING RNA AS A TOOL TO STUDY THE ROLE OF VIRAL AND HOST FACTORS IN TOMBUSVIRUS REPLICATION.....	2
Origin and synthesis of Defective Interfering (DI) RNAs.....	3
Viral replication proteins as factors influencing the formation/accumulation of DI-RNAs... ..	3
DI-RNAs as surrogate templates to study virus replication.....	4
Template selection and DI-RNA recruitment into replication.....	4
Factors affecting the assembly of the viral replicase complex.....	5
Factors affecting the replication of DI-RNA.....	6
Release of (+)DI-RNA progeny from the replicase complex and disassembly of replicase complex.....	6
Chapter 2. Defining the roles of <i>cis</i> -acting RNA elements in tombusvirus replicase assembly <i>in vitro</i>	11
INTRODUCTION.....	11
RESULTS.....	12
Defining a minimal RNA sequences required for the assembly of the tombusviral replicase complex <i>in vitro</i>	12
RII(+)-SL and RSE-gPR constitute the minimal RNA elements required for the assembly of the tombusviral replicase complex <i>in vitro</i>	13
Template competition reveals that the C•C mismatch in RII(+)-SL is important for competitiveness of an RNA template during <i>in vitro</i> replication.....	13
A novel two-component RNA system supports TBSV replication <i>in vitro</i>	14
RSE-gPR defines the template for RNA synthesis in the two-component RNA system <i>in vitro</i>	14
The RII(+)-SL is needed for the assembly of the TBSV replicase <i>in vitro</i>	15
DISCUSSION.....	16
The role of UL-DL in replication assembly.	16
Dual role of RII(+)-SL during template recruitment and the assembly of the viral replicase.	16
Cis-replication of the RNA template by the tombusvirus replicase depends on the presence of RSE.	17
Summarizing template recruitment and replicase assembly.	17
MATERIALS AND METHODS.....	17
Yeast and Bacterial strains.	17
E. coli expression plasmids.	18
Yeast expression plasmids.	18
RNA template production and annealing.	18
<i>In vitro</i> replication assay based on yeast CFE.....	19
Micrococcal nuclease protection assay.	19
Purification of the recombinant tombusvirus replicase from yeast.....	19

<i>In vitro</i> assembly and purification of the TBSV replicase.....	19
Protein purification from <i>E. coli</i>	19
<i>In vitro</i> RNA recruitment assay.....	20
<i>In vitro</i> RdRp reaction.....	20
S1 nuclease digestion of the RdRp products.....	20
Chapter 3. The host Pex19p plays a role in peroxisomal localization of tombusvirus replication proteins.....	37
INTRODUCTION.....	37
RESULTS.....	38
The Pex19p host protein binds to the tombusvirus p33 replication cofactor <i>in vitro</i>	38
Co-purification of p33 replication protein with Pex19p host protein from yeast.....	39
Pex19p is temporarily present in the viral replicase.....	39
Re-targeting Pex19p to the mitochondria leads to redistribution of p33.....	39
Re-targeting Pex19p to the mitochondria interferes with TBSV repRNA accumulation.....	40
Re-targeting Pex19p to the mitochondria decreases the efficiency of the tombusvirus replicase.....	40
DISCUSSION.....	41
MATERIALS AND METHODS.....	42
Yeast strains.....	42
Yeast and <i>Escherichia coli</i> plasmids.....	42
The source of Antibodies for Western blotting.....	44
<i>In vitro</i> pull-down assay with recombinant p33.....	44
GST-based pull-down of cross-linked Pex19p complex.....	44
A two-step His/FLAG affinity-based co-purification of the viral replicase and Pex19p.....	45
Confocal laser microscopy.....	45
Replication assay.....	46
<i>In vitro</i> replicase assay.....	46
Chapter 4. Protein-protein interaction domain of <i>Cucumber necrosis virus</i> p33 and p92 is needed for viral RNA binding and assembly of replication complex.....	58
INTRODUCTION.....	58
RESULTS.....	60
S1/S2 sub-domains mutations abolish TBSV replication.....	60
Wild type p33/p92 couldn't rescue the activity of loss of function S1/S2 mutants.....	60
Q ₂₄₅ F mutant inhibits the wt p33/p92 mediated RNA replication.....	61
LT and RA mutations in p92 ^{pol} reduces its efficiency of RNA recruitment.....	61
S1/S2 subdomains are required for efficient RNA binding of p33.....	62
Assembled and purified TCV or CNV RdRps are resistant to inhibitory effects of S1/S2 mutants.....	62
Q ₂₄₅ F doesn't alter the localization or the structures formed by wt-p33 in yeast cells.....	62
S1/S2 sub-domain determines the quality of replication complex.....	63
DISCUSSION.....	63
Role of S1/S2 in p33:p33/p92 interaction.....	63
Novel replication inhibitory dominant negative mutants.....	64
MATERIALS AND METHODS.....	65
Yeast and <i>E. coli</i> strains.....	65
Plasmids.....	65
Site directed mutagenesis.....	65
Cell free extract based <i>in vitro</i> replication assay.....	66
Purification of the recombinant tombusvirus replicase from yeast.....	66
<i>In vitro</i> RNA recruitment assay.....	66

<i>In vitro</i> assembly and purification of replicase complex.....	66
<i>In vitro</i> RdRp assay.....	66
Electromobility gel shift assay.....	67
Protein purification from <u>E. coli</u>	67
Confocal microscopy.....	67
Chapter 5. Summary.....	79
REFERENCES.....	81
VITA.....	90

LIST OF FIGURES

Figure 1.1. Genome and structural organization of TBSV genomic RNA and the prototypical DI-73 and DI-72 RNAs.	9
Figure 1.2. The predicted secondary and tertiary structure of the 3' UTR in DI-72(+) RNA.	10
Figure 2.1 Schematic representation of TBSV DI-73 (+)repRNA and its derivatives carrying the three known <i>cis</i> -acting replication elements.	22
Figure 2.2. UL-DL <i>cis</i> -acting element functions as an enhancer element for the replicase assembly (EERA).	23
Figure 2.3. A mini template with RII(+)-SL and RSE-gPR can efficiently support the <i>in vitro</i> assembly of the TBSV replicase.	25
Figure 2.4. RII(+) RNA inhibits the <i>in vitro</i> assembly of the TBSV replicase.	26
Figure 2.5. An efficient two-component RNA-based TBSV replicase assay.	28
Figure 2.6. RII(+)-SL and RSE-gPR sequences must be located in close vicinity during the assembly of the TBSV replicase.	30
Figure 2.7. <i>cis</i> -replication of the template RNA carrying RSE-gPR <i>in vitro</i>	32
Figure 2.8. RII(+)-SL is required for the <i>in vitro</i> assembly of the TBSV replicase.	34
Figure 2.9. RNA templates containing the MS2 CP hairpins are efficiently recruited, but they are replication incompatible <i>in vitro</i>	35
Figure 2.10. The known functions of the <i>cis</i> -acting replication elements in TBSV (+)RNA.	36
Figure 3.1. <i>In vitro</i> interaction between Pex19p and p33 depends on the redundant peroxisomal targeting sequences in p33.	48
Figure 3.2. Co-purification of p33 with Pex19p from yeast.	49
Figure 3.3. Temporary presence of Pex19p in the viral replicase preparation.	50
Figure 3.4. Re-targeting Pex19p via an MTS sequence leads to mitochondrial localization of a fraction of p33 replication protein.	52
Figure 3.5. Dominant negative effect of the mitochondrial targeted MTS-Pex19p on TBSV replication.	54
Figure 3.6. Reduced replicase activity of preparations obtained from yeast expressing the mitochondrial targeted MTS-Pex19p.	55
Figure 3.7. A model for the proposed transporter function of Pex19p during tombusvirus replication.	56
Figure 4.1. Mutations in S1/S2 domains of p33/p92 inhibits viral replication <i>in vitro</i>	69
Figure 4.2. Mutant replication proteins' activity can't be rescued by wild-type p33/p92.	70
Figure 4.3 Dominant negative effect of p33-Q ₂₄₅ F mutant during <i>in vitro</i> CFE replication.	72
Figure 4.4 <i>In vitro</i> RNA recruitment to membranes affected by p92 mutants.	74
Figure 4.5. p33-Q ₂₄₅ F mutant is inefficient in binding viral RNA.	75
Figure 4.6 p33 mutants do not exert dominant negative effect on the RdRp activity of purified replicase complexes.	76

Figure 4.7. Peroxisomal localization and punctate pattern of wt-p33 is not affected by expression of Q₂₄₅F-p33 mutant in yeast.....77

Figure 4.8. Denaturing PAGE analysis of the CFE-based replication assay.....78

LIST OF FILES

Kunj_Dissertation.pdf.....21.6 MB

Chapter 1. Introduction

Sir Peter Medawar (Nobel Laureate) said-“Viruses are a piece of bad news wrapped up in protein.” Precisely, they are nucleic acid piece(s) surrounded by a protective coat. They are very simple in structure. They have limited genetic resources but can perform many biological activities elegantly. For example, one of the most deadly viruses for human beings is hepatitis B virus with only four genes, yet clinically affecting over a million people each year [2]. Viruses neither possess the machinery to synthesize proteins nor for energy production but can still make millions of progeny very quickly. To do so they usurp the biochemical machinery of the host cells. For example, they use cellular ribosomes to translate their own proteins, use cellular compartments as microhabitats to multiply and even use cells’ well-established transport mechanisms to move within a cell as well as hitch a ride out of the infected cells (reviewed by [3-7]). Viruses possess all the qualities of successful parasites; they can borrow, steal, and subvert host resources.

Viruses are the only pathogens that can infect most organisms, including bacteria, blue-green algae, fungi, plants, insects and animals causing diseases and epidemics in humans, animals and plants leading to intense studies. The research has resulted in eradication of several deadly viruses like smallpox virus [8]. Nevertheless, emerging and re-emerging viral diseases never let up and scientists are working round the clock to tackle them.

Apart from causing diseases, viruses are also associated with positive effects. For example, viruses have taught us seminal lessons in molecular biology and cellular biology. Several Nobel Prizes awarded to virologists exemplify this. Likewise, viruses are the most abundant biological entity in freshwater and seawater and they help maintain the planktonic populations of the aquatic ecosystems (reviewed by [9]). Another example is reconsideration of use of bacteriophages as a weapon against antibiotic-resistant bugs (reviewed by [10]). Use of viruses as vectors in gene therapy to cure genetic diseases and as vehicle of drug delivery are also progressing (reviewed by [11]). On top of this, viruses are now becoming favorite tools in the hands of nanotechnologists trying to take advantage of their versatile nature as examples, to make highly efficient material for batteries and fuel cells (reviewed by [12]).

THE EXPERIMENTAL SYSTEM

How do the viruses intricately manipulate their much more complex host cells and take over? These are questions and the focus of research for many scientists. To answer some of these questions it is highly desirable to have a model virus-host system: A virus that has a small genome, is robust enough to be easily detectable; are some of the attractive characteristics of a model virus. Similarly, some of the desirable features of a host to work on can be: Simple, easy and cheap to maintain in the lab; full genetic resources available; well known cellular and biochemical pathways. Tombusvirus and yeast is a winning merger of “model” virus and “model” host to study the enigmatic interaction between virus and host. This system has been developed in Dr. Peter Nagy’s lab to discover hundreds of host factors affecting tombusvirus multiplication [5, 6, 13, 14]. Our lab members used the many genetic and proteomic screens available to discover the factors affecting tombusvirus multiplication [14-19]. They were also able to observe the real time evolution of tombusvirus in yeast in the absence of some particular genes [20, 21]. These discoveries have opened up a new era of systems biology approaches in virology [22].

TOMBUSVIRUS GENOME STRUCTURE

Nagy and Pogany (2006) have described tombusvirus genome structure in their review [6]: “Tombusviruses are a group of single-component RNA viruses of plants within the large Tombusviridae family. Among the five viral-coded proteins, only p33 and p92 are essential replication proteins [23-27]. The sequence of p33 overlaps with the N-terminal region of p92, yet the functions of these regions are different in the two proteins. p33 is a replication cofactor, which

is involved in binding to the viral RNA via its RNA-binding region (termed RPR), [28]. The RPR domain is essential for the function of p33, whereas it plays a lesser role in p92, which functions as the RNA-dependent RNA polymerase [29, 30]. p33 also includes two essential membrane-spanning domains [31] and an N-terminal domain with unknown but essential function in replication [30]. In contrast, the corresponding domains in p92 modulate the function of this protein, but they are not essential [30]. In contrast, the p33:p33/p92 interaction domain, which is important for multimerization of p33 molecules and binding between p33 and p92 [32], is essential for tombusvirus replication [30]. Both p33 and p92 are part of the active tombusvirus replicase, which is most active when it contains a 10–20-fold larger amount of p33 than p92 [32]. Based on biochemical and cellular studies, the emerging picture is that, in spite of the overlapping sequences, p33 and p92 perform noncomplementary functions during tombusvirus replication.”

DEFECTIVE INTERFERING RNA AS A TOOL TO STUDY THE ROLE OF VIRAL AND HOST FACTORS IN TOMBUSVIRUS REPLICATION

Viruses are thought to be the ultimate parasites, multiplying inside the host cells and utilizing the resources of their hosts to produce vast number of infectious progenies. Intriguingly, many viruses have their own parasites, including defective interfering (DI) RNAs, as well as satellite viruses and satellite RNAs. For viruses with RNA genomes, the DI molecules consist of RNA sequences derived from the parent RNA virus, whereas the origin of satellite RNAs are not known in most cases. Both classes of subviral RNA are parasitic, since they have to use proteins coded by viruses, called helper viruses, for their replication inside the host cells. This review will focus on the DI-RNAs and their intimate relationship with their parent viruses and host cells.

DI-RNAs are created spontaneously during the replication of the viral genome and they multiply rapidly and eventually lead to inhibition of the parent virus' multiplication [reviewed by 33, 34]. These RNAs are called "defective" because they have lost the capacity to code for all the necessary viral proteins for independent replication and thus are defective in the absence of the parent (also called helper) virus. Accordingly, the helper virus is required to provide the missing replication protein(s) in *trans*. DI-RNAs are referred as "interfering" because they can interfere with the multiplication of their helper virus [reviewed by 34, 35]. However, some defective RNAs do not interfere with multiplication of their helper viruses; in those cases they are simply called D-RNAs. In some cases, DI-RNAs can enhance the symptoms caused by their parent viruses. Importantly, DI-RNAs are distinct from other parasitic RNAs, called satellite (sat)RNA and satellite viruses, which are associated with helper viruses. The primary difference being that satRNAs do not show intensive sequence similarities with their helper viruses and the sources of their nucleic acid sequences remain uncertain [reviewed by 34]. The hierarchical game of parasitism does not stop here. To make the matter more complex, DI-RNA has been discovered even for a satellite virus [36]. This satellite derived DI-RNA strongly interfered with the parental *satellite panicum mosaic virus* (SPMV), which is one of the two sub-viral particles associated with *Panicum mosaic virus* (PMV). Thus, there is a unique complexity and dynamism in viral co-infections that include satellite RNAs, satellite viruses and DI-RNAs.

DI-RNAs are often observed during RNA virus infections of mammalian cell cultures when high multiplicity of infection is used [37]. DI-RNAs associated with plant virus infection has been mostly described from greenhouse samples or laboratory experiments [38-47]. DI-RNAs associated with viruses in the tombusvirus genus are among the most extensively studied. Also, the first DI-RNAs associated with a plant virus identified were derived from *Tomato bushy stunt virus* (TBSV) [43]. I used TBSV DI-RNA in the course of my entire research thus it will be discussed in detail.

There are several reviews [27, 33-35, 48], which comprehensively discuss the occurrence and genome structures of DI-RNAs. In this chapter, I will mainly focus on how they have shaped our understanding about the biology of parent virus replication.

Origin and synthesis of Defective Interfering (DI) RNAs

DI-RNAs are synthesized by the viral RNA-dependent RNA polymerases (RdRp) that also replicate the parental virus genomes. Most of the DI-RNAs consist of non-contiguous portions of their helper virus' genomes [48]. The popular model for DI-RNA formation is the viral polymerase driven template-switching mechanism [49].

RNA recombination plays a major role in producing DI-RNAs or defective RNA particles (i.e. packaged DI RNAs). The errors made by the RdRp, including template switching (also called replicase jumping), during the standard replication process of the viral genome is likely the main mechanism of genomic RNA-RNA recombination and also DI-RNA formation [49].

The replicase-driven template-switching model is supported by biochemical assays performed in cell-free systems with purified recombinant viral RdRps. The list includes two tombusviruses (TBSV and *Cucumber necrosis virus*, CNV), *Brome mosaic virus* (BMV), *Turnip crinkle virus* (TCV), *Cucumber mosaic virus*, *Bovine viral diarrhea virus*, and *Hepatitis C virus* [50-55]. The *in vitro* data from the above works suggested that breaks, strong hairpin structures, or AU-rich stretches in the template (donor) RNA promotes the viral replicase to switch template to the acceptor RNA and then use the nascent RNA as a "primer" for resumption of RNA synthesis on the acceptor RNA. Interestingly, *cis*-acting sequences as well as sequence complementarity between the nascent RNA and the acceptor RNA may guide the template-switching events [49]. Primer extension experiments with RNAs representing the nascent strand revealed that rather short (2-to-5 nt) sequence complementarity between the primer and the acceptor template was sometimes sufficient to promote re-initiation of the replicase [51, 52, 56-58]. Additional works revealed recombination "cold-" and "hot-spots", i.e. regions of decreased and increased recombination, respectively, in the BMV and TBSV genomes [51, 52, 59].

The formation of the prototypical TBSV DI-RNAs requires two or three recombination events, which likely occur sequentially [38]. For example, the TBSV-associated DI-72 RNA and other tombusvirus DI-RNAs are comprised of four noncontiguous RNA segments, namely Region I (derived from the 5' untranslated region [UTR]), Region II (representing portion of the p92^{pol} ORF), Regions III and IV (mostly derived from the 3' UTR) (Figure 1.1) [60] [48]. Interestingly, the junction sites among the four noncontiguous regions in the above DI-RNAs do not show long sequence similarity. Therefore, it has been suggested that the recombination events during TBSV DI-RNA formation are unlikely to be random, but guided by *cis*-acting replication sequences [27].

Another mechanism for RNA recombination based on RNA ligation has also been reported for Q-beta bacteriophage and poliovirus [61, 62]. The major evidence provided for RNA breakage and transesterification was the interference with recombination when the 3' OH group in the acceptor strand was altered to inhibit ligation. It is yet to be seen if this mechanism is involved in DI-RNA formation.

Viral replication proteins as factors influencing the formation/accumulation of DI-RNAs

Evidence to support the roles of replication proteins in DI-RNA formation has been obtained with the helicase-like protein 1a of BMV. Mutations within the 1a protein altered the sites of RNA recombination when compared with BMV infections containing the wt 1a [63]. In addition, mutational studies on BMV 2a polymerase also indicated the replicase's role in recombination [64]. A 2a mutation affected the precision as well as the location of RNA recombination sites. Similarly, mutation in the polymerase gene of influenza virus, led to an increase in the synthesis of DI-RNAs [65]. The authors proposed that the mutation destabilized the polymerase-viral RNA complex during the elongation step. A role for the replicase in RNA recombination was further bolstered by studies on the p33 auxiliary replication protein for CNV [66]. Frequency of recombination for tombusvirus DI-RNA was affected by mutations in the RNA binding (RPR)

domain of p33. Two p33 mutants tested enhanced the recombination and 5 of the 17 mutants tested slowed down the accumulation of recombinants. Interestingly, the recombination promoting mutants also increased the level of subgenomic RNA transcription [25]. The connection between transcription and recombination is not that surprising as both processes utilize the viral replicase complex. Mutations within the N-terminal portion of p92^{pol} polymerase, which overlaps with p33, did not have similar effects on recombination, suggesting different roles for RPR in p33 and p92^{pol} proteins with respect to RNA recombination. How these mutations affect recombination, or how they enhance template-switching remains to be tested.

Most plant RNA viruses code for two or more replication proteins and the amount and the ratio of the replication proteins could be another factor affecting RNA recombination and DI-RNA formation. This was tested with the tombusvirus p92^{pol} and p33 replication proteins in yeast, a surrogate model host [67]. High level of p33 was shown to increase the accumulation of recombinant DI-RNA. The effect on recombination was even more profound when p92^{pol} was expressed at a high level in yeast. In addition, the ratio of p33 and p92^{pol} also affected recombinant DI-RNA formation. It is possible that too high a level of p92^{pol} RdRp makes the viral replicase complexes less precise and more prone to template switching.

DI-RNAs as surrogate templates to study virus replication

DI-RNAs are versatile tools at virologists' disposal. DI-RNAs often multiply faster, are smaller than the full genome of the virus and contain the *cis*-acting replication elements for replication and other steps in viral multiplication cycle. Since many DI-RNAs do not code for proteins, mutational studies on DI-RNAs make the results easier to interpret due to separation of *trans*-acting protein factors and *cis*-acting RNA elements. Thus, critical *cis*-acting replication elements important for different steps in viral replication can be deductively discovered. These RNAs also are adapted to use *trans* (viral and possibly other) factors for their replication enabling a more experimental control over those factors so that a virologist can regulate them spatially and/or temporally. Indeed, using DI-RNAs combined with other modern tools, many *cis*-acting RNA elements for tombusviruses were deciphered [reviewed by 27, 68]. DI-RNAs also proved to be useful in discovering host factors modulating viral replication. To this end, a yeast system using TBSV DI-72 as an experimental replicon (rep)RNA was developed [13, 69]. In the above yeast system, the repRNA works as an independent replicon, capable of assembling the viral replicase complex and performing most of the steps in replication in the absence of a helper virus. Based on the yeast/TBSV repRNA system, genome-wide and proteomics-based screens have been performed [15-18, 20, 21, 70]. This in turn, accelerated the identification of more than hundred host factors affecting TBSV replication and ~40 host factors affecting RNA recombination. In addition, the system is also useful in dissection of the mechanisms by which these host factors affect viral replication and RNA recombination. To better explain the roles of *cis*-acting replication elements, viral and host factors discovered with the assistance of DI-RNA, I divide the replication cycle of the plus-stranded RNA viruses further into different steps in chronological order [reviewed by 5, 6].

Template selection and DI-RNA recruitment into replication.

Similar to the viral genomic RNA, DI-RNAs should also be recognized selectively from the large pool of host RNAs. The selection of the viral RNA requires specific interaction with viral- or host proteins. For TBSV DI-RNAs, the selective RNA recognition is mediated by the cytosol-exposed C-terminal portion of p33 replication protein in yeast [71, 72]. Detailed mutational studies on DI-RNA revealed the essential role for a C•C mismatch within the RII(+)-SL sequence (Figure 1.1) in binding to p33 [71]. When the C•C mismatch was mutated to G=C, then binding of DI-72 to p33 was lost and this DI-RNA was unable to replicate in the yeast system or the full-length TBSV genomic RNA carrying the comparable mutation in *N. benthamiana* plants [71, 72]. Thus, the C•C mismatch sequence can be regarded as the “identity card” of the virus, allowing

the viral replicase complex to achieve high selectivity to replicate only viral RNA. As expected, the C•C mismatch region is also required for replication of DI-72 repRNA in a yeast extract capable of supporting one full cycle of replication *in vitro* [55, 73].

In addition to interacting with the viral replication proteins, DI-RNA is likely bound by select host proteins. To identify the host proteins that bind viral RNA, TBSV DI-72 (+)RNA was used as a probe to screen RNA binding proteins in a yeast proteome-wide chip carrying 4,100 purified yeast proteins [18]. Five of the identified host proteins in the above screen were further confirmed with other approaches, e.g., gel-shift and pull-down assays. One of the factors discovered was translation elongation factor eEF1A. This protein also co-purified with the tombusvirus replicase. Further studies showed that eEF1A binds to the silencer sequence present in the 3'UTR (Figure 2.2) [18], which is required for the assembly of the tombusvirus replicase complex [74, 75]. A mutation affecting guanine exchange factor requirement of eEF1A inhibited DI-72 repRNA accumulation in yeast. It has been proposed that eEF1A interaction with DI-72 RNA might be needed for RNA recruitment into replicase complex or viral RNA synthesis [76]. Another host factor that exerts its effect on viral replication directly via binding to the viral RNA is Nsr1p (also known as nucleolin). This factor was discovered during screening of the yeast knock out (YKO) library for TBSV replication [15]. Virus replication was boosted three folds in the absence of NSR1. Further analysis revealed that Nsr1p binds to RIII in DI-72 (+)RNA [77]. Indeed the Nsr1p mediated inhibitory effect on DI-72 repRNA accumulation *in vivo* was lost when DI-72 repRNA missing RIII, the target for Nsr1 binding, was used as a replicon RNA in above study. This protein may inhibit TBSV replication via specific binding to the viral RNA and, thus, resulting in inefficient repRNA recruitment for replication.

After the RNA has been selected for replication, the viral proteins and RNA complex has to be transported to the site of replication. TBSV assembles the replicase complex on the cytosolic surface of peroxisomal membranes [30, 78, 79]. It has been shown that the host shuttle protein Pex19p, which is involved in peroxisomal membrane protein transport, play a role in TBSV protein transportation to the site of replication [80]. Another host protein involved in localization/transportation of the viral replication proteins is the heat shock protein 70 (Hsp70). Using a temperature-sensitive mutant of Hsp70 at nonpermissive temperature has led to cytosolic localization of p33 replication protein [81]. Shifting down to permissive temperature resulted in re-localization of p33 to the peroxisome membrane surface in yeast.

Overall, the above studies revealed that both viral- and host proteins are involved in RNA template selection and the recruitment of the viral RNA/p33/p92^{pol} complex to the site of replication.

Factors affecting the assembly of the viral replicase complex.

The assembly of the viral replicase complex is still a poorly understood process. Interestingly, the viral RNA plays an essential role in the replicase assembly both *in vivo* and *in vitro* [73, 75, 82, 83]. Detailed work with TBSV RNA revealed that RII(+) (Figure 1.1) is also crucial for the assembly of tombusvirus replicase complex in yeast [75]. In this study, the minimal *cis*-acting elements required for the assembly of the tombusvirus replicase complex was defined. The affinity purified viral replicase complex was active on external templates only when the full-length DI-72 repRNA was co-expressed with the p33 and p92^{pol} replication proteins in yeast. The minimal repRNA still capable of supporting the assembly of the replicase complex consisted of RII(+)-SL hairpin, the replication silencer element and genomic promoter (Figure 1.1) [75]. The exact role of the viral RNA in the assembly process is currently under heavy investigation and presented in the next chapter. The viral RNA might provide an assembly platform to bring together the viral and host proteins. The RNA may also play a role in making structural change(s) in the viral RdRp required for activation of the polymerase function of the RdRp. Recently long-range RNA interacting elements UL and DL in the TBSV genomic RNA have been discovered that play a role in replicase assembly [84]. Long distance base pairing between UL and DL

sequences juxtapose RII(+)-SL and the replication silencer and gPR within the 3'-UTR (Figure 1.1). These latter two elements had already been shown to be important in replicase assembly [73, 75]. It is interesting to note that UL-DL interaction is not crucial for replicase assembly in DI-73, probably because RII(+)-SL and the 3'-UTR are already in close proximity (Figure 1.1B), unlike in the genomic RNA, where they are 3000 nt apart (Figure 1.1A).

Both viral replication proteins of TBSV are essential for the assembly of the functional virus replicase [73, 82]. Interestingly, the p33:p33/p92^{pol} interaction domains in these replication proteins seem to be critical for the assembly, suggesting that these proteins are participating in multimeric complex formation, which is likely needed for the formation of membrane invaginations, called spherules. These spherules are the predicted structures supporting TBSV replication [78].

In addition to the viral RNA and viral replication proteins, host factors play a role in tombusvirus replicase assembly. The best-characterized host factor in the replicase assembly process is Hsp70. Proteomics analysis of the tombusvirus replicase complex revealed the presence of Hsp70 and 5-10 other host proteins within the replicase complex [17, 18, 70]. *In vitro* work indicated that Hsp70 plays a role in membrane insertion of the viral replication proteins [85]. The essential role of Hsp70 in the assembly of the TBSV replicase was confirmed by Pogany and colleagues, using a yeast extract depleted in Hsp70 [73]. The addition of purified recombinant Hsp70 to the above cell-free assay complemented the defect, leading to the assembly of the viral replicase complex and active replication of the DI-72 (+)repRNA *in vitro* [73].

Factors affecting the replication of DI-RNA.

After the assembly of the replicase complex is finished, the synthesis of the complementary (-) strand from the plus (+) stranded DI-RNA takes place. The newly made (-) strand then serve as a template for synthesis of new (+)DI-RNAs. The replication process of (+) stranded RNA viruses and associated DI-RNAs is asymmetrical, leading to 20-100-fold more copies of (+) RNAs than (-) strand RNA. One of the major factors in regulation of DI-RNA replication is the DI-RNA carrying *cis*-acting elements in both strands [reviewed by 27]. The *cis*-acting elements include the genomic promoter (gPR) in the 3' end of (+)DI-RNA [86], a complementary promoter element in the 3' end of (-)RNA [87] and replication enhancer elements in RI(-) and RIII(-) [88]. An intriguing replication modulator element is the replication silencer (Figure 1.2), which is involved in the assembly of the replicase complex and possibly in the regulation of the (-)-strand synthesis [74]. This element interacts with gPR, making the promoter recognition by the RdRp weaker *in vitro*. It is currently under investigation how this interaction is regulated and what viral- or host proteins are involved in modulating this interaction.

The asymmetrical RNA synthesis is affected not only by *cis*-acting RNA replication elements, but host factors as well. One such host factor is a metabolic enzyme called glyceraldehyde-3-phosphate dehydrogenase (GAPDH), which was discovered as a component of the tombusvirus replicase complex via a proteomics analysis of a purified viral replicase preparation [17]. When TBSV DI-72 RNA was replicated in yeast cells, the cellular distribution for GAPDH changed dramatically due to re-localization from the cytosol to the site of replication (peroxisome) [89]. Down-regulation of GAPDH levels in yeast correlated with reduced level of (+)-strand DI repRNA. GAPDH was shown to bind to (-)-strand of DI-72 repRNA via an AU pentamer sequence. It was proposed that the role of GAPDH is to retain the (-)-strand repRNA intermediate in the replicase complex, thus facilitating asymmetrical replication. The data from the yeast host were also validated in *N. benthamiana* host [89].

Release of (+) DI-RNA progeny from the replicase complex and disassembly of replicase complex.

After the synthesis of the new (+)DI-RNA progeny by the replicase, (+)RNA is released to the cytosol while the (-) RNA intermediate is kept within the spherule most or all the time [30].

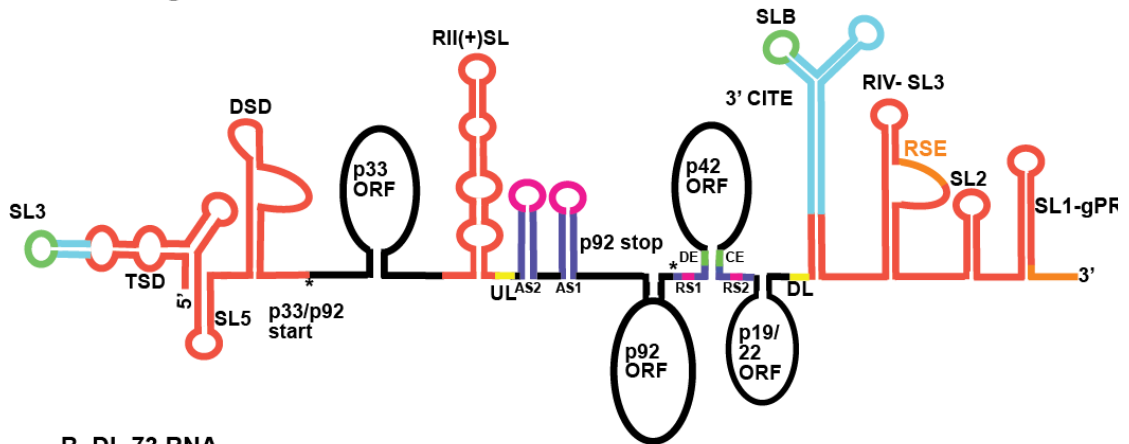
So far host factors and viral RNA sequences have not been discovered playing role(s) in the release of (+)RNA progeny. However, viral protein modification has been proposed to modulate this process [90]. This is based on the observation that p33 gets phosphorylated *in vivo* and *in vitro* as well [90, 91]. The phosphorylated form of p33 lost its ability to bind to (+)DI-72 RNA associated with TBSV and *in vitro* phosphorylation of the p33:DI-72 RNA complex led to the release of the RNA from the complex [90]. In contrast, p33 mutants mimicking the unphosphorylated stage of the protein bound efficiently to DI-72 RNA, suggesting that phosphorylation/unphosphorylation of p33 might regulate the release of (+)RNA from the replicase complex.

Roles of other host proteins in viral protein modification have also been demonstrated. A host ubiquitin conjugating enzyme Cdc34p as well as Rsp5p ubiquitin ligase have been shown to ubiquitinate p33 *in vitro* [70, 92]. However, the actual role of p33 ubiquitination is currently unknown. It is possible that this protein modification modulates the viral protein-protein or viral protein-host protein interactions important for viral replication.

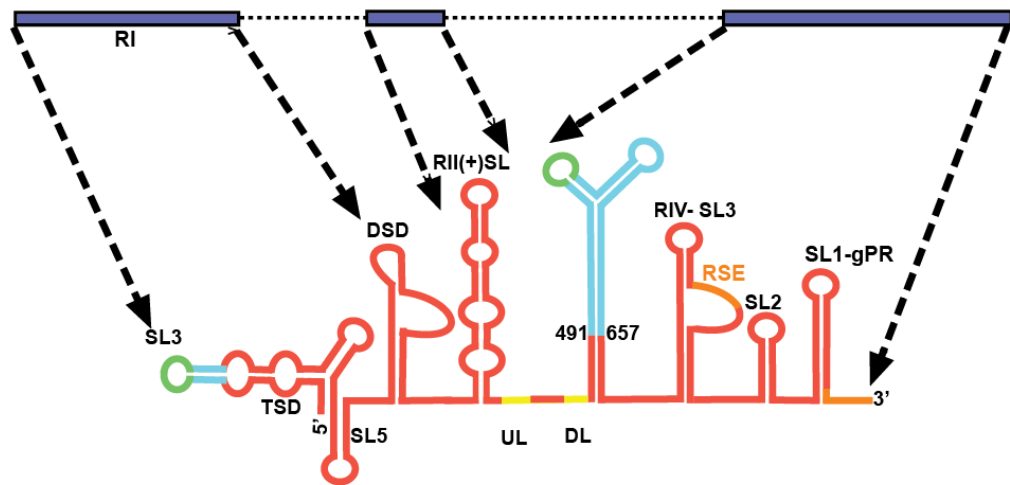
Altogether, the use of DI-RNA as surrogate template contributed a great deal to our understanding of viral RNA replication and virus - host interactions.

I exploited DI-RNAs to dissect the mechanism of virus replication: particularly the role of non-template function of RNA; the role of auxiliary protein p33 in assembly of replication complex and the role of a host protein. The subsequent chapters present my work in detail about the above-mentioned research.

A. TBSV genomic RNA



B. DI -73 RNA



C. DI -72 RNA

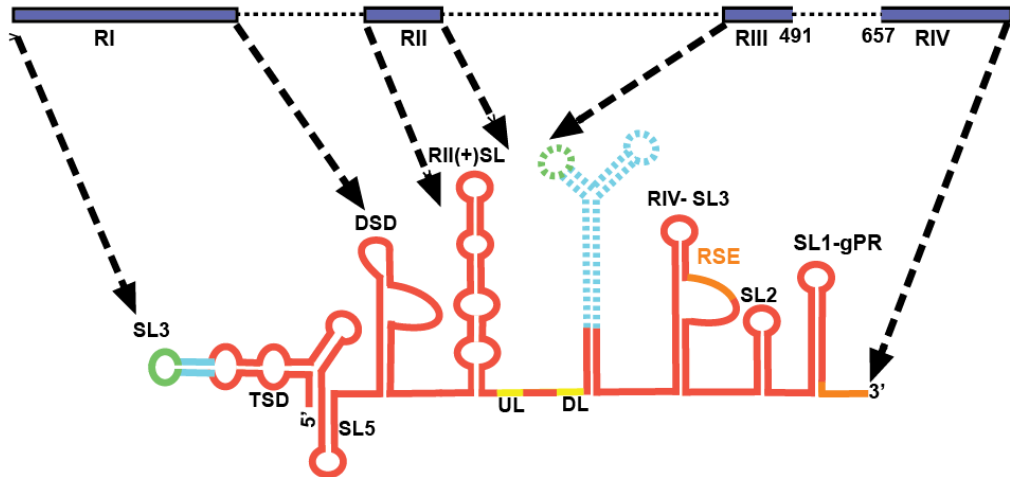


Figure 1.1. Genome and structural organization of TBSV genomic RNA and the prototypical DI-73 and DI-72 RNAs.

(A) A cartoon showing structural details of the ~4,800 nt TBSV genome (not to scale). The p33, p92^{pol}, p41 and the overlapping p19/p22 ORFs are depicted as black ovals and labeled accordingly. Note that p92^{pol} overlaps with p33, sharing the same initiation codon. Sequences playing role(s) in translation, genome replication and sgRNA transcription are shown in turquoise blue, red and purple, respectively. Sequences involved in RNA-RNA interactions are shown in matching colors. Note that translation requires SL3-SLB interaction, UL-DL and RSE-gPR interactions are required for replicase assembly and AS1-RS1, AS2-RS2 and DE-CE interactions are crucial for sgRNA synthesis. (Abbreviations used are DSD: downstream domain; TSD: T-shape domain; RSE: replication silencer element; AS: activator sequence; RS: receptor sequence; CE: core element; DE: distal element; UL: upstream linker; DL: downstream linker; CITE: cap independent translation enhancer; SL: stem loop) [84] (B) Structure of the ~800 nt DI-73 carrying three noncontiguous segments of the genomic RNA. Generation of DI-73 preserves critical replication elements (red) and the 3'CITE. The blue bars and dotted arrows depict the segments corresponding to genomic RNA. (C) Note that the other prototypical DI of ~620 nt, named DI-72 RNA, has an additional deletion of the 3'CITE.

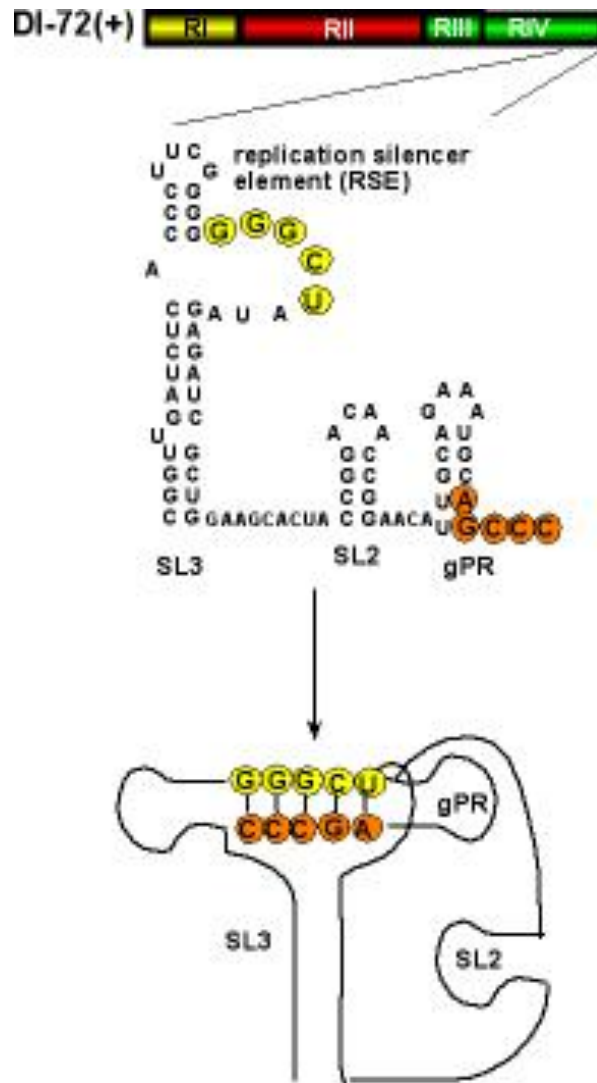


Figure 1.2. The predicted secondary and tertiary structure of the 3' UTR in DI-72(+) RNA.

A 5 nt base-pairing between RSE in the internal loop sequence of SL3 and gPR stabilizes the tertiary structure. This interaction is critical for the assembly of the functional TBSV replicase [74, 93].

Chapter 2. Defining the roles of *cis*-acting RNA elements in tombusvirus replicase assembly *in vitro*

This chapter is published [epub ahead of print] in *Journal of Virology*, 2011 Oct 19

INTRODUCTION

Plus-stranded (+) RNA viruses exhibit many similarities during genome replication, including the formation of membrane-bound viral replicase complexes, the production of (-)-strand and abundant (+)-strand RNAs, and the use of co-opted host factors [3, 5, 7, 94]. One of the best-studied (+)RNA viruses is *Tomato bushy stunt virus* (TBSV), which has a single 4,800 nt long RNA genome [27]. The two viral-coded replication proteins, p33 RNA chaperone and p92^{pol} RNA-dependent RNA polymerase (RdRp), participate in the formation of the membrane-bound viral replicase complex that also contains several host proteins [7, 17, 76, 95, 96].

Replication of TBSV and other (+)RNA viruses involve several sequential steps, including: selection of the viral (+)RNA template for replication; recruitment of the viral (+)RNA and the viral replication proteins from the cytosol to the subcellular membrane surfaces where replication takes place; the assembly/activation of the viral replicase; (-)-strand and then (+)-strand RNA synthesis; and the release of progeny (+)-strand RNAs from the replicase complex [5, 6, 97]. This complex process helps to ensure that authentic viral templates are replicated and that the replication process is rapid and efficient.

The TBSV (+)RNA plays multiple roles during viral replication. In addition to its main function as a store of genetic information, the viral (+)RNA also regulates its own intracellular localization and recruitment to the site of RNA replication [30, 71, 73, 75, 84]. Moreover, the TBSV (+)RNA serves as an assembly platform for the viral replicase, consisting of viral replication proteins, co-opted host proteins and host lipids/membranes [17, 18, 55, 73]. These replication related functions are guided by various *cis*-acting elements within the TBSV (+)RNA, most notably by RII(+)-SL located internally and RIV, positioned 3'-terminally [71, 72, 75, 84]. These two RNA segments (RII and RIV), along with additional *cis*-acting elements RI and RIII, are retained in TBSV defective interfering (DI) RNAs, which are small virus-derived replicons used to study sequence functions (Figure 1A) [98].

Other plant viruses also contain specific sequences in their viral (+)RNAs that affect RNA recruitment and the assembly of their cognate replicase complexes. For example, short stem-loops within the 3' UTR of *Tobacco mosaic virus* (TMV) (+)RNA can bind specifically to the TMV 126K replication protein *in vitro* [99, 100]. The *Brome mosaic virus* (BMV) 1a protein participates in template selection/recruitment via interaction with the 1a responsive element present in the BMV RNAs [101, 102]. A Y-shaped RNA element in the 3'UTR in RNA2 of *Red clover necrotic mosaic virus* is specifically recognized by its cognate viral replication proteins, aiding recruitment of this viral RNA into replication [103, 104].

Dissection of the actual function(s) of *cis*-acting RNA elements such as those mentioned above can be hindered by the sequential and cycling nature of the (+)RNA replication; *i.e.* where a particular replication step depends on the previous step(s) and portions of the process are repeated in many cycles. Consequently, mutations introduced into a viral RNA could directly or indirectly affect multiple steps in replication, making assignment of functions of specific *cis*-acting RNA sequences/structures challenging. To circumvent some of the above problems, I have previously developed an *in vitro* replicase assembly assay based on yeast cell-free extract (CFE) and purified recombinant tombusvirus replication proteins [73]. In our CFE assay, the viral (+)RNA has to be recruited to the membrane (derived from the organelles of yeast), followed by the assembly of the viral replicase complex and a single cycle of replication producing (-)-strand and abundant (+)-strand RNA progeny, which is released to the solution [55, 73].

In this paper, I employed the CFE assay to dissect the functions of various known *cis*-acting elements in the TBSV (+)RNA. I show that an essential internal stem-loop structure, RII(+)-SL, has a dual function: serving both as a (+)RNA recruitment element and mediator of viral replicase assembly, with the former activity being able to function in *trans*. Using a novel two-component RNA system in the replication assay, I also show that another *cis*-acting element, located in RIV and termed the replication silencer element (RSE), has to be present in the viral (+)RNA in order for it to serve as a functional template. These findings have provided further important insights into the detailed steps of the replication process in tombusviruses.

RESULTS

Defining a minimal RNA sequences required for the assembly of the tombusviral replicase complex in vitro.

Previous work with TBSV identified the extended stem-loop RII(+)-SL in RII and the two sub-elements RSE and SL1-gPR in RIV as distinct *cis*-acting RNA elements, required for the assembly of the TBSV replicase *in vivo*, either in plant cells or in yeast, a surrogate host [75, 84] (Figure 2.1A). The RSE and SL1-gPR interact via a 5 bp interaction and this feature is important for replicase assembly (Figure 2.1A) [74, 75]. In the context of the TBSV genome, RII and RIV are separated ~3 kb, but they can be brought into close proximity by an RNA base pairing bridge that forms between the UL (upstream linker) sequence just 3' to RII(+)-SL and its complementary DL (downstream linker) sequence, positioned near RIV (Figure 2.1A, lower panel). Formation of this UL-DL bridge mediates efficient replicase assembly *in vivo* in both yeast and plant cells [84].

To further define and dissect the functions of the abovementioned *cis*-acting RNA sequences during replication, I measured their effects on the assembly of the tombusvirus replicase complex *in vitro* (*i.e.* separate from their effects on template amplification) using our recently developed *in vitro* replicase assembly assay based on yeast CFE [73]. In this assay, the recombinant viral proteins are affinity-purified from *E. coli*, the various (+)-stranded TBSV DI-RNA-based templates, termed (rep)RNAs, are made via T7 transcription, while the CFE is prepared from yeast BY4741 strain (free of any TBSV components). The assembly assay contains ATP and GTP, but lacks CTP and UTP, thus preventing complementary RNA synthesis or replication (Figure 2.2A). After mixing these components the assembly assay is allowed to occur and then any assembled replicase complex is solubilized and affinity-purified; a process that leads to the loss of the original repRNA template. Subsequently, a (-)RNA template, DI-72(-), is added to the purified replicase preparations to measure the copying activity of the replicase *in vitro*, which provides a measure of the efficiency of replicase assembly (Figure 2.2A). In this replicase assembly assay, the originally added repRNA functions only in template recruitment and replicase assembly and does not act as a template for complementary strand synthesis or replication.

To determine if the UL-DL long-distance base-pairing interaction is required for the assembly of the tombusvirus replicase complex *in vitro*, I used wt DI-73 repRNA and mutants containing substitutions in UL, DL or both [84], as shown in Figure 2.2B. Mutations in either the UL or DL regions (mutants dD and dU in Figure 2.2B), which reduced base-pairing between UL-DL, decreased the *in vitro* assembly of the replicase by ~85% (lanes 2-3, 6-7 in Figure 2.2C-D). Restoring the base-pairing between UL-DL via complementary mutations in UL and DL (mutant cUD in Figure 2.2B) resulted in ~3- to 4-fold more efficient replicase assembly, versus the single mutants, for both replication competent and incompetent repRNAs (lanes 4 and 8, respectively, in Figure 2.2C). Including all four ribonucleotides in the assembly assay led to slightly increased recovery levels for the compensatory mutant (Figure 2.2D, lane 4), while not adding template under the same conditions resulted in no products (Figure 2.2E). Overall, as observed *in vivo* [84], the UL-DL interaction is also important for promoting replicase assembly

in vitro. Since the UL-DL interaction was not essential for this process, but did stimulate the *in vitro* assembly of the replicase (albeit, in a sequence independent manner), we define it as an enhancer element for a replicase assembly (EERA).

RII(+)-SL and RSE-gPR constitute the minimal RNA elements required for the assembly of the tombusviral replicase complex in vitro.

To test if RII(+)-SL and RSE-gPR elements (Figure 1.1A) together were sufficient for the assembly of the replicase *in vitro*, I constructed a minimal RNA (called “mini”) containing only these elements as shown in Figure 1.1B [75]. Comparing the *in vitro* replicase assembly efficiency of the mini RNA versus the full-length DI-72 (+)repRNA revealed comparable levels of replicase assembly in the CFE-based replicase assembly assay (Figure 2.3A, lanes 2 and 4 versus 1 and 3). Thus, these data demonstrate that RII(+)-SL and RSE-gPR elements together are sufficient for the efficient assembly of the TBSV replicase *in vitro*.

In the *in vitro* replication assay in CFE, all four ribonucleotides are added, along with the repRNA and purified p33 and p92, to the yeast extract, allowing for both assembly and RNA synthesis from the repRNA in the reaction (Figure 2.3B). Comparing the replication efficiency of the mini template versus DI-72 repRNA in the CFE revealed that the mini template was highly deficient in this replication assay (Figure 2.3B, lanes 3-4 versus 1-2). The larger RII/IV(+) template, carrying the additional sequences flanking RII(+)-SL and RSE-gPR, was also very inactive for RNA replication *in vitro* (Figure 2.3B, lanes 5-6). Interestingly, at the 40 min time point of the replication assay, both mini and RII/IV(+) templates were about two-times more sensitive to micrococcal nuclease treatment than DI-72 (+)repRNA (Figure 2.3C), suggesting that replicase assembly *in vitro* in the presence of the shorter templates could only partially protect these RNA templates from this nuclease.

The efficiency of *in vivo* assembly of replicase by DI-72 repRNA and mini template were also assessed using a modified *in vitro* replicase assay (Figure 2.3D, top). The affinity-purified replicase from yeast cells co-expressing the mini template and his-tagged p33/p92 (Figure 2.3D, bottom) showed reduced ability to copy the exogenously provided RI/III(-) template when compared with the replicase preparation from yeast co-expressing DI-72 and p33/p92 (Figure 2.3D, middle, lanes 3-4 versus 1-2). The decreased isolated replicase activity from yeast cells for the mini RNA is consistent with it being a poor template for replication *in vitro* (Figure 2.3B), thus there would be less of this template available for replicase assembly. These results show that the mini repRNA is good at facilitating the assembly of the TBSV replicase, but it is a poor replicon. This is likely due, at least in part, to the absence of important *cis*-acting replication elements such as RI, which is present in DI-72 (+)repRNA [27, 86-88, 105].

Template competition reveals that the C•C mismatch in RII(+)-SL is important for competitiveness of an RNA template during in vitro replication.

RII(+)-SL and RSE-gPR are important for forming an assembly platform for the replicase and RII(+)-SL is proposed to aid in RNA recruitment to the cellular membranes [73]. TBSV p33 is targeted to peroxisomal membranes [30, 78, 80, 106] and binds to RII(+)-SL with high affinity [71]. Accordingly, it has been proposed that a key function of RII(+)-SL is to facilitate the recruitment of the TBSV repRNA to the site of viral replication on membranes via its interaction with p33 [30, 71, 72].

To determine the importance of RII(+)-SL and RSE-gPR for replication in the CFE, I performed template competition experiments in our CFE replication assay (Figure 2.4 top). This involved adding defined viral segments containing different *cis*-acting elements as competitors to a replication assay for DI-72 (+)repRNA. Added the plus-stranded RI, RIII or RIV, as well as heterologous TCV satC RNA, exhibited relatively poor competition against the accumulation of DI-72 (+)repRNA template *in vitro* (Figure 2.4A, lanes 3-4, 1-2, 9-10 and 15-18, respectively), while RII was more competitive (Figure 2.4A, lanes 13-14). The C•C mismatch in mutant RII*,

which prevents the p33-RII(+)-SL interaction [71], reduced its competitiveness *in vitro* compared to wt RII (Figure 2.4A, cf. lanes 11-12 with 13-14). The mutant RIV*, in which the RSE-SL1-gPR interaction was disrupted (Figure 2.1A) [74], was slightly more competitive than its wt RIV counterpart (Figure 2.4A, cf. lanes 7-8 with 9-10). Since none of the above short RNA templates are replication competent in the CFE assay, these RNAs likely inhibit replication of DI-72 (+)repRNA *in vitro* by competing for diffusible factors during RNA recruitment or replicase assembly. Results from competition assays with larger RNAs containing two or more of the above segments were also consistent with the single segment results and indicated that wt RII has the greatest negative effect on DI-72(+) replication (Figure 2.4B). This effect was partially related to RII's ability to bind to p33, as RNAs containing mutant RII* [that are unable to bind to p33 [71]] showed a marked reduction in competitiveness. (Figure 2.4B). Thus, in this factor-limited *in vitro* environment, RII, alone or with other RNA elements, likely sequesters p33 or p92 away from the DI-72(+), leading to reduced replicase assembly and replication of DI-72(+).

A novel two-component RNA system supports TBSV replication in vitro.

To further dissect the roles of RII(+)-SL and RSE-gPR elements in TBSV RNA replication, I developed a novel two-component RNA replicase assembly assay based on CFE. One RNA, construct A (Figure 2.5A) contained RII(+)-SL and the other RNA, construct B, (Figure 2.5A) carried the RSE-gPR sequence. Constructs A and B also contained a 23 nt long region of complementarity at their 3' and 5' ends, respectively, that would allow them to interact via base pairing (Figure 2.5A). Testing the replicase activity of the affinity-purified TBSV replicase from CFE revealed that neither construct A nor construct B was able to efficiently support the assembly of the TBSV replicase when provided individually in the assembly assay (Figure 2.5B, lanes 4 and 5, respectively). However, when both RNAs were present, the assembly of the TBSV replicase was as efficient as the single-component mini-construct or DI-72(+)repRNA (Figure 2.5B cf. lane 3 with lanes 1-2.). This result demonstrates that both RII(+)-SL and RSE-gPR RNA elements are required for replicase assembly, but they do not have to be present in the same RNA molecule.

The complementarity between constructs A and B was important for *in vitro* RNA synthesis in the CFE replication assay, since constructs with 23 nt complementarity supported RNA synthesis more efficiently than constructs with 12 nt of complementarity (Figure 2.6B, lanes 5 versus 2) or that lacking extensive base pairing (Figure 2.6B, lanes 5 versus 3). Interestingly, mixing construct A(5'-29) and construct B, which share a tract of 29 bp complementarity, did not support RNA synthesis in the CFE assay (Figure 2.6B, lane 1). However, relative to construct A(23), the section of complementarity in construct A(5'-29) is at the opposite end of the RNA, which would result in a different and less proximal positioning of the RII(+)-SL and RSE-gPR [Figure 2.6, cf. A(23)+B with A(5'-29)]. This result suggests that not only do the two RNAs have to be physically close together in order to efficiently promote the assembly of the replicase and allow for RNA synthesis; there are also additional structural requirements with respect to their precise spatial orientation/proximity relative to each other. Another interesting finding from this analysis is that the functional replicase that assembled with the two-component system showed a preference for copying construct B, which contained RSE-gPR.

RSE-gPR defines the template for RNA synthesis in the two-component RNA system in vitro.

Results from Figure 2.6 indicated the TBSV replicase preferentially used construct B, carrying the RSE-gPR, as a template to make (-)RNA and this notion was confirmed by PAGE analysis of the RNA products synthesized (seen as a dsRNA in Figure 2.7B, lane 6). As expected, when heat-denatured, the dsRNA product became single-stranded (ssRNA in Figure 2.7B, lane 5) and similar results were observed when the samples were treated with S1 nuclease

prior to heating and gel analysis (Figure 2.7B, lanes 7 and 8), supporting the double-stranded nature of the faster moving product.

To test if construct A could be converted to an active template, I introduced SL1-gPR sequence (construct A/gPR, Figure 2.7A) or SL1-gPR and SL2 sequences (construct A/gPR/SL2) into RII(+)-SL-containing construct A at a 3' position. These new construct A-derivatives were able to serve as promoters in an *in vitro* replicase assay based on an active RdRp (Figure 2.7C, lanes 5-6 and not shown). In contrast, constructs A/gPR or A/gPR/SL2 did not produce complementary RNA products when mixed with construct B in the CFE replication assay (Figure 2.7B, lanes 9-16) and only construct B was copied in these two-component RNA systems. These data suggest that the RSE is an important determinant of template copying by the replicase and that, for *in vitro* replicase assembly in association with viral RNA, only an RNA carrying a complete RSE-gPR is used *in cis* by the replicase as a template for RNA synthesis.

The RII(+)-SL is needed for the assembly of the TBSV replicase in vitro.

RII(+)-SL has been designated as a template recruitment element [6, 71], However it is not known if this RNA element is also required for the subsequent replicase assembly step. To test this, I inactivated the recruitment function of RII(+)-SL [via a C-to-G mutation in the critical C•C mismatch, Figure 2.1A, [71]], but also introduced a heterologous "recruitment element", namely six RNA hairpins from bacteriophage MS2 that bind selectively to the coat protein (CP) of MS2 [30, 107] to obtain construct RII-G/C-M (Figure 2.8A). I also tagged the TBSV p92 protein with a monomer of MS2 CP [108], creating MS₂92 (Figure 2.8A) in order to promote binding of RII-G/C-M to the TBSV replicase via the heterologous MS2 CP domain (as depicted in Figure 2.8A). This arrangement was predicted to promote the viral RNA recruitment into replication by the binding of the MS2 hairpins in RII-G/C-M to the MS2-CP part of the p92 fusion protein, MS₂92.

In vitro assembly of the TBSV replicase with purified recombinant p33 and MS₂92 fusion protein (Figure 2.8C) in the CFE assay revealed that construct RII-G/C-M did not support replication (Figure 2.8B, lane 2.8). However, the *in vitro* RNA recruitment assay in CFE showed that wt p33 and the MS₂92 fusion protein did recruit RII-G/C-M RNA to the membrane ~ 3-fold more efficiently than did wt p33 and p92 (Figure 2.8D, cf. lane 9 with 8). Thus, I conclude that the heterologous MS2-CP hairpins work with p33/MS₂92 fusion proteins in template recruitment. Importantly, the insertion of the six MS2-CP hairpins did not hinder replication when inserted in wt DI-72 (i.e. construct WM, Figure 2.8A) (Figure 2.8B, lanes 2) and the hybrid MS₂92 was functional for replication (Figure 2.8B, lane 6).

I also performed a second test with a dual MS2-CP-tagged p33 [(MS₂)₂33] where the viral replication proteins were expressed in yeast [55] via co-expression of (MS₂)₂33 fusion protein and p92 only (in the absence of TBSV repRNA, Figure 2.9B). After preparing the CFE from the above yeast, various RNA templates were introduced and an *in vitro* replication assay was performed (Figure 2.9A). Although (MS₂)₂33 was expressed at a lower level than wt p33 in yeast (Figure 2.9B), the CFE containing (MS₂)₂33/p92 supported the replication of wt DI-72 (+)repRNA to similar levels as p33/p92 (Figure 2.9A, compare lanes 4 and 1). The same CFEs also allowed for replication of WM, albeit at reduced levels (Figure 2.9A, lanes 2 and 5), but did not support the replication of RII-G/C-M RNA (Figure 2.9A, lanes 3 and 6). The *in vitro* RNA recruitment experiments with CFE containing (MS₂)₂33/p92 revealed efficient recruitment of RII-G/C-M RNA to the membrane (Figure 2.9C, lanes 12), suggesting that this step was performed more efficiently by (MS₂)₂33/p92 with RII-G/C-M RNA than p33/p92 did with the wt DI-72 (+)repRNA (Figure 2.9C, lane 2). Based on these data, I conclude that replacing the recruitment function of RII(+)-SL with the heterologous MS2-CP hairpins is sufficient for RNA recruitment to the membrane, but not sufficient to promote the functional assembly of the TBSV replicase. Thus, RII(+)-SL may have an additional essential function during the assembly of the TBSV replicase complex.

DISCUSSION

The role of UL-DL in replication assembly.

The two critical *cis*-acting elements, RII(+)-SL and RSE-gPR, are located ~3 kb apart in the TBSV genomic RNA. However, a long-distance base-pairing interaction between UL-DL sequences brings RII(+)-SL and RSE-gPR into close proximity (Figure 2.2B) [84]. I found that UL-DL interaction is not necessary for the assembly of the TBSV replicase *in vitro*, but it boosts the assembly by ~10-fold (Figure 2.2). The UL-DL interaction is not needed when RII(+)-SL and RSE-gPR are located at nearby positions (see template “mini” lacking UL-DL, Figure 2.3), therefore, it represents a unconventional type of enhancer element for replicase assembly (EERA) that does not directly interact with proteins.

The two-component system confirmed the importance of the UL-DL interaction and revealed that RII(+)-SL and RSE-gPR could function when not covalently linked to each other. This suggests that there is no processive tracking of components along the RNA between RII(+)-SL and RSE-gPR during replicase assembly. Nonetheless, the base-pairing requirement between the two RNAs underscored the importance of proximity for these two elements. In addition to general proximity, their relative orientations and/or precise proximity also seem to be significant, as base pairing between sites that were not similar in relative location to the UL-DL interaction, did not lead to functional replicase assembly [Figure 2.6, A(5'-29)+B]. Thus, the UL-DL interaction acts indirectly to enhance the assembly process by optimally positioning RII(+)-SL and RSE-gPR relative to one another.

Dual role of RII(+)-SL during template recruitment and the assembly of the viral replicase.

Two of the most intriguing non-template roles of the viral (+)RNA are essential functions for template recruitment and assembly of the viral replicase complex [73, 75, 84]. These functions are mediated by distinct *cis*-acting elements in the viral (+)RNA. In tombusviruses, one of these elements is the internally located RII(+)-SL (Figure 2.1A), which binds to p33/p92 replication proteins via a C•C mismatch present in an internal loop [71, 72]. Template competition experiments using our CFE replication assay revealed that RII(+)-SL, and particularly the C•C mismatch, is required for the template to inhibit the replication of the full-length DI-72 repRNA *in vitro* (Figure 2.4). In contrast, other important regions of DI-72 (+)repRNA did not efficiently compete in the CFE-based replication assay, suggesting the lack of contribution by these sequences to viral RNA recruitment or direct binding to the viral replicase. These observations are consistent with the model that RII(+)-SL is an authentic RNA recruitment element that determines if a particular RNA is selected/recruited for replication by the tombusvirus replicase.

However, this result or previous data [71, 75, 84] have not precluded the possibility that, independent of template recruitment, RII(+)-SL also plays a role in the assembly of the replicase complex. These two activities are difficult to separate, since the assembly of the replicase depends on the prior RNA recruitment step. Consequently, in order to separate these two functions, I utilized a heterologous recruitment approach based on the specific MS2 CP-MS2 RNA hairpin interaction [30, 107, 108] using chimeric RNAs and fusion proteins. This alternative recruitment scheme was able to direct RNA templates to membranes, however no replicase assembly was observed (Figs. 2.8 and 2.9). This suggests that the RII(+)-SL-p33/p92 interaction mediated by the C•C mismatch is also critical for replicase assembly. Indeed it is possible that this interaction both tethers the template for protein-mediated transport to membranes and, at the same time, establishes the foundation from which a replicase complex can assemble. The requirement for this specific interaction may be related to allosteric effects on p33/p92 that are important for subsequent interactions and/or for precise positioning of these

viral factors relative to host factors, which facilitates complex formation. Indeed, such a strategy of coupling the RNA-protein interaction with template recruitment and replicase assembly would streamline these consecutive processes and potentially provide a fitness benefit to the virus by minimizing unnecessary steps.

Cis-replication of the RNA template by the tombusvirus replicase depends on the presence of RSE.

The novel two-component RNA system was used to confirm that the RSE-gPR *cis*-acting sequence is also absolutely necessary for the assembly of the viral replicase *in vitro* (Figs. 5-6). Surprisingly, however, this system also revealed that only one of the two RNAs is used as a template by the newly assembled/activated membrane-bound replicase. Analysis of various modified template pairs indicated that selection of an RNA for copying required the presence of the RSE element in that template and that neither the promoter for minus strand synthesis, gPR, nor a longer version of it, gPR+SL2, would suffice for this function (Figure 2.7). This finding is in contrast with the data obtained with the solubilized and purified tombusvirus replicase, which efficiently used RNAs carrying gPR or gPR+SL2 sequences at 3' terminal positions, but lacking RSE (Figure 2.7). Indeed, this solubilized replicase is not associated with viral RNA and thus is able to encounter promoter sequences in the template RNAs added to the reaction. Conversely, in *de novo* replicase assembly, our data indicates that the nascent replicase may assemble with the viral RNA in such a manner that positions its active site in proximity to the gPR, where minus-strand synthesis initiates. Our results also suggest that RSE, in cooperation with covalently linked gPR, would be integral for this to occur. This type of tight coupling could be limited to the pioneering round of minus-strand synthesis, as initial copying of the template would presumably dislodge any replicase/cofactor contacts involved in replicase assembly that were not involved in the RNA synthesis step. Nonetheless, this strategy would help to ensure that only templates capable of assembling functional replicase would be templates for replication. This and other *cis*-preferential replication strategies would be particularly beneficial at the early stage of infections initiated at low multiplicity of infection.

Summarizing template recruitment and replicase assembly.

Replication of a viral RNA requires the preceding processes of template recruitment and replicase assembly. In TBSV, RII(+)-SL interacts with p33/p92 which targets the RNA for replication by shuttling it to membranes (Figure 2.10). RII also likely directly contributes to replicase complex assembly in a manner that is, at least partially, linked to its p33/p92 binding activity. RSE-pPR forms part of the replicase assembly platform (Figure 2.10) and binds to eEF1A, which is a component of the replicase complex [18, 76]. RSE-gPR also specifies the template for minus-strand synthesis and harbors the core promoter for initiation, gPR. UL-DL plays an indirect role in replicase assembly by bringing RII(+)-SL and RSE-gPR into proximity in the proper orientation. Collectively, this diverse group of core RNA elements function jointly to mediate efficient replicase complex assembly.

MATERIALS AND METHODS

Yeast and Bacterial strains.

Saccharomyces cerevisiae strains BY4741 α (*MATa his3 Δ 1 leu2 Δ 0 met15 Δ 0 ura3 Δ 0*) was obtained from Open Biosystems (Huntsville, AL, USA). *Escherichia coli* Top10 (Invitrogen, Carlsbad CA, USA) and Epicurion BL21-codon-plus (DE3)-RIL cells (Stratagene, La Holla, CA, USA) were used to propagate plasmids and for expression of recombinant proteins, respectively. *E. coli* strain Stb12 (Invitrogen, Carlsbad CA, USA) was used for maximizing the stability of the plasmids containing direct repeats [such as (MS2)₂p33]. Also, I changed the typical growing temperature from 37°C to 30°C when using Stb12.

E. coli expression plasmids.

pMAL-33 and pMAL92 were described earlier [28]. pET-His-MBP-p33, expressing p33 with dual tags 6xHis/MBP, was also obtained earlier [73]. pMAL-MS₂33, containing TBSV p33 fused in-frame with bacteriophage MS2 coat protein (MS2-CP), was obtained by PCR amplification of MS2-CP open reading frame (ORF) from pGBK-MS2-CFP [30] using primers #1576 (5'-GGAGTCTAGAGCTTCTAACTTTACTCAG) and #3269 (5'-CCGCCATGGGTAGATGCCGGAGTTTGC) appended with *Xba*I and *Nco*I restriction sites. While TBSV p33 ORF was amplified from pMAL92 using primers #3313 (5'-CGGACCATGGGAGACCATCAAGAGAATG) and #2744 (5'-CGGCTGCAGCTATTTGACACCCAGGGAC) appended with *Nco*I and *Pst*I respectively. To get the desired clone, after gel-isolation of the restriction enzymes digested PCR products, I ligated the PCR products into pMAL-c2X digested with *Xba*I and *Pst*I.

To obtain pMAL-MS₂92, the TBSV p92 ORF was fused in-frame in fusion with MS2-CP ORF, which was PCR-amplified from pGBK-MS2-CFP [30] using primers #1576 and #3269 appended with *Xba*I and *Nco*I restriction sites. The TBSV p92 ORF was PCR-amplified from pMAL92 using primers #3313 and #3529 (5'-CCAGCTGCAGTCAAGCTACGGCGGAGTCGAGG) appended with *Nco*I and *Pst*I respectively. After gel-isolation of the restriction enzymes digested PCR products, I ligated the PCR products into pMAL-c2X digested with *Xba*I and *Pst*I.

Yeast expression plasmids.

pGBK-His33 and pGAD-His92, expressing only 6xHis-tagged p33 and p92, respectively, from the *ADHI* promoter and pYC-DI72 were described previously [13]. pGBK-Cup-(MS₂)₂-33 was obtained by fusing the CNV p33 ORF in-frame with two copies of bacteriophage MS2-CP [(MS₂)₂ representing directrepeats of MS2-CP ORF linked with a short linker (GAPGIHPGM) and also containing an internal polyHis-tag]. The sequence of (MS₂)₂ was amplified from p(MS₂)₂PCBP2 [108] using primers #4194 (5'-CGGACCATGGCGGATATCGAAGGTCCCACC) and #4196 (5'-CCAGCCATGGGTTCGTTTGGGTGATGGTGATGGTGGTGGCTGCCGCGTGG) appended with *Nco*I restriction site and cloned into *Nco*I digested and dephosphorylated vector pGBK-His33/Cup1 [67]. Similarly, pGAD-Cup-(MS₂)₂-92 was obtained by fusing the CNV p92 ORF in-frame with (MS₂)₂ using primers #4194 and #4196 appended with *Nco*I restriction site and cloned into *Nco*I digested and dephosphorylated vector pGAD-His92-Cup1 [70].

pYC-DI(C:G)6XMS₂(+) was generated by PCR-amplifying Region I and II of DI-72(+) from pYC-DI(C₉₉:G) [71] using primers #542 and 1565 [88]. The PCR product was digested with *Hind*III and *Bam*HI and used to replace the corresponding region in pYC-DI72(+)/MS₂ [30] treated with the same pair of enzymes. To create pYC-DI(C:G)-6XMS₂(-), similar strategy was used based on the vector pYC-DI72(-)/MS₂ [30].

RNA template production and annealing.

Single-stranded (ss)RNA templates were obtained by *in vitro* transcription with T7 RNA polymerase using PCR amplified DNA templates [88, 109]. The reaction mixture was incubated at 37°C for 2 hours. 2 µl of DNaseI (10 U/ml from Roche) was added, and incubated for ~20 min at 37°C. After phenol-chloroform extraction, RNA was precipitated twice with isopropanol-ammonium acetate (10:1). To synthesize radioactively labeled RNA similar T7 reaction was performed, except for using 5 µl of 10 mM rATP, rGTP rCTP and 1mM of rUTP supplemented with 0.1 µl of [³²P]UTP. RNA annealing was done with RNA samples mixed in equimolar ratio (20 pmols each) in 20 µl buffer containing 50 mM NaCl, 10 mM Tris-Cl and 1 mM EDTA. The samples were incubated in a thermocycler at 95°C for 5 min and then cooled to 25°C by reducing the annealing temperature by 1°C per minute.

In vitro replication assay based on yeast CFE.

The cell-free extract was prepared from yeast strain BY4741, untransformed or transformed with pair-wise combinations of pGBK-His33/Cup1; pGAD-His92-Cup1; pGBK-Cup1-(MS2)₂-33; and pGAD-Cup1-(MS2)₂-92 (see Figure 2.9) as described [55, 73]. Briefly, the CFE (1 μ l) was pre-incubated on ice for 10 min in 10 μ l cell-free replication buffer containing 50 mM HEPES-KOH, pH 7.4, 150 mM potassium acetate, 5 mM magnesium acetate, 0.2 M sorbitol, and 0.4 μ l actinomycin D (5 mg/ml). Then, the reaction volume was adjusted to 20 μ l with 1x cell-free replication buffer also containing 2 μ l of 150 mM creatine phosphate; 2 μ l of 10 mM ATP, CTP, and GTP and 0.25 mM UTP; 0.3 μ l of [³²P]UTP, 0.2 μ l of 10-mg/ml creatine kinase, 0.2 μ l of RNase inhibitor, 0.2 μ l of 1 M dithiothreitol, and 0.5 μ g RNA transcript. The reaction mixture also contained 4 pmol MBP tagged TBSV p33 and 1 pmol MBP-p92 purified from *E. coli* cells. This reaction mixture was incubated at 25°C for 3 h. The reaction was terminated by adding 110 μ l stop buffer (1% sodium dodecyl sulfate [SDS] and 0.05 M EDTA, pH 8.0), followed by phenol-chloroform extraction, isopropanol-ammonium acetate precipitation, and a washing step with 70% ethanol as described earlier. The RNA samples were electrophoresed under denaturing conditions (5% PAGE containing 8 M urea) and analyzed by phospho-imaging using a Typhoon (GE) instrument as described [75].

Micrococcal nuclease protection assay.

The CFE-based *in vitro* replication assay was conducted as described above. Micrococcal nuclease digestion of the samples was performed at 25°C for 15 min using 0.04 U/ml, final concentration, and 1 mM CaCl₂ at various time points as described [55, 73]. To terminate the action of micrococcal nuclease, I added EGTA (2.5 mM, final concentration), followed by further incubation of the cell-free replicase assay mixture at 25°C for 2.5 hrs. In the control assay, only CaCl₂ and EGTA were added to the reaction mixture in the absence of the nuclease.

Purification of the recombinant tombusvirus replicase from yeast.

Yeast cells transformed with pGBK-His33, pGAD-His92 and pYC-DI72 were pre-grown in SC-ULH⁺ medium containing 2% glucose for 15 h at 29 °C with shaking at 250 rpm. The affinity-purification of the solubilized tombusvirus replicase was performed using ProBond resin (Invitrogen) as described [82]. The obtained template-dependent replicase was then used in a standard replicase reaction using either DI-72(-) or RI/RIII(-) exogenous templates and [³²P]UTP [75, 82].

In vitro assembly and purification of the TBSV replicase.

The cell free replication assay was conducted at 20°C for 1 h as described above except for following changes: The reaction volume was increased to 200 μ l, while the final concentration of DTT was reduced from 10 mM to 2.5 mM. In addition, only rATP and rGTP were used, while [³²P]UTP was omitted. The recombinant p33 was dually tagged with both MBP and 6xHis. After incubation, the assay mixture was diluted with 800 μ l chilled solubilization buffer and affinity-purification was done exactly as described [75, 82].

Protein purification from E. coli.

The MBP-tagged p33, p92, MS₂33, MS₂92 and *Turnip crinkle virus* p88C were purified from *E. coli* as described previously [28, 110]. Briefly, expression of the MBP tagged proteins was induced by isopropyl-d-thiogalactopyranoside (IPTG) in Epicurion BL21-codon-plus (DE3)-RIL cells (Stratagene). Cells were suspended in the column buffer (10 mM Tris-HCl [pH 7.4], 1 mM EDTA, 25 mM NaCl, 10 mM β -mercaptoethanol) and were broken by sonication, and then the cell lysate was passed through the equilibrated amylose columns to bind MBP tagged

proteins. After passing the cell lysate, the columns were washed three times with ice-cold column buffer and eluted with column buffer containing 10 mM maltose and stored at -80°C until further use.

In vitro RNA recruitment assay.

The recruitment assay was performed as described [76]. Briefly, recruitment assay based on yeast CFE and recombinant p33/p92 is similar to the replication assay, except for the following changes: [³²P]-labeled RNAs (2 pmol) were added to the CFE. In addition, only rATP and rGTP were used, while [³²P]UTP was omitted. The assay was performed at room temperature for 1 h. Then, the mixture was suspended in 980 µl of pre-chilled Buffer A and centrifuged at 35,000g for 30 min at 4°C. Supernatant was discarded and the washing of the membrane pellet was repeated twice. After final washing, the pellet was dissolved in 120 µl of stop buffer (1% sodium dodecyl sulfate [SDS] and 0.05 M EDTA, pH 8.0). Afterwards standard RNA extraction and purification was performed followed by autoradiography of the electrophoresed RNA samples as described [75].

In vitro RdRp reaction.

Affinity-purified recombinant TCV p88C or affinity-purified CNV replicase from yeast in an RdRp assay were used as described [82, 110]. Briefly, the RdRp reaction was performed in 100 µl volume containing RdRp buffer [40 mM Tris pH 8.0, 10 mM MgCl₂, 10 mM DTT, 0.2µl RNase inhibitor, 1 mM ATP, CTP, GTP, 0.1 µl radioactive [³²P]UTP and 50 µl RdRp fraction. As an external template, 300 ng of DI-72(-) RNA or RI/III(-) RNA were added. Samples were incubated at 25 °C for 2 h. The reaction was terminated by adding 70 µl SDS/EDTA (1% SDS, 50 mM EDTA pH 8.0) and 100 µl phenol-chloroform (1:1). The analysis of RdRp products was as described [82, 110].

S1 nuclease digestion of the RdRp products.

The RNA products from the *in vitro* RdRp assays were purified and divided into two aliquots of 8 µl each. S1 digestion was performed with one aliquot in a 20 µl reaction containing 0.1 µl S1 nuclease (400U/µl from Boehringer), 1X S1 nuclease buffer and 2.5 µl 3M NaCl. The other aliquot was treated similarly, except without S1 nuclease. After incubation at 37°C for 30 min, standard RNA analysis was performed [82, 110].

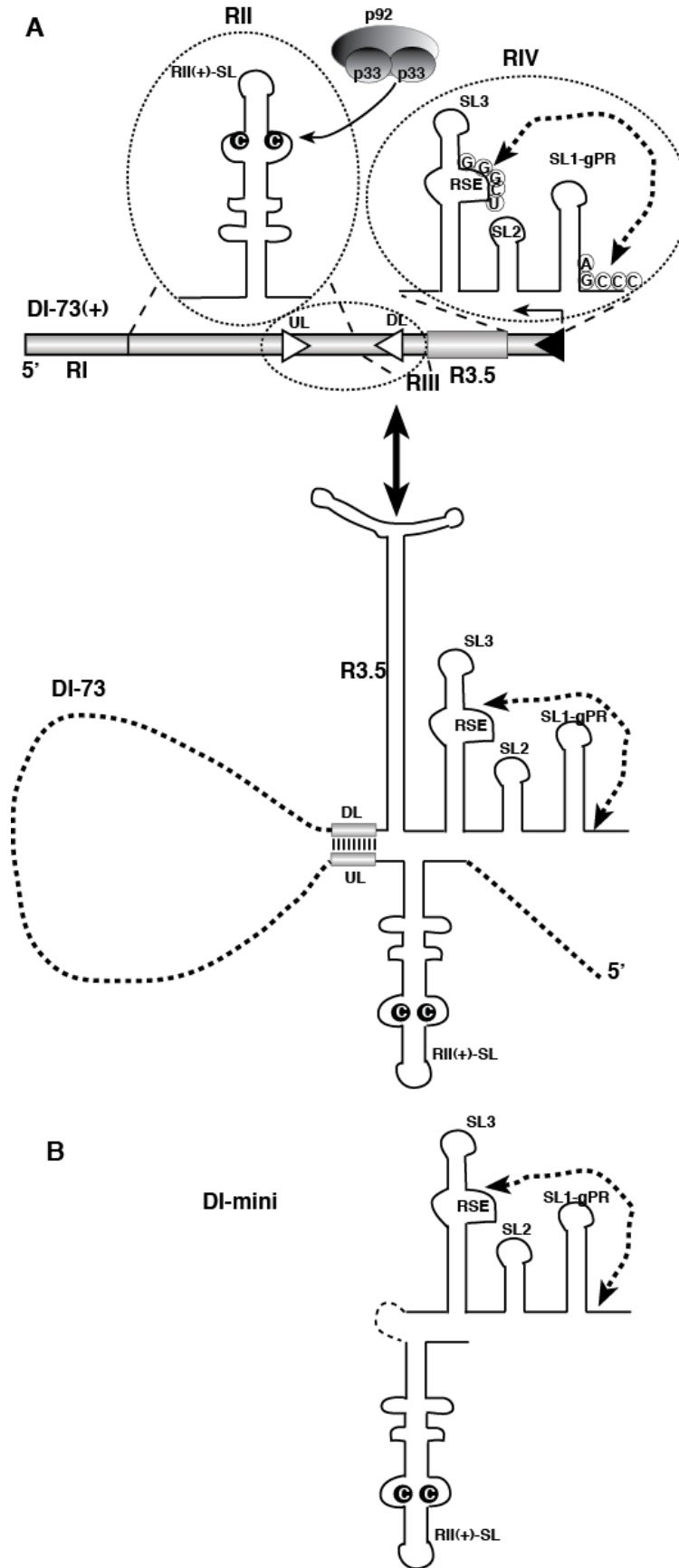


Figure 2.1 Schematic representation of TBSV DI-73 (+)repRNA and its derivatives carrying the three known *cis*-acting replication elements.

(A) Top: The three *cis*-acting sequences are circled. The characteristic C•C mismatch, which is critical to bind to p33/p92 replication proteins, within the RII(+)-SL is highlighted. The complementary nucleotides in the replication silencer element (RSE) and the genomic promoter (gPR) that form a 5 bp-long region are depicted with an arrow. Note that R3.5 serves as a translation enhancer, which is missing from DI-72 repRNA. Bottom: A long-range interaction between UL-DL elements brings RII(+)-SL and RSE/gPR into proximal positions as shown. (C) Predicted secondary structure of mini RNA used as a model template for testing the assembly of the TBSV replicase complex *in vitro* in yeast CFE. Note that the UL-DL interaction and other portions of DI-73 repRNA are replaced by a short sequence from RIV(+).

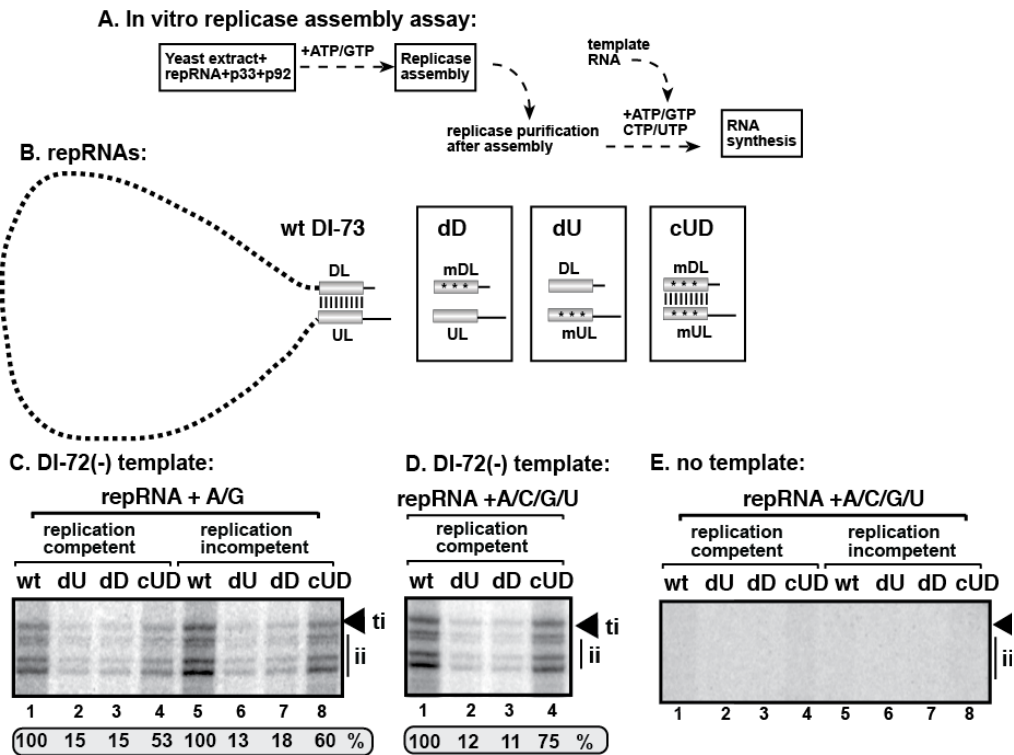
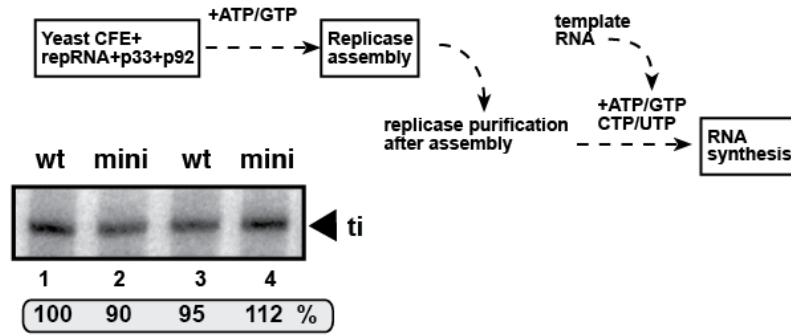


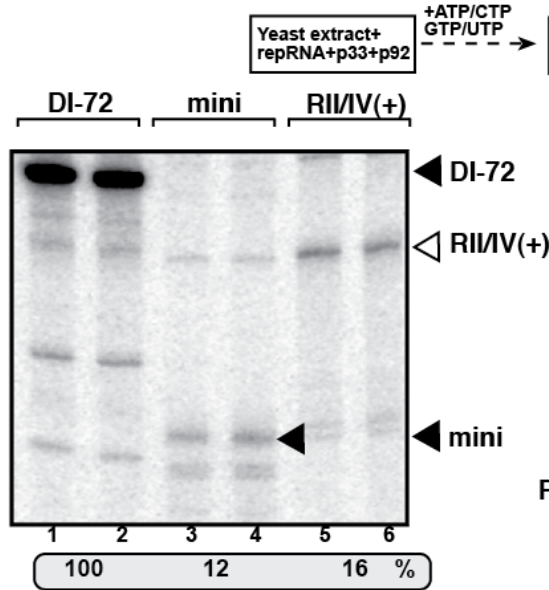
Figure 2.2. UL-DL *cis*-acting element functions as an enhancer element for the replicase assembly (EERA).

(A) The scheme of the *in vitro* TBSV replicase assembly assay performed with yeast CFE. Note that the recombinant p33 and p92^{pol} are purified from *E. coli*, while the CFE was prepared from BY4741. After 1-hour reconstitution, the membrane-bound replicase was solubilized with Triton X-100/SB3-10 detergent, followed by purification on Ni-column of the 6xHis/MBP-tagged p33, which is integral part of the replicase complex. The activity of the affinity-purified TBSV replicase was tested on DI-72(-) RNA added to each sample using the same amount of RNA. (B) Mutations within UL-DL, which interfere with base-pairing, or reform base-pairing due to complementary mutagenesis, are shown. (C-D) Representative denaturing gels of ³²P-labeled RNA products synthesized by affinity-purified TBSV replicase preparations obtained in TBSV replicase assembly assays *in vitro* with yeast CFE in the presence of all four or two rNTPs. The replicase assembly assay contained the wt DI-73 (+)repRNA or mutated versions within UL-DL region as shown in panel A. The replication competent RNA was DI-73-based, while the replication-incompetent carried a debilitating mutation in RI in DI-73 repRNA. The template RNA was DI-72(-)repRNA, which produces both full-length (terminal initiation [ti]) and shorter (due to internal initiation [ii]) complementary products in the *in vitro* assay with the purified TBSV replicase. The level of full-length RNA synthesis was compared to that of the replicase activity obtained with DI-73 (+)repRNA (100%). (E) No RNA template was added into the *in vitro* assays with the purified TBSV replicase preparations, while the shown repRNAs were used during the TBSV replicase assembly assays *in vitro* with yeast CFE prior to affinity-purification of the TBSV replicase.

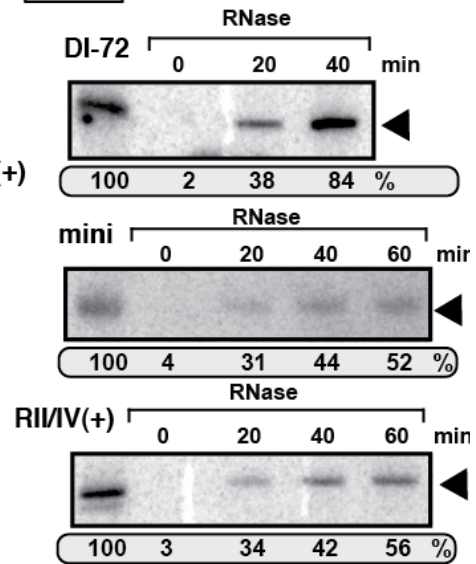
A. In vitro replicase assembly assay:



B. In vitro replication in CFE



C. In vitro replication in CFE



D. In vitro replicase assay:

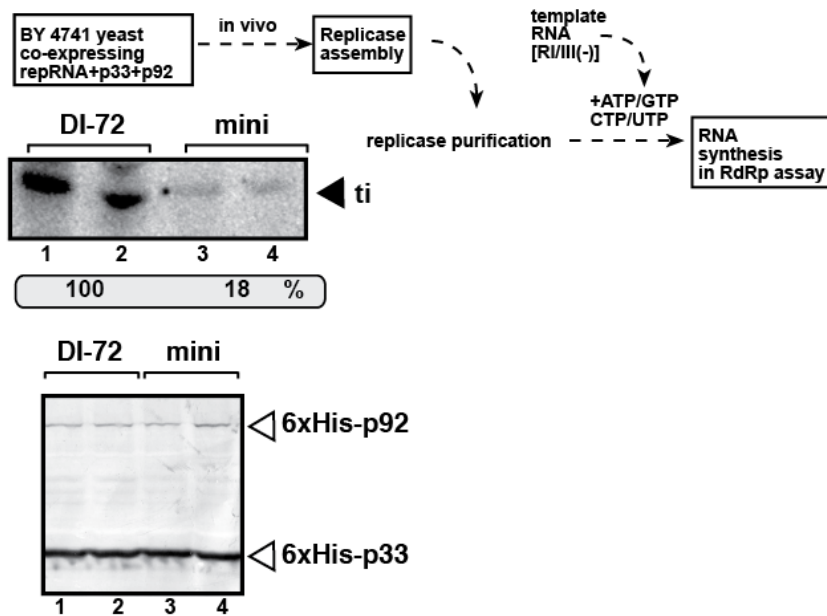


Figure 2.3. A mini template with RII(+)-SL and RSE-gPR can efficiently support the *in vitro* assembly of the TBSV replicase.

(A) Denaturing PAGE analysis of the *in vitro* reconstituted TBSV replicase in the presence of repRNAs. The replicase reconstitution assay contained CFE, affinity purified recombinant TBSV p33 and p92^{pol}, ATP/GTP and the same amount of TBSV repRNAs. After assembly and affinity-purification, the activity of the replicase preparations was tested on DI-72(-)RNA template *in vitro*. See further details in Figure 2. (B) Denaturing PAGE analysis of the CFE-based replication assay. The *in vitro* replication assay contained yeast CFE, affinity purified recombinant TBSV p33 and p92^{pol}, and 4 pmol of various TBSV repRNAs (as shown in Figure 1). The full-length products are depicted with arrowheads on the right. Note that the repRNA serves both as an assembly factor and a template in this assay. (C) The *in vitro* assembled TBSV replicase with DI-72(+) forms a structure more ribonuclease-resistant than with mini or RII/IV(+) repRNAs in the CFE. The *in vitro* replicase assay in CFE was done using one of the shown RNAs. Note that I applied a 15-min treatment with ribonuclease (micrococcal nuclease) at the 0, 20, 40 or 60 min time points for 15 minutes, followed by inactivation of the nuclease and continuation of the *in vitro* replicase assay up to 2 hours. The denaturing PAGE analysis of the ³²P-labeled repRNA products obtained is shown. (D) Denaturing PAGE analysis of the *in vitro* replicase assay. The assay contained the purified replicase from yeast co-expressing p33 and p92^{pol}, and the (+)repRNAs (as shown). The activity of the affinity-purified TBSV replicase was tested on RI/RIII(-) RNA added to each sample using the same amount of RNA. Note that the assembly of the replicase took place in yeast cells in the presence of co-expressed p33/p92 and actively replicating repRNA. The bottom image shows a Western blot demonstrating equivalent amount of p33/p92 replication proteins in the purified tombusvirus replicase preparations used for the *in vitro* assay.

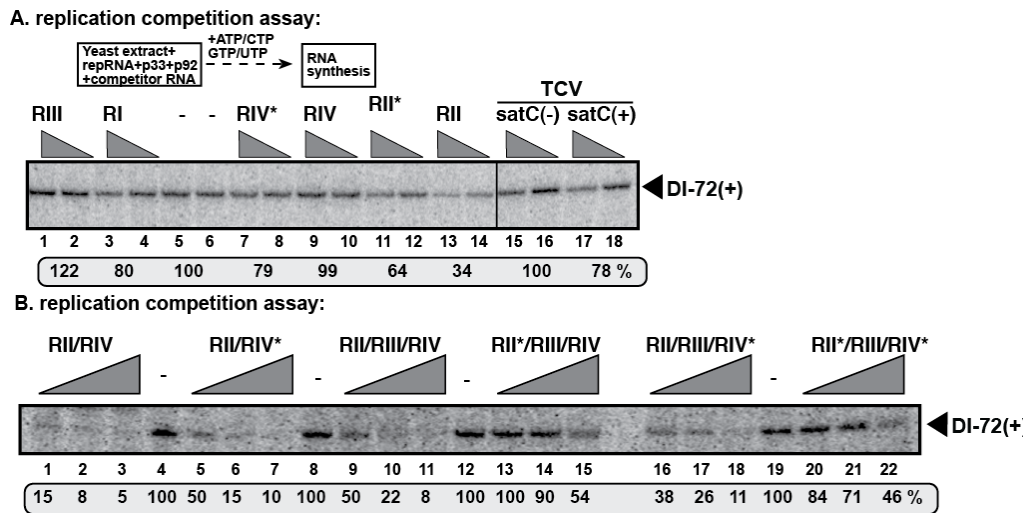
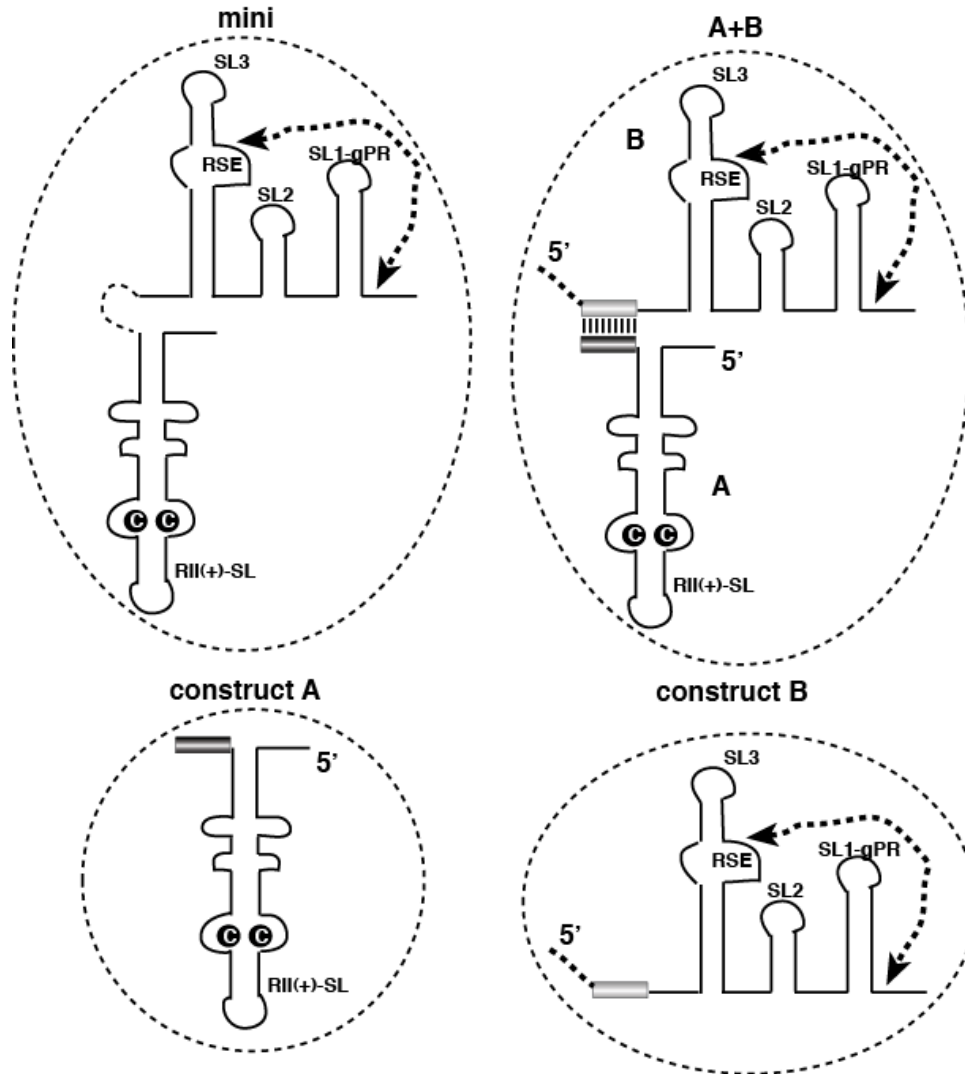


Figure 2.4. RII(+) RNA inhibits the *in vitro* assembly of the TBSV replicase.

(A) Denaturing PAGE analysis of the CFE-based replication assay. The *in vitro* replicase reconstitution assay contained yeast CFE, affinity purified recombinant TBSV p33 and p92^{pol}, and the same amount of TBSV DI-72 (+)repRNA plus increasing amounts of competitor TBSV-derived RNA templates (RI, RII, RIII and RIV are shown in Figure 2.1) or the TCV associated satC templates. The samples contained 0, 2 and 8 mg of competitor RNA and each had 0.4 mg of DI-72(+) RNA template. The full-length DI-72-derived RNA products are depicted with arrowheads on the right. Note that the repRNA serves both as an assembly factor and a template in this assay, while the competitor RNA cannot assemble a functional replicase, but it can interfere with the replicase assembly process. The level of DI-72 repRNA replication in the “no competitor” samples was chosen as 100%. (B) Another template competition in CFE-based replication assay. The competitor RNA contains the wt regions (RII, RIII or RIV), a mutated RII (marked with an asterisk, and represents a C-to-G mutation in C•C mismatch, Figure 2.1A) or a mutated RIV (marked with an asterisk, and represents a G-to-C mutation in gPR, Figure 2.1A). These mutations are known to interfere with the *cis*-acting replication functions of these regions. See further details in panel A. The samples contained 0, 3 and 9 mg of competitor RNA and each had 0.4 mg of DI-72(+) RNA template.

A. RNA constructs:



B. In vitro replicase assembly assay:

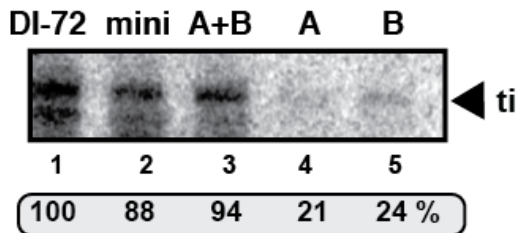
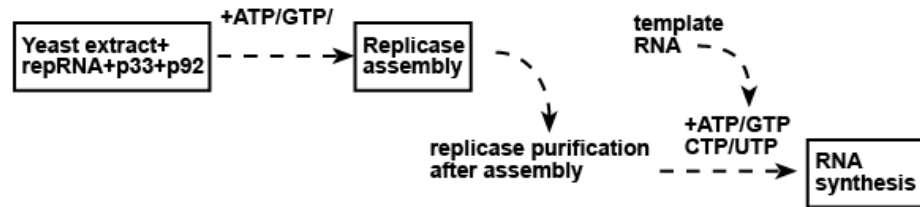
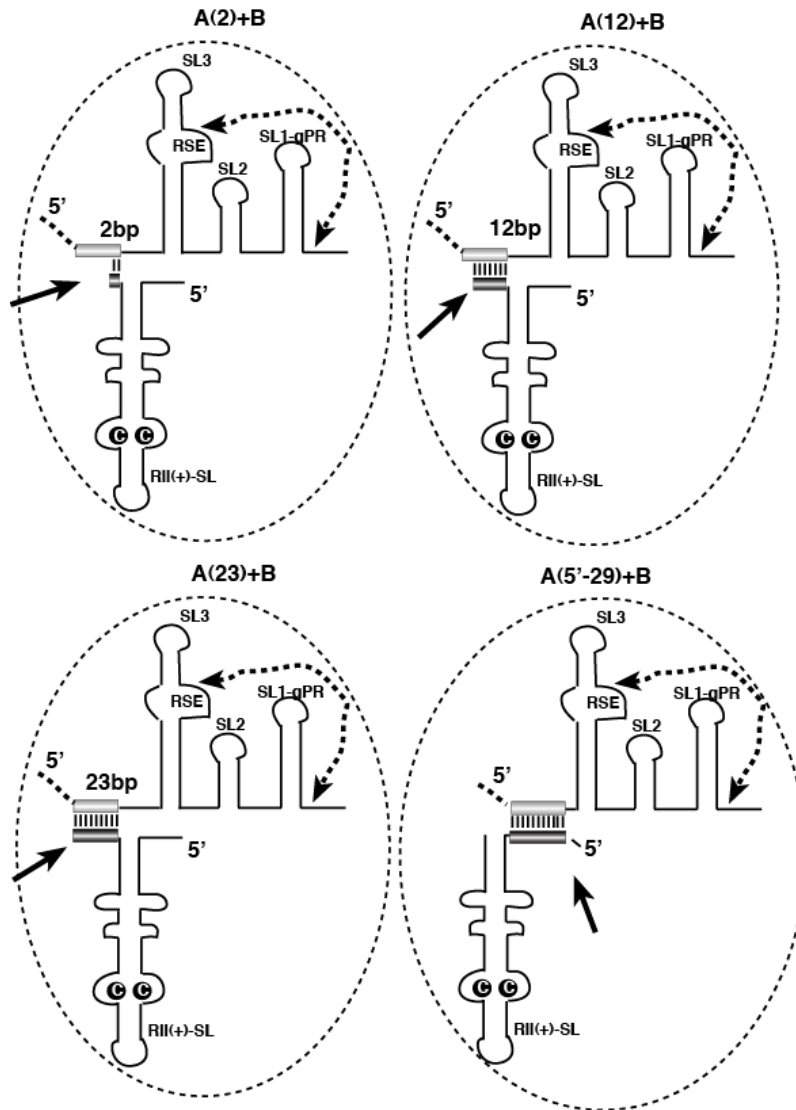


Figure 2.5. An efficient two-component RNA-based TBSV replicase assay.

(A) Schematic representation of the RNA constructs used in the replicase assembly assay. Construct A contains functional RII(+)-SL, while construct B carries RSE-gPR element. Note that constructs A and B can form a 23 bp heteroduplex that holds the two RNAs together as shown for “A+B”. (B) Denaturing PAGE analysis of the CFE-based replication assay. The *in vitro* reconstitution assay contained yeast CFE, affinity purified recombinant TBSV p33 and p92^{pol}, and the same amount of various TBSV repRNA templates (as shown). After the *in vitro* reconstitution, the activity of the purified replicase preparations was tested using RI/RIII(-) template. The full-length RNA product is depicted with an arrowhead on the right. Note that the repRNAs (panel A) serve only as assembly factors in this assay.

A. RNA constructs:



B. In vitro replication assay in CFE:

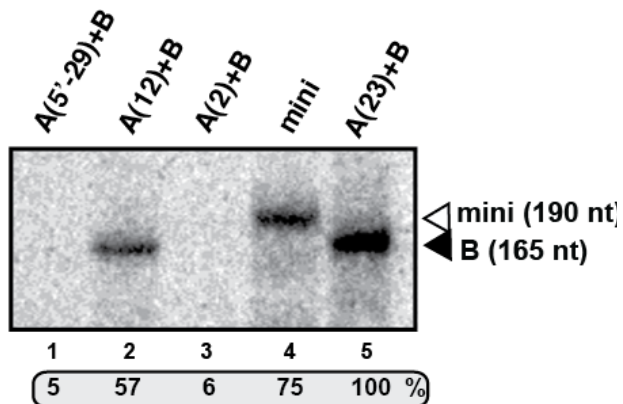
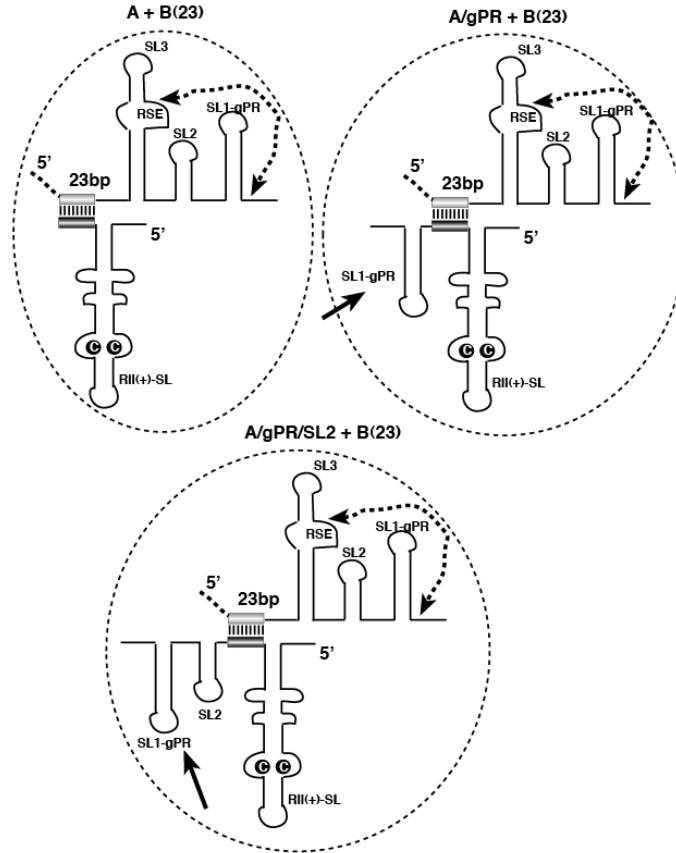


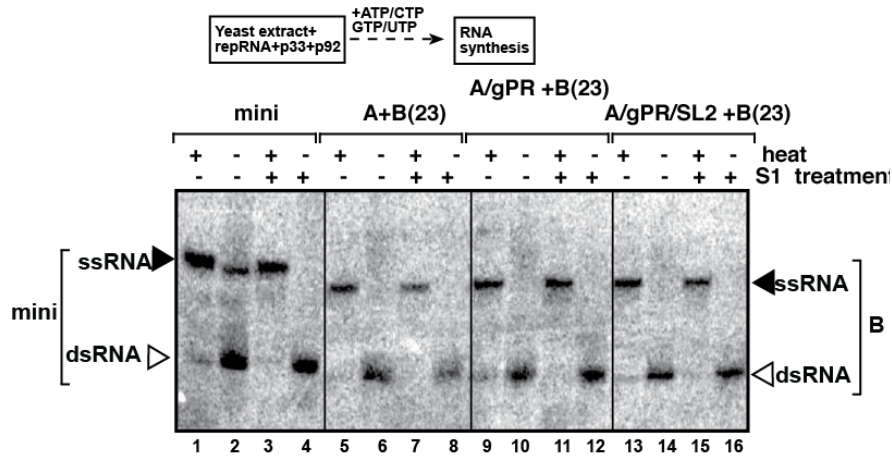
Figure 2.6. RII(+)-SL and RSE-gPR sequences must be located in close vicinity during the assembly of the TBSV replicase.

(A) Schematic representation of the two-component RNA constructs used in the replicase assay. See further details in Figure 2.5A. (B) Denaturing PAGE analysis of the CFE-based replication assay. The *in vitro* reconstitution assay contained yeast CFE, affinity purified recombinant TBSV p33 and p92^{pol}, and the same amount of various TBSV repRNA templates (as shown). Note that the repRNAs (panel A) serve both as assembly factors and templates in this assay. The full-length RNA products are depicted with arrowheads on the right.

A. RNA constructs:



B. In vitro replication assay in CFE:



C. In vitro RdRp assay:

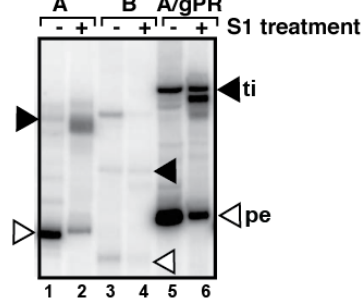
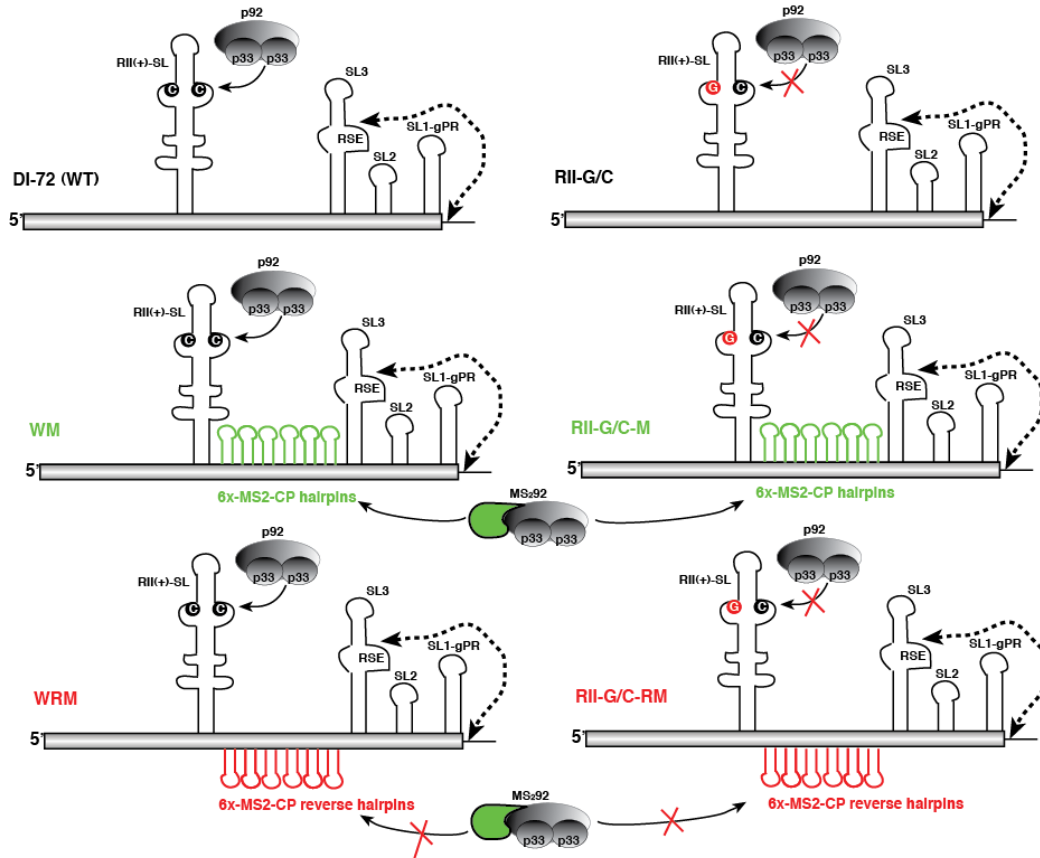


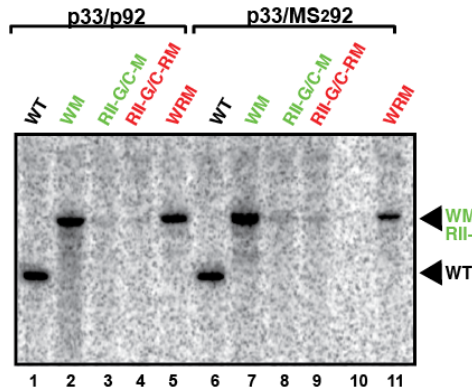
Figure 2.7. cis-replication of the template RNA carrying RSE-gPR *in vitro*.

(A) Schematic representation of the two-component RNA constructs used in the replicase assay. See further details in Figure 2.5A. (B) Non-denaturing PAGE analysis of the CFE-based replication assay. The *in vitro* reconstitution assay contained yeast CFE, affinity purified recombinant TBSV p33 and p92^{pol}, and the same amount of various TBSV repRNA templates (as shown). Note that the repRNAs (panel A) serve both as assembly factors and templates in this assay. The full-length ssRNA and dsRNA products are depicted with arrowheads on the right. Note that only construct B carrying RSE-gPR can produce complementary (-)RNA product *in vitro*, since ssRNA is only visible after denaturation of dsRNA product. (C) Representative denaturing gel of ³²P-labeled RNA products synthesized by TCV p88C RdRp *in vitro* in the presence of 1 mg of RNA transcripts as shown. The *de novo*-initiated terminal products are marked with arrowheads (“ti”). The samples were treated with S1 nuclease to show the 3'-terminal extension products (shown as “pe”), which change migration after treatment [110]. Each experiment was repeated three times.

A. RNA constructs:



B. In vitro replication assay:



D. In vitro RNA recruitment assay:

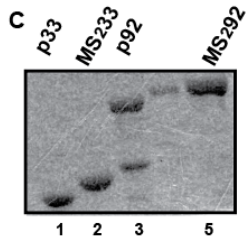
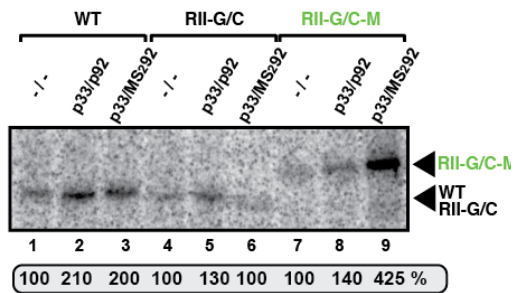


Figure 2.8. RII(+)-SL is required for the *in vitro* assembly of the TBSV replicase.

(A) Schematic representation of the RNA constructs used in the *in vitro* replication assay. Constructs WM and RII-G/C-M contain 6 copies of the MS2-CP hairpin (green), which can specifically bind to MS2 CP. p92 was fused to MS2 CP (green) as indicated. Constructs WRM and RII-G/C-RM contain 6 copies of the complementary MS2-CP hairpin sequence (red), which cannot bind to MS2 CP. The predicted binding of the RNA constructs to p33/p92 or the MS2-CP fusion proteins is shown with black arrows (positive binding) or crossed with red (no binding). (B) Denaturing PAGE analysis of the CFE-based replication assay. The *in vitro* replication assay contained yeast CFE, affinity purified recombinant TBSV p33 and p92^{pol}, or the MS2 CP fusion p92 protein and the same amount of various TBSV repRNA templates (as shown). The full-length products are depicted with arrowheads on the right. Note that the repRNAs serve both as assembly factors and templates in this assay. (C) SDS-PAGE analysis of the affinity-purified recombinant proteins. (D) Denaturing PAGE analysis of the *in vitro* RNA recruitment assay. The assay contained CFE, affinity purified recombinant TBSV p33 and p92^{pol} or the MS2 CP fusion p92 protein, and the same amount of ³²P-labeled TBSV repRNA templates. After the recruitment assay, the membrane-associated P³²-labeled repRNAs were quantified.

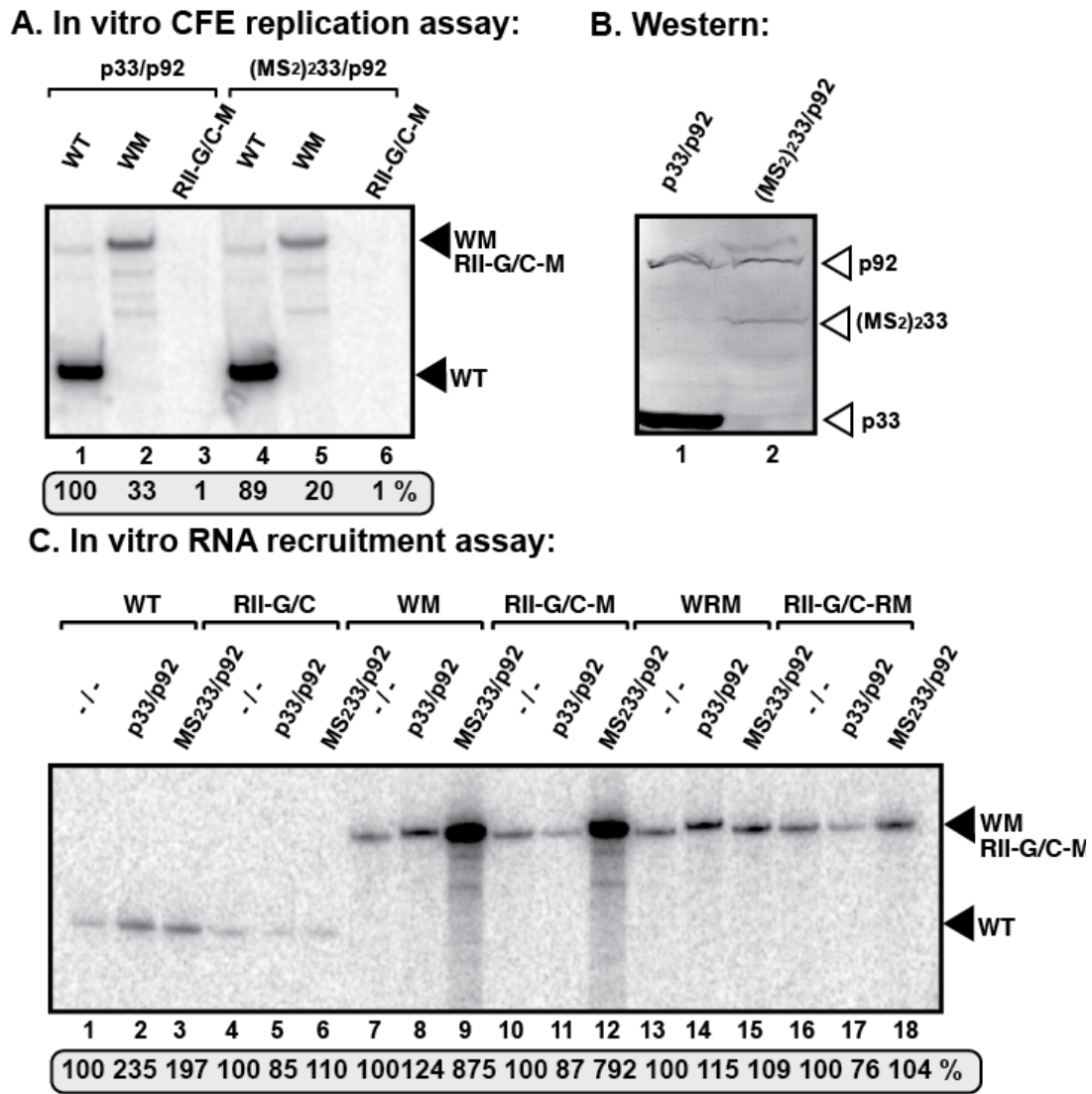


Figure 2.9. RNA templates containing the MS2 CP hairpins are efficiently recruited, but they are replication incompatible *in vitro*.

(A) Denaturing PAGE analysis of the CFE-based replication assay. The *in vitro* replication assay contained CFE prepared from yeast co-expressing p33 and p92 or (MS₂)₂33 fusion protein (containing the dimeric CP of MS2) and p92, and the same amount of various TBSV repRNA templates (as shown). The full-length products are depicted with arrowheads on the right. Note that the repRNAs serve both as assembly factors and templates in this assay. (B) Western blot analysis of p33, p92 and (MS₂)₂33 fusion proteins in yeast CFE. (C) Denaturing PAGE analysis of the *in vitro* RNA recruitment assay. The assay contained CFE (as in panel A), and the same amount of P³²-labeled TBSV repRNA templates. After the recruitment assay, the membrane-associated P³²-labeled repRNAs were quantified.

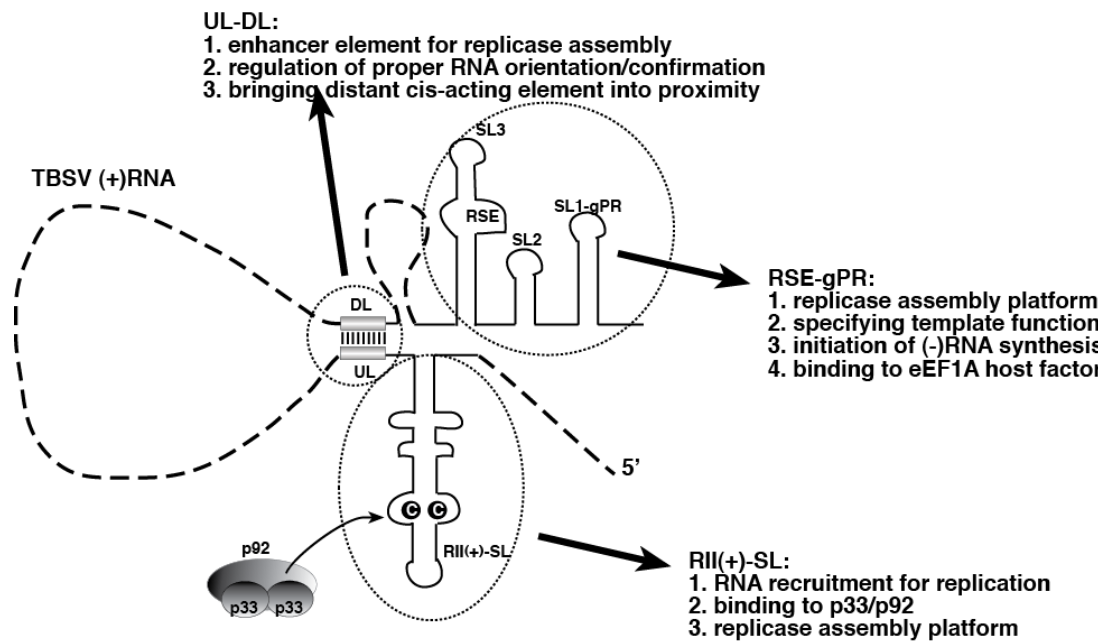


Figure 2.10. The known functions of the cis-acting replication elements in TBSV (+)RNA.

Since RII(+)-SL could not be replaced by a heterologous RNA recruitment element, I propose that RII(+)-SL is not only needed for RNA recruitment into replication, but it is also required for the assembly of the replicase complex. The RSE-gPR element is required for the assembly of the replicase and also determination of the template for the replicase, since only those RNAs, which carry the RSE element, are used as templates by the TBSV replicase. I propose that the role of UL-DL is not only to bring the RII(+)-SL and RSE-gPR elements into close proximity, but to assure their proper orientation needed during the replicase assembly.

Chapter 3. The host Pex19p plays a role in peroxisomal localization of tombusvirus replication proteins.

This chapter is published in *Virology*, 2008, 379(2):294-305.

INTRODUCTION

Similar to animal viruses, plant viruses containing RNA genomes of plus-strand polarity replicate on the cytosolic surfaces of intracellular membranes. For different viruses, these membranes include different organelles, such as endoplasmic reticulum, mitochondria, chloroplast, peroxisomes, vacuoles or unique subcellular membranes induced specifically by viral infections [6, 111-114]. Why different viruses choose different subcellular membranes for their replication and how the viral replication proteins are targeted to those membranes are currently under intensive investigations. Once the replication proteins and the viral RNA are delivered to the precise membrane locations, then they form, likely with the help of yet unidentified host proteins, membrane invaginations (called spherules) that contain narrow openings facing toward the cytosol [115]. These spherules contain the viral replicase complex and are the places for viral RNA synthesis [78, 115, 116].

Targeting of the viral replication proteins to the particular membrane location is likely driven by host transport proteins that might recognize specific targeting signals within the viral replication proteins. In spite of intensive studies, I know only a few cases, where host proteins are implicated in intracellular transport of the viral replication proteins. For example, the 126K replication protein of *Tobacco mosaic virus* (TMV) is bound to TOM1 and TOM2 transmembrane proteins, which might anchor the TMV replication protein to the membrane [117]. Also, the transport of BMV replication proteins and the BMV (+)RNAs within the host cells is affected by the Lsm1-7p/Pat1p/Dhh1p complex [118]. This complex has been suggested to facilitate the pre-assembly of the BMV replicase complex in the P-bodies, prior to the transportation of the viral replication proteins and RNAs to the ER, the site of replication [118].

There are some viruses other than tombusviruses that utilize peroxisomes at some stage of their multiplication cycle albeit not replication per se (reviewed by [119]). E.g. Rotavirus' spike protein VP4 is targeted to peroxisomes and may utilize lipid metabolic machinery [120]. Nef protein of *Human immuno deficiency virus* (HIV) interacts physically and functionally with a peroxisomal thioesterase that also might get some help in the fatty acid modification of proteins [121]. Moreover, NS1 of influenza viruses interacts with a multifunctional peroxisomal enzyme 17 β -HSD4/MFP-2 [122]. Exact relevance of this interaction for virus or the host is not clear presently.

Interaction of the NS5A and NS5B replication proteins of *hepatitis C virus* (HCV) with intracellular membranes is affected by hVAP-A SNARE-like protein. The proposed function of hVAP-A is to serve as a membrane receptor and to anchor the replication proteins to the intracellular membrane [123]. Moreover, FBL2, a geranylgeranylated cellular protein might be involved in recruitment of HCV NS5A to intracellular membranes [124]. Overall, none of the above cellular proteins fit the definition of a traditional transporter protein, which is expected to be released and recycled from the membrane after delivering the cargo viral proteins/viral RNA.

Among the (+)RNA viruses of plants, tombusviruses have emerged as highly suitable model viruses for studying basic questions in viral RNA replication and recombination, including the role of the host [6, 68]. The genomic (+)RNA of TBSV and the closely related *Cucumber necrosis virus* (CNV) codes for p33 and p92^{pol} replication proteins, which are produced via translational readthrough strategy [27]. p33 is an essential replication co-factor involved in selection/recruitment of the viral RNA template [30, 71, 72], and in the assembly of the viral replicase [75], whereas p92^{pol} is a RNA-dependent RNA polymerase (RdRp) [13, 25, 125]. Both

replication proteins are integral parts of the tombusvirus replicase complex in combination with 4-10 host proteins [17, 32, 89]. One of the major breakthroughs in tombusvirus research is the development of yeast as a model host for virus - host interactions, allowing the utilization of powerful genomics and proteomics tools developed for yeast [13]. Yeast cells expressing tombusvirus p33 and p92^{pol} replication proteins can efficiently replicate a short TBSV-derived replicon (rep)RNA, which is a defective interfering (DI) RNA identified in TBSV infected plants [13, 82]. The tombusviral repRNA not only serves as a template for replication, but as an assembly platform for the viral replicase complex as well [75, 82].

Replication of both TBSV and CNV RNAs takes place on the cytosolic surfaces of the peroxisomal membranes in plant and yeast host cells [30, 78]. The peroxisomal membranes contain the typical virus-induced membrane spherules and the viral replicase [30, 78], suggesting that transport of the viral replication proteins to peroxisomal membranes likely occurs in TBSV infected cells. Deletion analysis of the p33 replication cofactor in combination with intracellular localization studies revealed that three redundant peroxisomal targeting sequences are present in p33 [78]. Unfortunately, among ~160 host genes identified in recent systematic genome-wide screens of single gene knock out library and the essential gene library of yeast that affected TBSV replication or recombination [16, 20, 21, 75], I could not yet identify any outstanding host protein candidates for transportation of the tombusvirus replication proteins to the peroxisomes. This is likely due to gene/functional redundancy within the yeast host. Indeed, later works demonstrated that replication of TBSV and the closely related *Cymbidium ringspot virus* (CyRSV) was able to switch to the ER membrane in the absence of peroxisomes in yeast [106, 126]. This unexpected finding suggested that the membrane requirement for tombusvirus replication is flexible and that tombusvirus replication proteins can be transported to the ER by default [106].

The objective of this work was to identify the host transporter protein for p33 replication cofactor to the peroxisomal membrane, where TBSV RNA replication takes place [30, 78]. I reasoned that p33 likely interacts with host proteins involved in intracellular trafficking of peroxisomal membrane proteins. To identify those host proteins that could be involved in transportation of the tombusvirus p33 replication co-factor to peroxisomal membranes, I tested whether yeast proteins involved in transport to peroxisome membrane could bind to p33 *in vitro*. These preliminary experiments have led to the identification of Pex19p that bound to p33 specifically under *in vitro* conditions. Further approaches validated that the Pex19p- p33 interaction is important for intracellular transport of p33. Altogether, data presented in this work support the model that Pex19p is the transporter for p33 replication protein.

RESULTS

The Pex19p host protein binds to the tombusvirus p33 replication cofactor in vitro.

To identify if one of the yeast proteins involved in transportation of membrane proteins to the peroxisome could interact with p33 replication cofactor, I performed preliminary pull-down experiments with purified recombinant p33 fused with the Maltose binding protein (MBP) immobilized on beads and five separately expressed GST-tagged host proteins affecting transport to peroxisomes. These experiments have shown that Pex19p bound to MBP-p33, but only poorly to the MBP control (Figure 3.1B, lane 1 versus 2). The GST protein expressed in yeast serving as a control for Pex19p-GST, did not bind to MBP-p33 in the pull-down experiments, confirming that the *in vitro* interaction took place between Pex19p and p33 and was not facilitated by the sequence tags.

To test if the previously defined three peroxisomal membrane-targeting sequences (mPTS) in p33 [78] are important for the interaction with Pex19p, I purified recombinant MBP-p33 proteins with defined deletions. These experiments revealed that p33DPTS that lacked all three mPTS sequences (Figure 3.1A) bound poorly to Pex19p in the pull-down experiment (Figure 3.1C, lane 3). Similarly, p33C, which misses the entire N-terminal domain, including the 3 mPTS sequences and the two predicted transmembrane domains (Figure 3.1A) bound poorly to

Pex19p *in vitro* (Figure 3.1C, lane 4). Deletion of the N-terminal 11 amino acids in p33, which includes one of the mPTS sequences and an ER-targeting sequence [78], did not inhibit its binding to Pex19p *in vitro* (Figure 3.1C, lane 2). Interestingly, deletion of short N-terminal stretches did not inhibit the peroxisomal localization of p33 in *N. benthamiana* or yeast cells [30], whereas deletion of all three mPTSs did inhibit p33 localization [78].

To define if the C-terminal sequence of Pex19p is involved in interaction with p33, I tested a C-terminally-truncated Pex19p, termed Pex19-N206. The C-terminal portion of Pex19p is known to bind to other cargo peroxins that are transported to the peroxisomal membrane by Pex19p [127]. The *in vitro* pull-down experiment has shown that Pex19-N206 did not bind to p33 (Figure 3.1D, lane 2). This was expected, since the N-terminal portion of Pex19p is involved in binding to Pex3p docking protein, not to the cargo proteins [127].

Co-purification of p33 replication protein with Pex19p host protein from yeast.

To test if Pex19p and p33 replication cofactor form a complex in yeast, first I cross-linked proteins with formaldehyde in intact yeast cells co-expressing GST-Pex19p and p33HF (6xHis/FLAG-tagged), followed by quenching with glycine. Then, the cells were broken and GST-Pex19p was affinity purified. Western blot analysis of the GST-affinity purified Pex19p revealed that p33HF was readily co-purified with GST-Pex19p, but not with GST (Figure 3.2A, lane 1 versus 3).

To test if the presence of the peroxisomal membrane is important for p33 and Pex19p interaction, I repeated the co-purification experiment from *pex3D* yeast, which lacks peroxisomes and peroxisomal “ghosts” or membranes [128-131]. I co-purified p33 from *pex3A* yeast, suggesting that the peroxisomal membrane is not necessary for Pex19p-p33 interaction. Since the co-purified p33 was less from *pex3A* yeast than from the wt yeast, it is possible that the peroxisomal membrane might increase/stabilize the Pex19p-p33 interaction. I also tested if the 3 mPTS sequences are important for p33 co-purification with Pex19p. These experiments have demonstrated that p33DPTS that lacked all three mPTS sequences (Figure 3.1A) was not co-purified efficiently with GST-Pex19p (Figure 3.2B, lane 3), whereas p33ΔN11 with deletion of the N-terminal 11 amino acids [that includes one of the mPTS sequences and an ER-targeting sequence [78]], was co-purified with Pex19p (Figure 3.2B, lane 4). Overall, these co-purification data from intact yeast cells are in agreement with the *in vitro* binding experiments, further supporting the model that the mPTS sequences in p33 are important for p33 - Pex19p interaction.

Pex19p is temporarily present in the viral replicase.

To test if Pex19p is present within the membrane-associated tombusvirus replicase, I purified the replicase from yeast actively replicating the TBSV repRNA. I have used a two-step purification procedure based on FLAG-6xHis double-tagged p33 solubilized from the membrane fraction of yeast lysate that results in a replicase preparation, which still has RNA-dependent RNA polymerase activity and contains a small number of host proteins in addition to the viral p33 and p92^{pol} [17]. Western blot analysis of the two-step purified tombusvirus replicase using anti-Pex19p antibody revealed trace amount of Pex19p, which was absent in the control preparation (Figure 3.3, lane 3 versus 4). The control was prepared using the same procedure, but the sample was based on yeast expressing a single 6xHis-tagged p33 [17].

As Pex19p is known to interact with other peroxins only temporarily [132, 133], I cross-linked proteins with formaldehyde prior to breaking the cells, followed by the above two-step affinity purification. Western blotting with anti-Pex19p antibody revealed that Pex19p was present in the highly purified replicase preparation, while it was missing in the control preparations (Figure 3.3, lanes 1 versus 2). Altogether, the higher recovery rate for Pex19p in the cross-linked samples than in the uncross-linked preparations (Figure 3.3, lanes 1 versus 3) supports that Pex19p is likely present in the tombusvirus replicase temporarily.

Re-targeting Pex19p to the mitochondria leads to redistribution of p33.

Finding evidence that supports the relevance of Pex19p in tombusvirus replication is challenging for several reasons. First, deletion of *PEX19* results in the complete loss of

peroxisomes in yeast [130]. Second, p33 is re-targeted to the ER in *pex19Δ* yeast that could be due to the lack of Pex19p or the absence of peroxisomal membranes. Moreover, TBSV replication takes place efficiently in the ER membrane in *pex19Δ* yeast [106], due to apparent functional redundancy in the cell that can support TBSV replication.

To circumvent the above problems, I redirected Pex19p to the mitochondria using a strong viral mitochondrial targeting sequence [MTS, derived from the N-terminal portion of *Carnation Italian ringspot virus*, CIRV [134]]. I reasoned that if Pex19p interacts with p33 in the cell, then MTS-Pex19p should re-direct the localization of a fraction of p33 to the mitochondria. Confocal laser microscopy analysis revealed that p33-YFP co-localized with a mitochondrial marker (MTS-CFP) [134] in yeast co-expressing MTS-Pex19p (Figure 3.4., panel A). The co-localization occurred even at an early time point (7 hours), suggesting that MTS-Pex19p can redirect p33-YFP to the mitochondria. Similar mitochondrial localization of p33-YFP was observed in *pex19Δ* yeast expressing MTS-Pex19p (Figure 3.4A, right panels). Over-expression of the 6xHis-tagged Pex19p did not lead to co-localization of p33-YFP and MTS-CFP (Figure 3.4B). Moreover, expression of MTS-CFP in the absence of MTS-Pex19p in wt BY4741 or *pex19Δ* yeast did not lead to co-localization of p33-YFP and MTS-CFP (Figure 3.4C), arguing against the possible role of MTS-CFP in the mitochondrial localization of p33-YFP in yeast also over-expressing MTS-Pex19p (Figure 3.4A). Altogether, the presented data is in agreement with the model that re-targeting of Pex19p to the mitochondria results in re-localization of p33-YFP to the mitochondria as well.

Re-targeting Pex19p to the mitochondria interferes with TBSV repRNA accumulation.

Re-targeting of the tombusvirus replication proteins to the mitochondria via MTS-Pex19p might cause problems during the assembly of the viral replicase, because other key peroxisomal membrane proteins, such as Pex3p docking protein, which is localized to the peroxisomes via the ER pathway and not via the cytosolic Pex19p-driven pathway [128, 129], will not be present in the mitochondrial membrane. To test the effect of re-targeting of MTS-Pex19p-p33 complex to the mitochondrial membranes, I measured TBSV repRNA accumulation in yeast cells expressing 6xHis-tagged MTS-Pex19p. These experiments have shown 60% reduction in TBSV repRNA accumulation when compared with yeast expressing a short peptide from the pYES plasmid (compare lanes 4-6 with 10-12 in Figure 3.5A). Additional control was yeast expressing 6xHis-tagged Pex19p, which affected TBSV repRNA accumulation by less than 30% in wt yeast, whereas expressing HisMTS did not affect repRNA accumulation (Figure 3.5A, lanes 1-3 and 7-9). The trend was similar in *pex19Δ* yeast, in which the re-targeted 6xHis-tagged MTS-Pex19p inhibited TBSV repRNA accumulation (lanes 16-18), while the control proteins did not. Overall, these data are consistent with a model that the re-targeted MTS-Pex19p can interfere with TBSV replication.

Since the expression level of 6xHis-tagged MTS-Pex19p was low in yeast (Figure 3.5B, lanes 4-6 and 16-18), I also expressed MTS-Pex19p, which was expressed to a level comparable to that of His-Pex19p (Figure 3.5C). In these experiments, I used p33-YFP, and p92H replication proteins to support TBSV repRNA replication, because the evidence on re-distribution of p33 to the mitochondria was obtained using this system (see Figure 3.4). I found that expression of MTS-Pex19p inhibited TBSV repRNA accumulation by 70-75% in wt and *pex19Δ* yeast (Figure 3.5C), confirming the dominant negative effect of MTS-Pex19p on TBSV replication.

Re-targeting Pex19p to the mitochondria decreases the efficiency of the tombusvirus replicase.

Re-targeting of the tombusvirus replication proteins to the mitochondria via expression of the dominant negative MTS-Pex19p could inhibit TBSV replication due to several reasons, including affecting the assembly of the viral replicase. To test if the viral replicase is active in yeast expressing MTS-Pex19p, I isolated the tombusvirus replicase, which was present in a membrane-enriched fraction. This replicase preparation is highly active *in vitro* [75, 82], as

shown in the control sample obtained from yeast expressing a short peptide from pYES plasmid (Figure 3.6A, lanes 10-12). On the contrary, the replicase preparation obtained from yeast expressing MTS-Pex19p showed poor replicase activity (down by 80%, Figure 3.6A, lanes 1-3), albeit the amount of p33 replication protein was comparable to the control samples (Figure 6B, lane 3 versus lanes 1 and 2). The additional control replicase samples obtained from yeast expressing either 6His-tagged Pex19p or MTS-CFP showed 100% and 70% activities, respectively (Figure 3.6A, lanes 4-9). Overall, the *in vitro* assays revealed that the activity of the tombusvirus replicase is poor when isolated from yeast expressing the functional viral replication proteins in the presence of the re-targeted MTS-Pex19p.

DISCUSSION

The assembly of replicase complexes of (+)RNA viruses requires the targeting of the viral replication proteins from the site of translation (cytosol or rough ER) to specialized subcellular membranes [111, 135]. For example, the tombusvirus p33 and p92^{pol} replication proteins are targeted to the peroxisomal membranes in plant and wt yeast cells [30, 78]. For the targeting of the viral replication proteins, tombusviruses might take advantage of host proteins involved in subcellular protein transportation. Indeed, this work shows evidence that Pex19p could serve as a transporter for the p33 replication protein in the yeast model host. The following evidence has been obtained: (i) the binding of Pex19p to p33 requires the 3 mPTS sequences in p33, which are also known to be essential for peroxisomal targeting in plant cells [78]; (ii) Pex19p was shown to be present, at least temporarily, in the viral replicase complex (Figure 3.3); (iii) re-targeting the Pex19p to the mitochondria has led to re-distribution of p33 to the mitochondria as well; (iv) Pex19p with the mitochondrial targeting sequence had a dominant negative effect on TBSV repRNA accumulation; and (v) expression of the MTS-Pex19p also reduced the activity of the tombusvirus replicase.

Based on the above evidence, I propose that Pex19p is the primary transporter of tombusvirus p33 replication protein (Figure 3.7, step 1), and likely p92^{pol} as well due to the presence of overlapping sequence at the N-terminus of p92^{pol} and the requirement of the N-terminal region of p92^{pol} for peroxisomal localization [30]. It is also possible that a fraction of p92^{pol} is ‘piggy-backing’ on p33 to reach to the peroxisomal membranes [30]. Based on the proposed function of Pex19p in yeast, it is likely that the Pex19p-p33 complex can directly reach the peroxisome from the cytosol (Figure 3.7A, step 2), without entering the ER or the Golgi compartment [130, 133]. After reaching the peroxisomal membrane, the Pex19p-p33 complex might bind to Pex3p, which is the docking protein for Pex19p [136]. Binding to Pex3p might facilitate the unloading of the cargo p33 from Pex19p, which could then be recycled to the cytosol for new rounds of transport (Figure 3.7A, step 3).

What makes the function of Pex19p in tombusvirus replication difficult to study is the presence of a default pathway that targets p33/p92^{pol} efficiently to the ER in the absence of the peroxisomes [30, 106, 126]. Thus, the function of Pex19p is not essential for tombusvirus replication in yeast. Yet, re-targeting of Pex19p to the mitochondria inhibited TBSV replication and reduced the activity of the viral replicase. This dominant negative function of MTS-Pex19p suggests that the peroxisomal pathway for tombusviruses is the primary pathway, while the ER targeting pathway is secondary. Moreover, I interpret the dominant negative effect of MTS-Pex19p as the consequence of the inappropriate environment in the mitochondrial membrane for assembling fully functional viral replicase complexes. It is possible that the short N-terminal sequence of p33 adapted to the peroxisomal membrane is not fully functional when inserted into the outer membrane of the mitochondria. In addition, the MTS-Pex19p - p33 complex could be more stable in the mitochondrial membrane due to the absence of Pex3p docking protein than in the peroxisomal membrane where Pex3p is present to recycle Pex19p. Also, due to the transmembrane domains within the MTS sequence, MTS-Pex19p likely stays integrated into the mitochondrial membrane, where it could inhibit p33 functions. Unfortunately, I cannot study the

effect of Pex19p - p33 complex on the viral replicase in the peroximal membrane in the absence of Pex3p, because there are no peroxisomes present in *pex3Δ* yeast [128, 133].

I should mention that the mitochondrial environment could be supportive for tombusviruses, since CIRV does replicate on the surfaces of the mitochondria [134]. In addition, re-targeting CyRSV p33/p92 proteins from peroxisomes to the mitochondria via replacing the mPTS-carrying N-terminal sequence with the longer MTS sequence in p33/p92^{pol} resulted in active CyRSV replication [137, 138]. However, I have to point out that, in these experiments, the mitochondrial transport system was likely recruited by the chimeric tombusvirus replication proteins carrying MTS, thus resulting in proper transport and unloading of the replication proteins to the outer membrane of the mitochondria. Alternatively, the original N-terminal sequence of p33 does not have the optimal sequence for the proper insertion to the mitochondrial membrane, unlike the chimeric MTS-p33/p92^{pol} proteins that carried the entire N-terminal portion of CIRV p36 protein, which are adapted to the mitochondrial membrane, where CIRV replicates [134]. Altogether, in our experiments, the p33 tombusvirus replication protein did not have MTS, and therefore its transport, unloading and/or insertion to the outer membrane of the mitochondria as the MTS-Pex19p / p33 complex could have taken place "improperly", thus, inhibiting the assembly/function of the viral replicase complex.

The known cellular functions of Pex19p fit well with the proposed role in p33 transportation to the peroxisomes. Pex19p is a cytosolic chaperone protein that binds to selected peroxin proteins and targets them for insertions to the peroxisomal membranes with the help of the Pex3p docking protein [132, 133, 136]. Re-cycling of the Pex3p after cargo delivery to the cytosol allows the multiple use of this protein for transport. Altogether, this work adds Pex19p as a new host factor to the growing list of host factors that are involved in tombusvirus replication. Future experiments will address if Pex19p is also involved in recruitment of additional host proteins to the viral replicase complex.

MATERIALS AND METHODS

Yeast strains.

Saccharomyces cerevisiae strains BY4741α (*MATa his3Δ1 leu2Δ0 met15Δ0 ura3Δ0*) and its derivatives *Pex19Δ* and *Pex3Δ* were obtained from Open Biosystems (Huntsville, AL, USA). The yeast GST-ORF over-expression library was provided by Dr Brenda Andrews, University of Toronto, Ontario, Canada.

Yeast and Escherichia coli plasmids.

pEG(KT/KG)-GST6xHis-pex19 and pEG(KT/KG)-GST6xHis were from the yeast GST library [139]. pESC-DI72-p33, co-expressing 6xHis-tagged p33 of CNV from the *GALI* promoter and TBSV DI-72 repRNA from the *GALI0* promoter was obtained as follows: The p33 ORF with the N-terminal 6xHis-tag was amplified by high-fidelity PCR using primer #1402 (GCGGCAGATCTTACCAT-GGGGGGTTCTCA) and #1403 (GCCGCTCGAGCTATTTACACCAAGGGACTCA) and then ligated to pESC vector (Invitrogen) digested with *Bam*HI and *Xho*I. In addition, the full-length cDNA of DI-72(+), including the 3' ribozyme [82] was cloned between *Eco*RI and *Sac*I sites. Construct pESC-DI72-YFPp33 expressing 6xHis-tagged p33 and the yellow fluorescent protein (YFP) at the N-terminus from the *GALI* promoter was described earlier [30, 106]. Plasmids pGBK-HF33 and pGAD-HF92 expressing 6xHis/FLAG-tagged p33 and 6xHis/FLAG-tagged p92, respectively, were described previously [17]. pHisGBK-His33 and pGAD-His92, expressing 6xHis-tagged p33 and 6xHis-tagged p92, respectively from the constitutive *ADHI* promoter were described [13].

For the *in vitro* binding assays, I used pMAL-33 (full length), pMAL-33C, and pMAL-empty as described earlier [28]. To obtain pMAL-p33ΔN11, a portion of p33 ORF was amplified by PCR using primers #2020 (GAGGAATTTCGAAATTTTATTGGCACGTTTC) and #871 (CCCGTCTAGAGGCCTCCCTATTTACACCAAGGGA), followed by cleavage with *Eco*RI

and *Xba*I and dwerectional cloning into vector pMAL-c2X digested with same pair of restriction enzymes. pMAL-p33ΔPTS was constructed by a two-step ligation of p33 cDNA fragments. The 5' portion of the p33 ORF was amplified with PCR using primers #2020 and #1703 (GCCGCTAGCCCATTGGCTGCACAATCTGT), followed by treatment with *Eco*RI and *Nhe*I. A 3' portion downstream from the 130 aa position of p33 was amplified using primers #2041 (GCCGCTAGCCCTAAGAAAGGCTTGCTACTG) and #871, followed by cleavage with *Nhe*I and *Xba*I. After gel-isolation of both PCR products, I ligated them and then used PCR with primers #2041 and #871 to amplify the correctly ligated PCR product. The obtained PCR product was cloned into pMAL-c2X digested with *Eco*RI and *Xba*I.

To obtain pESC-DI72-HisFLAGp33, the p33 ORF together with the N-terminal 6xHis/FLAG tag was amplified from pGBK-HF33 [17] by using primers #1402 (GCGGCAGATCTTACCATGGGGGGTTCTCA) and #1403 (GCCGCTC-GAGTATTTACACCAAGGGACTCA) digested with *Bgl*II and *Xho*I and then ligated to pESC digested with *Bam*HI and *Xho*I. For generating the pESC-HisFLAGp33ΔN11 and pESC-HisFLAGp33ΔPTS, the ORFs of p33ΔN11 and p33ΔPTS were amplified by PCR from pMAL-p33ΔN11 and pMAL-p33ΔPTS using primers #2222 (CGACGGATCCAAAGAAATTTTTATTGGCACGTTCGCGA) and #1403 (GCCGCTCGAGCTATTTACACCAAGGGACTCA), followed by digestion of the PCR product with *Bam*HI and *Xho*I and cloning into pESC-HisFLAGp33 plasmid digested with the same pair of restriction enzymes.

To obtain pYES-HIS-PEX19, the *PEX19* ORF was amplified by PCR from yeast genomic DNA with primers #1915 (CCCGGATCCATGCCAAA-CATACAACACGAAGTAATG) and #1916 (CCCCTCGAGTTATTGTTGTTT-GCAACCGTCGGT), followed by cloning into pYES at *Bam*HI and *Xho*I sites.

To generate pYES-MTS-PEX19, the first 666 base pairs of CIRV p36 ORF sequence (containing the MTS) was amplified from pGAD-CIRVp95 by PCR using primers #969 (CCGCGAAGCTTAAAGAT-GGAGGGTTTGAAGGCTGAGTCT) and #2609 (CCAGGGATCCATCC-TTACCCTTGAGCTC), followed by ligation with *PEX19* cDNA generated by PCR using primers #1915 and #1916 via three-piece ligation into pYES digested with *Hind*III and *Xho*I.

To construct pYES-MTS-CFP and pGAD-MTS-CFP, I PCR-amplified the MTS of CIRV p36 ORF sequence amplified from pGAD-CIRVp95 by PCR using #969 (CCGCGAAGCTTAAAGATGGA-GGGTTTGAAGGCTGAGTCT) and #2609 (CCAGGGATCCATCCTTACCCTTGAGCTC), followed by ligation to the CFP ORF, PCR-amplified from pYES-CFP using primers #1291 (CGGCGGATCCGTGAGCAAGGGCGAGGAGCTGTTCA) and #2044 (CGACCTCGAGTCATCTAGACTTGACAGCTCGTCCATGC). Three-piece-based cloning into pYES-NT/C resulted in pYES-MTS-CFP, and cloning into pGAD generated pGAD-MTS-CFP.

To construct pYES-HIS-MTS-PEX19, I PCR amplified the MTS-PEX19 ORF from the expression plasmid pYES-MTS-PEX19 using primers #642 (GGAGGAATTCATGGAGGGTTTGAAGGC) and #1916, followed by cloning into the multiple cloning site of pYES-NT/C via *Eco*RI and *Xho*I sites.

To generate pYES-HIS-MTS, the 5' 684 base pairs of CIRV p36 ORF sequence was amplified from pGAD-CIRVp95 by PCR using primers #642 (GGAGGAATTCATGGAGGGTTTGAAGGC) and #2692 (GGACTCGAGTTACCGAGCAGGCTCAACCAA) and then cloning into pYES-NT/C via *Eco*RI and *Xho*I sites. To construct pYES-HIS-PEX19-N206, the 5' portion of *PEX19* ORF representing the N-terminal 206 aa was PCR amplified using primers #1915 (CCCGGATCCATGCCAAAACATACAACACGAAGTAATG) and #2290

(CCCTCGAGTTATGTTATTGCGTCGTCCATCTC) and cloned into pYES/NT-C digested with *Bam*HI and *Xho*I.

The source of Antibodies for Western blotting.

I used the following antibodies in standard Western blotting as described [67]: Anti-His (dilution of 1:20000) from GE Healthcare, Piscataway, NJ, USA; Anti-FLAG (dilution of 1:10000) from Sigma-Aldrich, St Louis, MO, USA; Anti-GST (dilution of 1:2000) from Santa Cruz Biotechnology, Inc Santa Cruz, CA, USA. Anti-pex19 (dilution of 1:20000) from Dr. R. Erdmann, Bochum, Germany; Anti-Mouse conjugated Alkaline Phosphatase (dilution of 1:20000) from Sigma-Aldrich St Louis, MO, USA; Anti-Rabbit Alkaline Phosphatase (dilution of 1:5000) from Sigma-Aldrich, St Louis, MO, USA; and Anti-Mouse Horse Radish Peroxidase (dilution of 1:15000) from Bio-Rad, Hercules, CA, USA.

In vitro pull-down assay with recombinant p33.

The recombinant TBSV p33, and its derivatives p33 Δ N11, p33 Δ PTS and p33C (the C-terminal half of p33, Figure 3.1A) were expressed as fusion proteins with maltose binding protein (MBP) in *E. coli* Epicurian BL21-CodonPlus (DE3)-RIL (Stratagene, La Jolla, CA, USA) and purified as described earlier [26, 28]. The purified recombinant MBP-p33, its derivatives and MBP were bound to amylose beads as described [28].

Yeast strains expressing GST/6xHis-tagged Pex19p or only GST/6xHis as a control were from the yeast GST-ORF library, in which the expression is driven by *GALI* promoter [139]. Yeast cells were first pre-grown in SC-U⁻ with 2% glucose at 29°C and then in SC-U⁻ media with 2% galactose at 29°C until mid-logarithmic phase (an optical density at 600 nm = 0.8-1.0). Cells were suspended in binding buffer (20 mM Tris pH 7.5, 100 mM NaCl, 1mM EDTA, 10% Glycerol, 0.1% NP-40, 10 mM β -mercaptoethanol and 1% yeast protease inhibitor mix) and were broken using Talboys™ high throughput homogenizer (Thorofare, NJ, USA). The total yeast lysate was cleared by centrifugation at 21,000 \times g for 10 min at 4°C and then it was loaded on either MBP-p33 or MBP-immobilized amylose beads. The binding reaction was performed at 4°C for 1 hour with gentle rotation. This was followed by washing the beads twice with 1 column volume of binding buffer containing 100 mM NaCl, followed by two washings of 150 mM NaCl binding buffer and finally with two more washings of binding buffer containing 200 mM NaCl. Proteins retained on the beads were eluted by incubation in SDS-PAGE loading buffer at 85°C for 10 min and centrifugation. Samples were subjected to SDS-PAGE followed by Western blotting with anti-His antibody as described [75].

GST-based pull-down of cross-linked Pex19p complex.

Yeast BY4741 and *pex3* Δ strains were co-transformed with pEG(KT/KG)-GST6xHis-pex19 and pESC-HisFLAGp33 or with pESC-HisFLAGp33 and pEG(KT/KG)-GST6xHis as a control. For additional analysis, BY4741 strain was also co-transformed with pEG(KT/KG)-GST6xHis-pex19 and pESC-HisFLAGp33 Δ N11 or pESC-HisFLAGp33 Δ PTS. Transformed yeast cells were cultured in 15-ml culture tubes containing 3 ml SC-UH⁻ (2% glucose) media for 24 h at 29°C. Yeast cells were pelleted, and washed with SC-UH⁻ (2% galatose) media, followed by inoculation to 200 ml SC-UH⁻ (2% galatose) and culturing at 29°C until reaching A_{600} 0.8-1.0. Yeast was pelleted, and washed once with 1X Phosphate Buffered Saline (PBS) buffer, then suspended in 200 ml 1X PBS buffer, and cooled on ice. The yeast cells then were treated with 5.5 ml of 37% formaldehyde (1% final concentration) and incubated for 1 h on ice. The cross-linking reaction was stopped by quenching in 10 ml 2.5 M glycine (final concentration 0.125 M). Yeast was then pelleted, washed once with 1X PBS buffer, and stored at -80°C. This was followed by breaking yeast cells in the lysis buffer (1X PBS, 10% Glycerol, 1mM EDTA, 0.1% NP-40, 1% yeast protease inhibitor cocktail™ [Sigma-Aldrich] and 10mM β -mercaptoethanol) using a homogenizer as described above. The unbroken cells were removed by centrifugation at 100g for 5 min. The total yeast lysate was solubilized in the lysis buffer also containing 0.5 M NaCl and 1 % NP-40 via rotation at 4°C for 1 h, followed by further incubation at 37°C for 5 min and snap

chilling on ice. The solubilized membrane fraction was centrifuged at 21,000 g for 10 min at 4°C. The supernatant was loaded onto GST-resin (Bio-Rad™ Spin chromatography column) equilibrated twice with the lysis buffer with 0.5 M NaCl and 1% NP-40. The samples were rotated for 1 h at 4 °C. The affinity column was drained by gravity flow, washed twice with 600 µl lysis buffer containing 0.5 M NaCl and 1 % NP-40, and then twice with 600 µl lysis buffer, followed by centrifugation at 1000 g for 2 min. The bound proteins were then recovered from the column in 50mM Tris buffer containing 20mM glutathione in a two-step elution. Finally, the protein samples were incubated at 100°C for 20 min to reverse cross-linking, and mixed with the SDS sample buffer and subjected to SDS-PAGE and Western blotting using anti-FLAG antibody. The detection of FLAG was via chemiluminescence according to manufacturer's recommendations (GE Healthcare, Piscataway, NJ, USA).

A two-step His/FLAG affinity-based co-purification of the viral replicase and Pex19p.

This procedure is the modification of a previously published approach [17]. Briefly, yeast SC1 strain was transformed to express 6xHis/FLAG-tagged p33 or only 6xHis-tagged p33 together with plasmids expressing p92 and DI-72 repRNA. The yeast were grown at 23°C until reaching OD₆₀₀ 0.8-1.0. 200 mg of yeast was resuspended and homogenized in TG buffer (50 mM Tris-HCl [pH 7.5], 10% glycerol, 15 mM MgCl₂, and 10 mM KCl) buffer supplemented with 0.5 M NaCl, 0.1% Nonidet P-40 (NP-40), and 1% yeast protease inhibitor cocktail by glass beads using Talboys™ high throughput homogenizer (Thorofare, NJ, USA). The cell debris was removed by centrifugation for 5 min at 100 × g at 4°C. The enriched membrane fraction containing the active viral replicase complex was collected by centrifugation for 15 min at 21,000 × g at 4°C and then solubilized in 1 ml TG buffer with 0.5 M NaCl, 1% NP-40, 5% SB3-10 [caprylyl sulfobetaine] [Sigma] via gentle rotation for 2 h at 4°C. The samples were then incubated at 37°C for 5 min and centrifuged at 21,000 × g at 4°C g for 15 min. 5mM imidazole was added to the supernatant, followed by gentle rotation for 1 h at 4°C with ProBond resin (Invitrogen) pre-equilibrated with TG buffer supplemented with 0.5 M NaCl and 1% NP-40 and 5% SB3-10. The unbound materials were removed by gravity flow, and the resin was washed twice with TG buffer supplemented with 0.5 M NaCl, 1% NP-40, and 1% SB3-10. The resin-bound proteins were eluted in 200 µl TG buffer supplemented with 0.5 M NaCl, 1% NP-40, 1% SB3-10 and 300 mM imidazole. The eluates were then loaded onto anti-FLAG M2-agarose affinity gel (Sigma) pre-equilibrated with 0.6 ml TG buffer supplemented with 0.5 M NaCl, 1% NP-40, 1% SB3-10 and 1% yeast protease inhibitor cocktail. After 2 h gentle rotation at 4°C, the unbound materials were removed by gravity flow and the resin-column was washed 3 times with 1 ml TG buffer with 0.5 M NaCl, 1% NP-40, and 1% SB3-10 and twice with 1 ml TG buffer with 150 mM NaCl and 0.1% NP-40. Proteins bound to affinity bead were eluted by incubating in SDS-PAGE loading buffer at 85 °C for 10 min and the subjected to SDS-PAGE and Western blotting with anti-Pex19 antibodies (generous gift from Dr. R. Erdmann).

Confocal laser microscopy.

Yeast strains BY4741 and pex19Δ were co-transformed with pESC-DI72-YFPp33 under GAL1 promoter, pGAD-MTS-CFP (as mitochondrial protein marker) under ADH1 promoter and pYES-MTS-PEX19 or pYES-PEX19 behind GAL1 promoter. In another set of experiments, above strains were transformed with GAL1 controlled pYES-MTS-CFP and pESC-DI72-YFPp33. Yeast transformants were pre-grown in SC-ULH⁺ media supplemented with 2% glucose for 16 hrs at 29 °C and then transferred to 2% galactose media, followed by shaking at 29 °C. Samples were collected at 7 h and 24 hours for confocal microscopy. Confocal laser scanning micrographs were acquired on a Olympus FV1000 microscope (Olympus America Inc., Melville, New York) as described earlier [106]. ECFP was excited using 440 nm laser light, attenuated to 4.5-11.0% of the maximum laser power, while EYFP was excited using 515 nm laser line (3.5-8.0% of the maximum laser power). The images were acquired using sequential line-by-line

mode in order to reduce excitation and emission cross-talk. The primary objective used was a water-immersion PLAPO60XWLSM (Olympus). Image acquisition was conducted at a resolution of 512x512 pixels and a scan-rate of 10 ms/pixel. Image acquisition and exportation of TIFF files were controlled by using Olympus Fluoview software version 1.5. Figures of micrographs were assembled using Photoshop 9.0 (Adobe Systems Incorporated, San Jose, CA).

Replication assay.

The p92 replication protein with N-terminal 6xHis-tag was expressed constitutively in *S. cerevisiae* strains from pGAD-His92 plasmid under *ADHI* promoter, while the 6xHis-tagged p33 and the full-length DI-72(+)RNA were launched from a dual-expression construct, pESC-DI72-p33 based on the galactose-inducible *GALI* and *GALI0* promoters, respectively. Pex19p and its mutant derivatives were expressed under *GALI* promoter. Yeast strains (BY4741 and pex19 Δ) were pre-grown in SC-ULH⁻ medium containing 2% glucose. After 16 h shaking at 29°C, the cultures were transferred to 2% galactose media and grown for additional 24 h at 29°C. Total RNA extraction and Northern-blotting was performed as described [21] using probe RIII/IV(-), which selectively binds to the 3' end region of the plus-stranded TBSV DI-72 RNA. The quantitative analysis was performed using phospho-imaging with a Typhoon (GE) instrument as described [21, 82].

In vitro replicase assay.

The isolation of the membrane-enriched fraction from yeast was similar to that developed earlier [75, 82]. The template activities of the obtained replicase preparations were tested after adjusting for the same amount of p33 proteins in the samples [75].

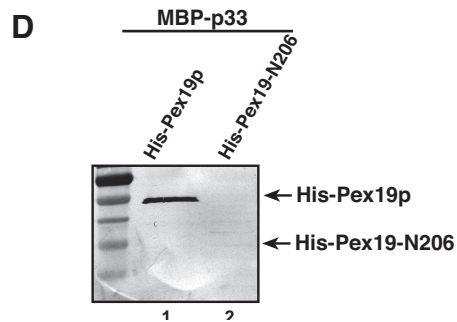
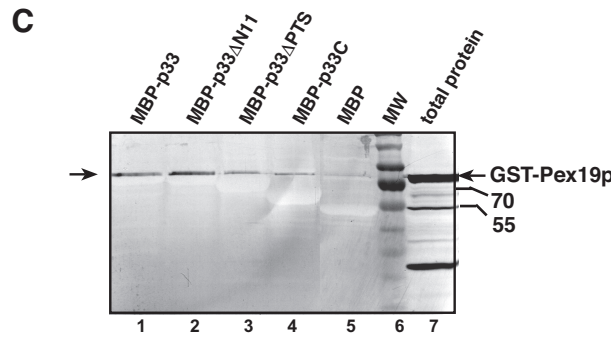
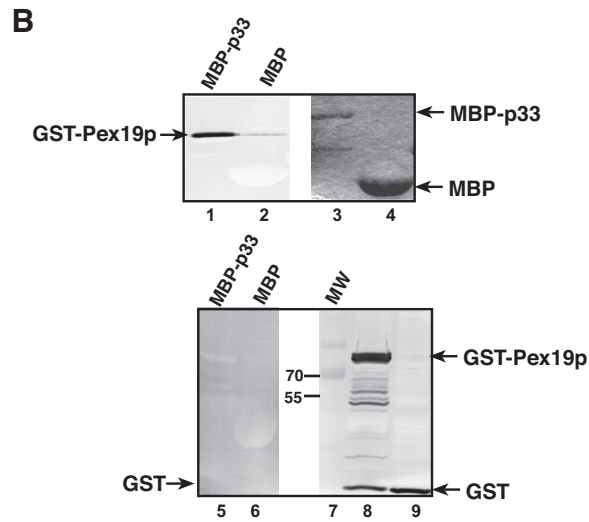
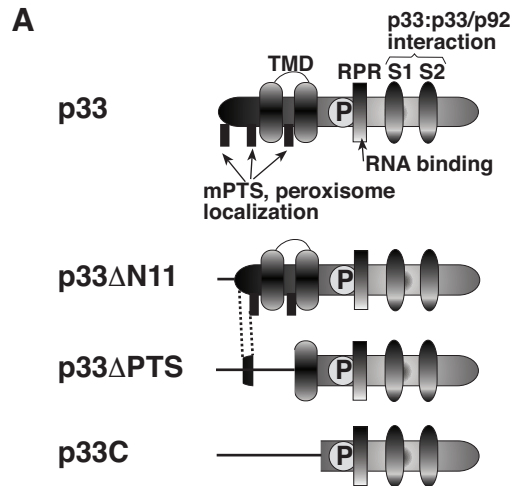


Figure 3.1. *In vitro* interaction between Pex19p and p33 depends on the redundant peroxisomal targeting sequences in p33.

(A) Schematic representation of known domains in p33 and its deletion derivatives used in this study. PTS is the peroxisomal targeting sequence; TMD is the predicted transmembrane domain; P indicates phosphorylation site; RPR is a proline-arginine-rich motif involved in viral RNA binding; while S1 and S2 represent subdomains involved in p33:p33/p92 interactions. The deleted sequences are represented with thin lines. (B) A pull-down experiment demonstrates interaction between p33 and Pex19p *in vitro*. The purified recombinant MBP-p33 or the controls MBP were immobilized on affinity beads. GST-Pex19p (top panel) or the control GST (bottom panel), both of which carry a 6xHis tag, were expressed in yeast and the yeast lysates were applied to the affinity columns with immobilized MBP-p33 or the control MBP. This panel shows the Western analysis (lanes 1-2 and 5-9) with anti-His antibody or the coomassie blue stained gel (lanes 3-4). (C) Western blot analysis of GST-Pex19p bound to the affinity columns with immobilized MBP-p33 derivatives or MBP as a control. (D) A pull-down experiment demonstrates the lack of interaction between p33 and a Pex19p mutant *in vitro*. Pex19p-N206 lacks the C-terminal 137 amino acids involved in binding to cargo peroxin proteins. See further details in panel B.

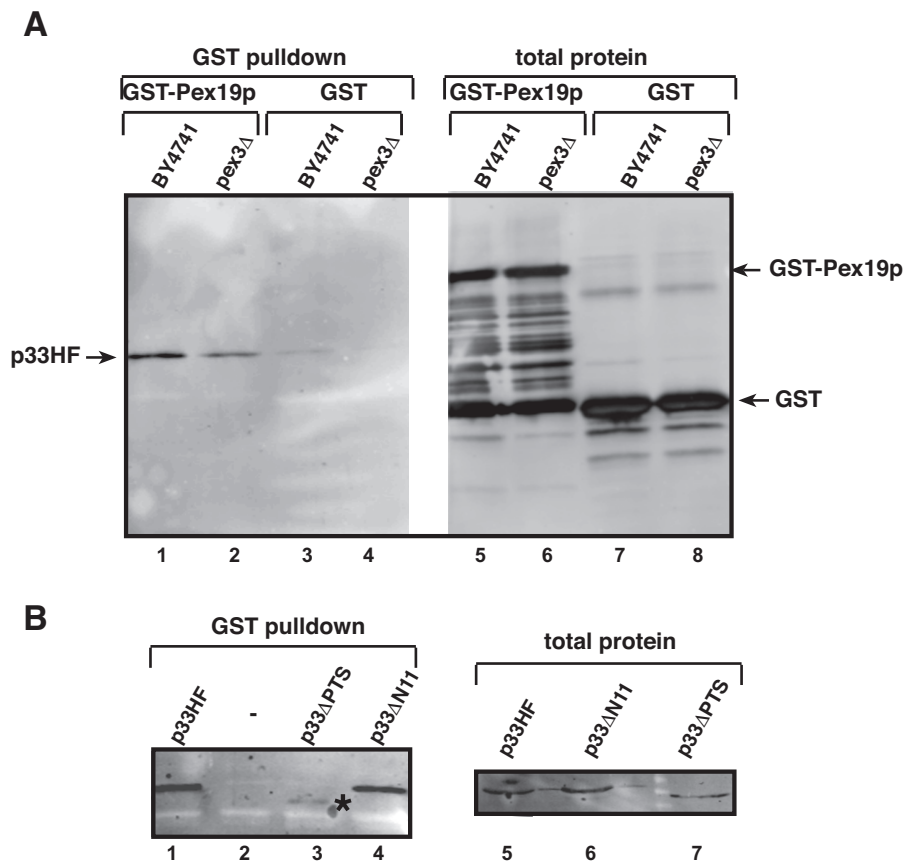


Figure 3.2. Co-purification of p33 with Pex19p from yeast.

(A) GST-Pex19p or GST were purified via GST-affinity purification from the wt (BY4741) and *pex3* Δ yeast co-expressing the FLAG/6xHis-tagged p33HF. Proteins were cross-linked with formaldehyde in intact yeast cells, followed by quenching with glycine, breaking the cells and affinity purification. The Western-blotting was done with anti-FLAG antibody to detect the co-purified p33HF (lanes 1-4). Total proteins were analyzed with Western blotting using anti-GST antibody (lanes 5-8). (B) Demonstration of co-purification of p33 derivatives with GST-Pex19p. The Western-blotting was done with anti-FLAG antibody. See further details in panel A. Asterisk marks the co-purified minute amount of p33 Δ PTS.

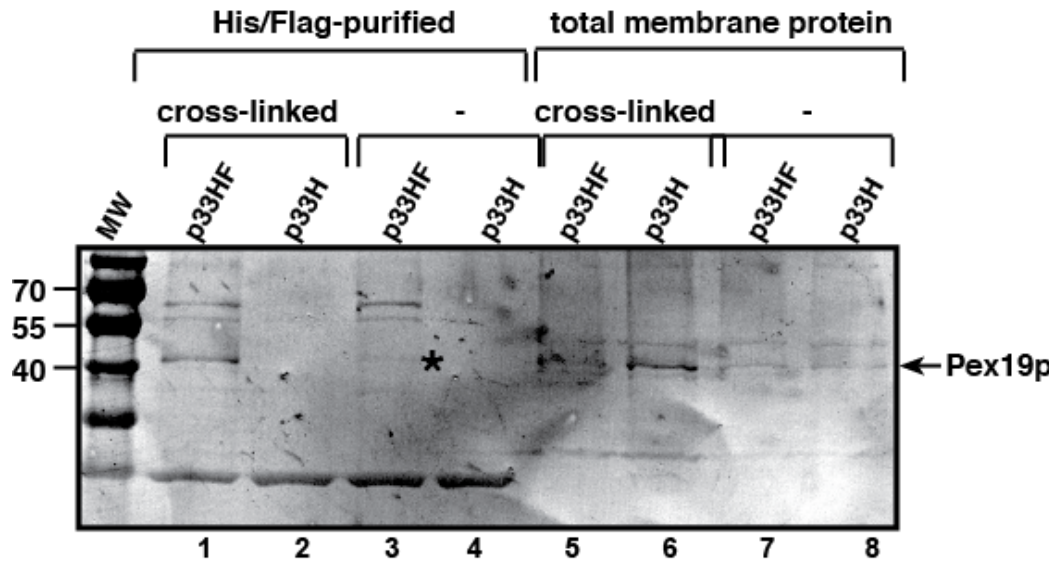


Figure 3.3. Temporary presence of Pex19p in the viral replicase preparation.

Protein cross-linking was done in intact yeast cells as described in Figure 3.2. The yeast cells expressed p33 from a plasmid and wt Pex19p from its natural chromosomal location. The membrane-enriched fraction of yeast was solubilized with 1% NP-40 + 5% SB3-10 detergents, followed by a two-step affinity purification of p33HF based on nickel and FLAG columns. The presence of Pex19p was detected with Western blotting of the proteins eluted from the affinity columns using anti-Pex19p antibody. Note that the control p33H (single 6xHis-tagged) samples were also used for two-step purification to identify nonspecific binders to the columns. The position of the wt monomeric Pex19p is marked with an arrow. The trace amount of Pex19p present in the purified sample obtained without cross-linking is indicated with an asterisk. A slower migrating Pex19p-specific band in the purified samples could be either Pex19p dimer or Pex19p-p33 heterodimer (not fully denatured by heating the samples at 100 °C). The presence of this band does not change the interpretation of the data, because it is only present in the samples also containing p33HF and monomeric Pex19p (lanes 1 and 3), excluding that it is a contaminating protein nonspecifically recognized by the anti-Pex19p antibody.

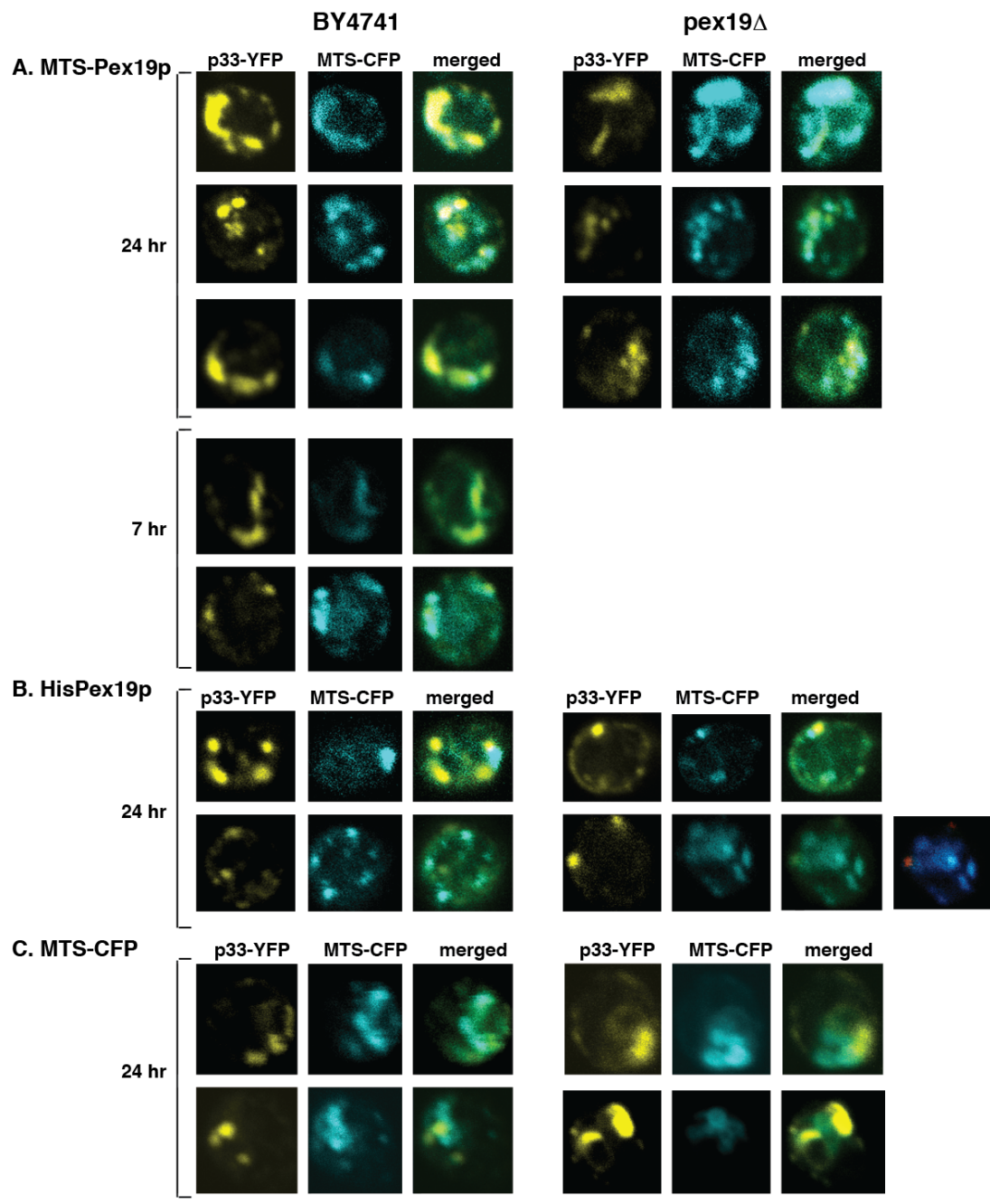
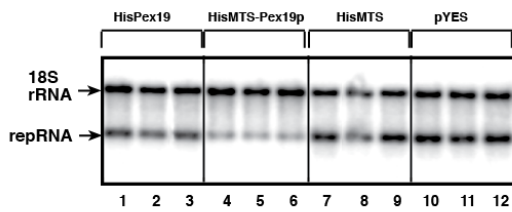


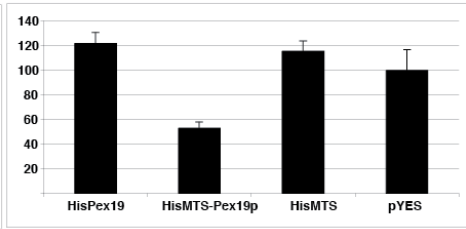
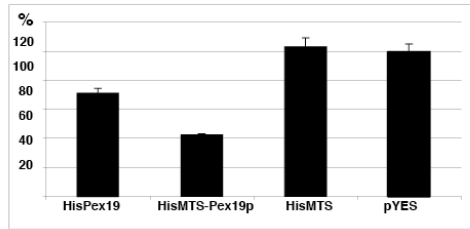
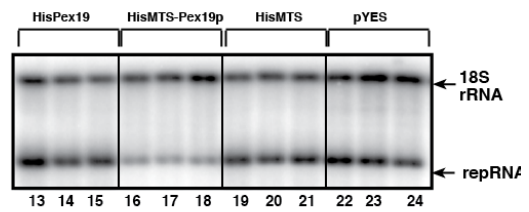
Figure 3.4. Re-targeting Pex19p via an MTS sequence leads to mitochondrial localization of a fraction of p33 replication protein.

(A) Confocal laser microscopy analysis of subcellular localization of p33 in the presence of mitochondrial-targeted Pex19p. The images were taken at 24 or 7 hours time points. MTS-Pex19p and p33-YFP were expressed from the *GALI* promoter, whereas the mitochondrial marker MTS-CFP was expressed from *ADHI* promoter in wt BY4741 (left panels) or *pex19Δ* (right panels) yeast cells. (B) Confocal laser microscopy analysis of subcellular localization of p33 in the presence of cytosolic Pex19p (6xHis-tagged). A false color, blue/red image is shown on the right to highlight the lack of co-localization in the merged image. See further details in panel A. (C) Confocal laser microscopy analysis of subcellular localization of p33 in the presence of mitochondrial-targeted CFP. Note that the expression of MTS-CFP did not result in re-localization of p33-YFP to the mitochondria.

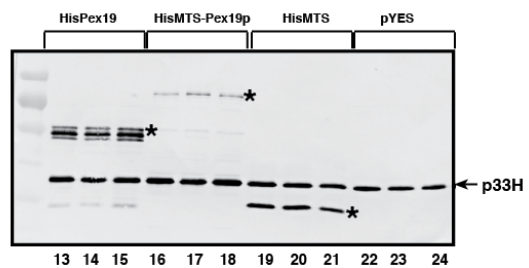
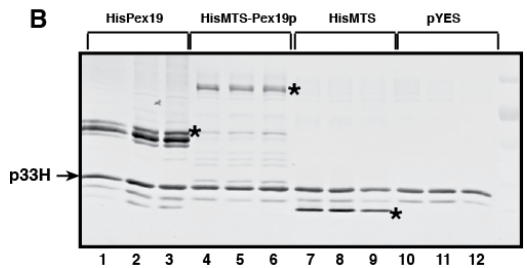
A BY4741



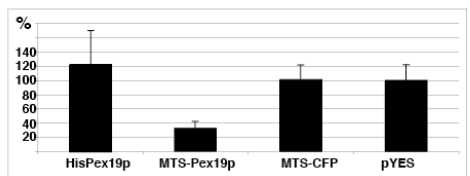
pex19Δ



B



C. BY4741



pex19Δ

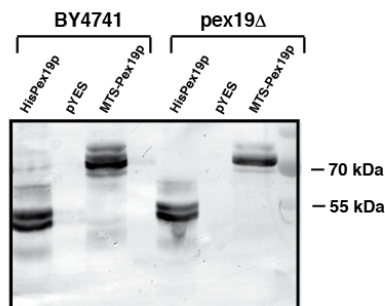
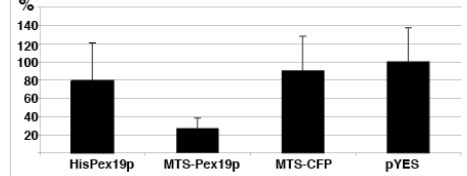


Figure 3.5. Dominant negative effect of the mitochondrial targeted MTS-Pex19p on TBSV replication.

(A) Northern blot analysis of TBSV repRNA accumulation in BY4741 (left panels) or *pex19D* (right panels) yeast cells co-expressing the 6xHis-tagged MTS-Pex19p with p33/p92/repRNA. The control yeast samples contained 6xHis-tagged Pex19p, 6xHis-tagged MTS sequence and a short peptide from pYES. RepRNA accumulation in yeast carrying pYES was taken as 100%. The 18S ribosomal RNA was used as a loading control. Quantification was done with Imagequant software. The experiments were repeated 3-8 times. (B) Western blot analysis of p33 (6xHis-tagged) and the co-expressed proteins using anti-His antibody. Asterisks point at the host proteins expressed with various tags as shown. The yeast samples were the same as used for Northern blotting in panel A. (C) Accumulation of repRNA in BY4741 (left panels) or *pex19D* (right panels) yeast cells co-expressing MTS-Pex19p (without extra-tag) and p33/p92/repRNA. I analyzed 12 independent samples per experiment. See further details in panel A. The Western blot (bottom panel) was done using anti-His antibody.

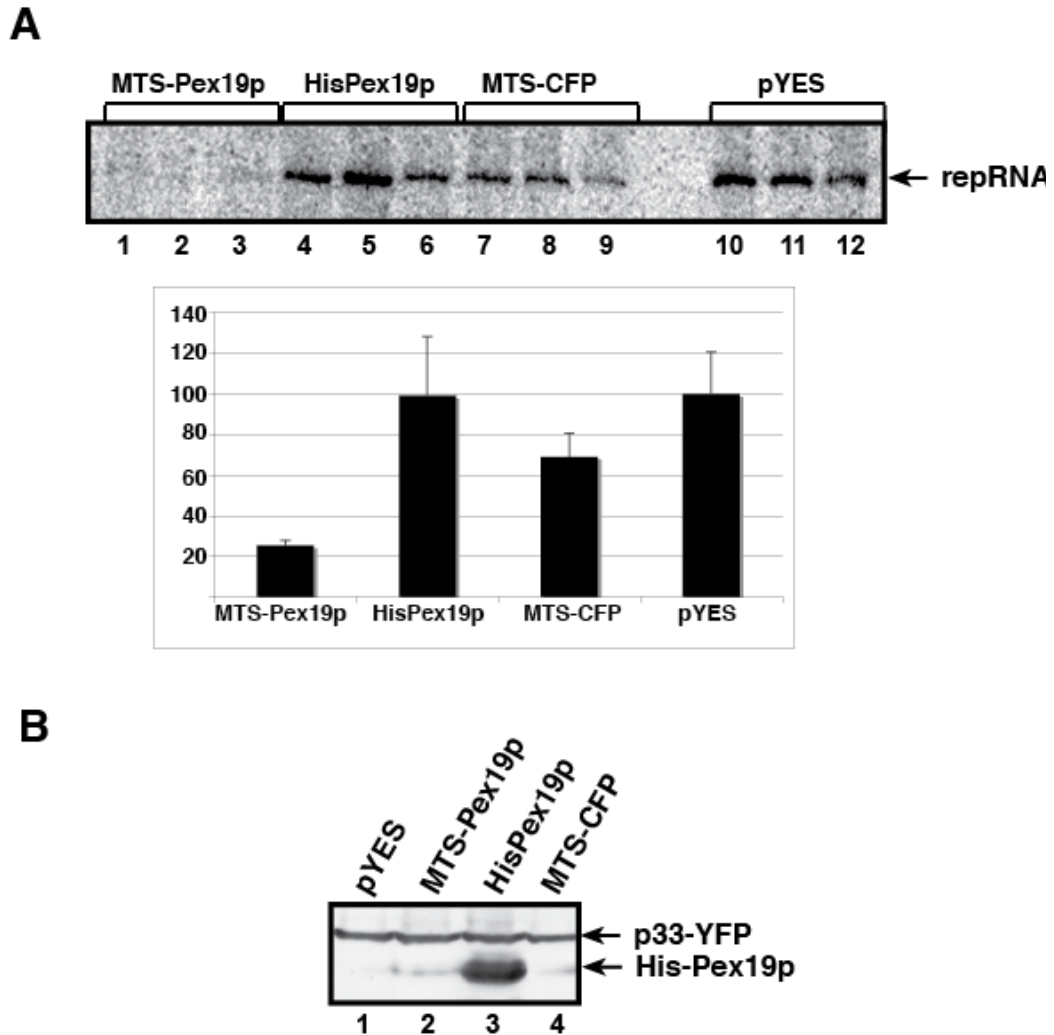


Figure 3.6. Reduced replicase activity of preparations obtained from yeast expressing the mitochondrial targeted MTS-Pex19p.

(A) Standard tobusvirus replicase assays with membrane-enriched fraction prepared from BY4741 yeast cells expressing MTS-Pex19p, 6xHis-tagged Pex19p, MTS-CFP or a short peptide from pYES are shown. Note that these replicase preparations contain the co-purified repRNA, which is used as a template during the *in vitro* assay in the presence of ^{32}P -UTP and cold additional ribonucleotides. The replicase activity of the preparation obtained from yeast carrying pYES was taken as 100%. (B) Western blot analysis of p33-YFP (6xHis-tagged) and the co-expressed proteins using anti-His antibody. The yeast samples were the same as used in the replicase assay in panel A.

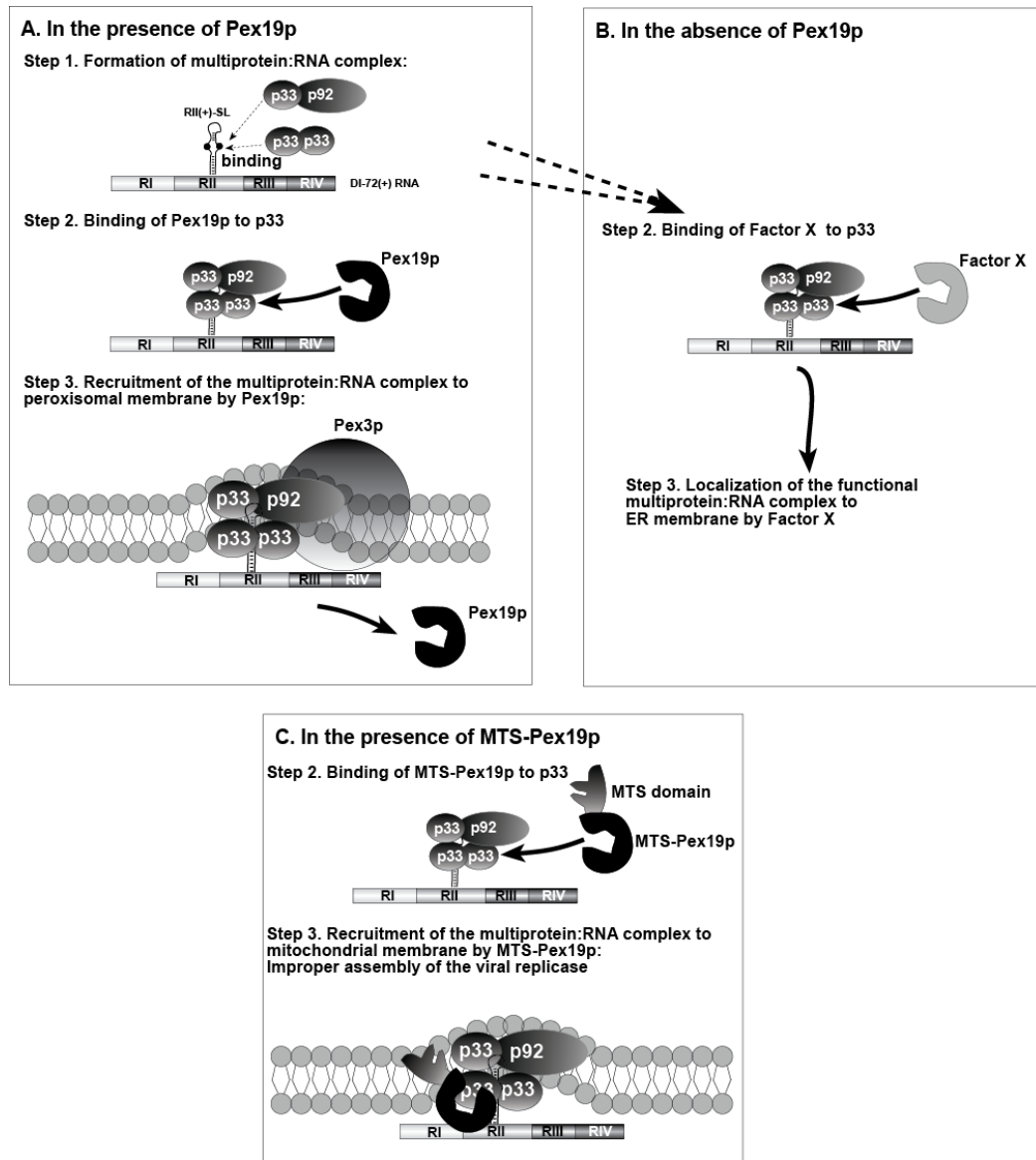


Figure 3.7. A model for the proposed transporter function of Pex19p during tombusvirus replication.

(A) In the wt yeast cells, the cytosolic Pex19p is proposed to bind to p33 replication co-factor after translation and shuttle p33, which likely forms a multiprotein-viral RNA complex as shown, to the peroxisomal membrane. There, the membrane-bound Pex3p “cargo-docking” protein might help unloading the p33 cargo and recycling the Pex19p protein to the cytosol. (B) In the absence of Pex19p in *pex19D* yeast, an unknown host protein, shown as host factor X, is suggested to transport the p33/multiprotein-viral RNA complex to the ER as a default mechanism [106]. Note that TBSV replication is as efficient in the ER as in the peroxisomes. (C) I propose that the MTS-Pex19p targeted to mitochondria facilitates the re-localization of p33 to the outer membrane of

the mitochondria, where p33 might be less efficient in assembling the functional tombusvirus replicase complex. See the text for further details.

Chapter 4. Protein-protein interaction domain of *Cucumber necrosis virus* p33 and p92 is needed for viral RNA binding and assembly of replication complex

INTRODUCTION

Positive strand (+) RNA viruses are the largest group of viruses affecting plants and animals. Their genome is gene-deficient when compared to the genomes of their hosts. To compensate for a lack of their own proteins, (+)RNA viruses usurp host proteins [5, 7, 113] and exploit their limited genetic information to get maximum number of proteins [140]. Apart from polymerase proteins, most of the (+) RNA viruses code for multi-functional ancillary replication proteins. Viral RNA translation, replication and virion assembly depend upon the ability of viral proteins to interact with themselves, other viral proteins, viral RNA and cellular proteins. Viral replication proteins perform several functions important for replication like: selectively recognizing the RNA template, followed by recruiting the RNA to the site of replication, targeting cellular membranes followed by assembling replicase complexes and finally producing the progeny RNAs (reviewed by [68] and [27]). The emerging picture is that almost all of the above-mentioned processes utilize viral protein-protein interactions. With a deeper understanding of the biochemistry of protein-protein interaction during viral multiplication it has become possible for virologists to develop chemical inhibitors that can specifically disrupt the viral protein-protein complexes and thus jeopardize viral functions [141]. Many examples for critical protein-protein interaction exist for virus replication; e.g. BMV protein 1a via interacting to other 1a and 2a molecules forms replication complexes on ER membranes [142, 143]. Another example is from Tobacco mosaic virus (TMV) 126K that is also known to interact with other 126K molecules and the polymerase 186K. Using temperature sensitive mutants of the same this interaction was shown to be critical for viral replication [144, 145]. Other examples of interaction between replication proteins important for (+)RNA viral replication are: poliovirus [146-148]. Hepatitis C virus [reviewed by [149]], cucumovirus [150] and potyviruses [151]. In general, there are many evidences of protein-protein interaction of viral replication proteins but detailed mechanisms by which this affects viral replication is not fully elaborated.

Apart from the polymerase p92, TBSV codes for p33, a multifunctional protein, which also forms the NH₂-terminal third of p92, latter being a translational read-through product of p33. These two proteins are indispensable for viral replication both in plant and yeast a model host [13]. Other TBSV proteins are expressed via two subgenomic RNAs are involved in virion assembly, cell-to-cell movement, and suppression of gene silencing [27, 68]. The auxiliary replication protein p33 is emerging as a major player in TBSV/CNV replication by regulating various steps in the viral replication like: (i) specifically binding to the viral RNA via RPR domain [25, 28] (ii) recruiting the RNA and other proteins to site of replication via two transmembrane domains and three peroxisomal targeting signals [30, 80, 152] (iii) ubiquitination of p33 to regulate the ESCRT pathway is crucial in formation of replication complex [95, 153] (iv) binding to multiple host proteins viz. Ssa1p, Tdh1p, Cpr1p, pex19p, Tef1p [19, 76, 80, 85, 89] that is important for successful replication and (v) also has RNA chaperone activity [96].

The importance of ability of p33 to interact with p33/p92 was discovered using systematic site-specific single amino acid mutations [26]. The study revealed two subdomains S1 and S2 important in p33:p33/p92 interaction. Also the tyrosine and arginine at 244 and 246 positions respectively were found to be critical for viral RNA replication [26]. In follow up work surface plasmon resonance (SPR) was used to study the kinetics of this interaction which revealed that S1 sub-domain has stronger affinity to other S1 [32]. Also the correlation among interaction

data and replication was found. The replication studies were conducted in vivo so each or all of the steps during replication process like: template selection, recruitment, replicase assembly and RNA synthesis could have been affected because of a lack of interaction between p33:p33/p92. This lack of pinpoint detail was addressed in this study.

This chapter describes the novel use of cell free yeast extract based (CFE) replication system to figure out the exact mechanism by which interaction among p33 and p92 affects CNV/TBSV replication. Recently, CFE has been developed that can launch an authentic RNA replication using membranes, host factors, a TBSV defective interfering RNA DI72(+) as a replicon (repRNA) and *E. coli* purified p33 and p92 [73].

I studied the S1 and S2 single amino acid mutants in the CFE replication system and found strong correlation between interaction and viral RNA replication. *In vitro* gel-shift assays showed deficient viral RNA binding ability by some mutants. Assembly of replicase complex was the final step that was negatively affected due to mutations in the S1/S2 sub-domains. Some mutants showed strong inhibition of replication launched even by wild type p33/p92. This inhibitory effect was gone if already assembled and purified replicase from *Turnip crinkle virus* (TCV) or *Cucumber necrosis virus* (CNV) was tested. These data not only establish the role of protein-protein interaction for RNA template selection and replicase assembly but also adds 'dominant negative replication protein interaction mutants' as a novel tool into the antiviral repertoire.

RESULTS

S1/S2 sub-domains mutations abolish TBSV replication.

Previously, using yeast two hybrid and Surface Plasmon Resonance (SPR) assays, Rajendran and co-workers showed that TBSV replication proteins p33 and p92 interact with themselves via two subdomains S1 (241-252 amino acid positions) and S2 (271-283 amino acid positions) respectively [32]. Trans-membrane domain together with RPR and S1/S2 domains (Figure 4.1A) play roles to make p33 a functional molecule for RNA replication in yeast and in plants. One indication was that protein-protein interaction domain is likely important for initial steps of RNA replication. To gain insight into the mechanisms by which protein-protein interaction domain might affect the TBSV replication, I utilized the recently developed cell free (CFE) replication system. I fused MBP tag to the N-terminus of p33 or p92 and to their respective S1/S2 mutants (created by Quick change mutagenesis®: see *Materials and methods*) and used them in CFE replication assay programmed with repRNA DI72(+). In these assays, C₂₇₃F (CF) and Q₂₄₅F (QF) mutations on p33 reduced the level of replication to 4% and 2% respectively almost to the levels of our negative control MBP (Figure 4.1A, Lanes 1-3). Another mutation on p33, I₂₄₃V (IV) halved the activity and C₂₇₂T (CT) activity was 14% when compared to wild type levels (Figure 4.1A Lane 4, 5 vs 6, 7). R₂₄₁A (RA) and LI₂₄₂₋₂₄₃CT (LT) failed to show any activity CF reduced the activity five-fold (Figure 4.1A Lanes 8-10). Coomassie blue staining analysis of SDS-PAGE (Figure 4.1B) showed that the different levels of activities were not because of the variations in amounts of recombinant proteins. Thus, the S1 and S2 domains are very critical for replication proteins p33 and p92 to retain their *in vitro* replication ability.

Wild type p33/p92 couldn't rescue the activity of loss of function S1/S2 mutants.

Protein-protein interaction domains have been indicated to play roles in assembly of replication complex of TBSV and CNV [26, 30, 32]. It is envisaged that p33 dimers help the formation of vesicular structures on the peroxisomal membranes [30, 80, 152] and ER in the absence of peroxisomes [106] together with the help of host factors like ESCRT proteins and HSP70 [73, 85, 95]. Inactivity of the above discovered mutants might be because of less-efficient formation of replicase complex due to poor dimerization or oligomerization. To check if the poorly formed replication complexes in the mutant replication proteins could gain some function if wild type replication proteins were supplied exogenously I utilized the CFE replication assay. This *in vitro* replication was programmed with repRNA and only two (rATP, rGTP) of the four nucleotides to arrest the replication process just after RNA recruitment and replication complex assembly. Assay consisted of wild type proteins (Figure 4.2A Lanes 1-4, left and right panels) or p92 mutants (Figure 4.2A Lanes 5-10, left panel) or p33 mutants (Figure 4.2A Lanes 5-10, right panel). After washing and removal of supernatant the supplementation of wild type p92 to the replication complexes assembled by using p92 mutants had minimal effect on the RNA accumulation (Compare lanes 5-7 vs 8-10 in Figure 4.2A, left panel). Also p92 mutants couldn't affect the activity of replication complexes assembled with wild type p33 and p92 (Lane 1 vs 2-4 in Figure 4.2A, left panel). In case of p33 mutants the addition of wild type p33 improved the activity marginally from 39% to 47% in case of IV (lane 5 vs 8 in Figure 4.2A, right panel) and 10% to 17% in CT (lane 7 vs 10 in Figure 4.2A, right panel). Similar to p92 mutants p33 mutants also couldn't affect the activity of replicase complexes assembled with wild type p33 and p92 (compare lane 1A to 2-4 in Figure 4.2A right panel). Overall, the mutant replication proteins could neither inhibit the activity of wild-type replicase complex nor the wild-type proteins could rescue the low activity of replication complexes assembled by mutant proteins when provided after the assembly process.

It is known that for the proper membrane insertion, TBSV replication proteins depend on host factors (especially chaperones from Hsp70 family) [85, 154], which are provided by the supernatant in CFE replication assay. The inability of wild type p33 and p92 to rescue the inactivity of their respective mutants in the above experiments might be due to a lack of host factors in the 2nd step of replication. To test, if providing host factors in the above experiments

could reverse the outcome, I provided supernatant together with the wild type p33 to the complexes assembled using p33 mutants. (Figure 4.2B lanes 4-6). The replication activity of the mutant proteins was minimally changed using the supernatant together with wild-type p33. Also, when mutant p33 proteins were provided to replicase assembled with wild type p33/p92 (Figure 4.2B lanes 1-3), the activity was 100%, 94% and 75% for Q₂₄₅F, C₂₇₂T and ΔRPR mutant p33 respectively. Altogether, these results suggested that replicase complexes assembled using mutant replication proteins either are permanently deranged beyond the capability of wild-type proteins to be able to rescue the lethal effects or too closed structures to be entered by huge proteins like MBP-p33 (75 kDa) or MBP-p92 (134 kDa).

Q₂₄₅F mutant inhibits the wt p33/p92 mediated RNA replication.

In the previous experiments, the p33 or p92 mutant proteins were unable to decrease the activity of replication complex assembled using wild type p33/p92. It has to be noted that the mutant proteins were added after the assembly of replicase complexes. It is possible that the p33 mutants, due to their inability to interact properly with p33 will form an improper replication complex if added together with them. To test these predictions, I used CFE replication assay and programmed it with repRNA, wild type replication proteins. 0.5, 1, 2 and 4 pmol of wild type p33 or mutant p33 were added simultaneously to the reaction (Figure 4.3A). Q₂₄₅F mutant reduced the replication to 3% and 7% at the highest concentration when compared to wt p33 or MBP only (Figure 4.3A, compare lane 18 vs lanes 1-3 and lane 24 vs lanes 25-27). IV and CT reduced the replication to 31% and 45% respectively with high standard deviation (Figure 4.3A lanes 6 and 12).

Assembly of replicase complex *in vitro* mostly occurs during the first hour of the CFE replication assay [55, 73]. Later on, the replicase complexes probably form special structures that are nuclease as well as proteinase resistant. To investigate that indeed the dominant negative p33 mutants are exerting their deleterious effect on replication during or before replicase assembly I performed a time-course experiment. To this end, I added Q₂₄₅F or ΔRPR or MBP only as a control protein to *in vitro* CFE reaction at different time points as indicated in Figure 4.3B. Maximum negative effect on replication (5% and 6% respectively) was observed when the mutant proteins were added simultaneously with wild-type replication proteins (compare Figure 4.3B lane 8 vs 7 and 14 vs 13). The deleterious effect was gradually reduced to only upto 45% and 67% of the mock treated sample (compare Figure 4.3B. lane 12 vs 7 and lane 18 vs 13) for Q₂₄₅F and ΔRPR respectively. As expected, minimal effect was observed on the replication levels by addition of MBP (Figure 4.3B. lanes 1-6). Consistent with the results in Fig 1A, the mutant replication proteins exert their dominant negative effect on TBSV replication during early events *viz.* RNA recruitment, replicase assembly.

LT and RA mutations in p92^{pol} reduces its efficiency of RNA recruitment.

The *in vitro* replication assays indicated that the mutants are debilitated in their ability to perform some of the early events during replication. To determine, if the mutations on the replication proteins had any effect on their ability to recruit viral RNA to the membrane, I performed an *in vitro* RNA recruitment assay. For this purpose, I purified the MBP tagged versions of wild type and mutant proteins and tested them in CFE with equal amounts of radiolabeled RNAs (i) Wt-RIISL(+) that is known to positively bind to the viral replication proteins and (ii) a C→G mutation containing RNA (G:C-RII-SL(+)) as a control as it is unable to bind to viral replication proteins efficiently. Only two of the four ribonucleotides (rATP and rGTP) were supplied so that the reaction wouldn't progress to replication. Autoradiography of the RNA samples isolated from the pelleted and washed membranes, revealed that LT and RA mutants were able to recruit only 17% and 26% of the viral RNA when compared to wild type p33/p92 (Compare lanes 2,3 to 4 in Figure 4.4, left panel). Please note that there was 11% recruitment (Lane 9 Figure 4.4, left panel) of viral RNA, in spite of absence of any replication proteins. Also the G:C-RII-SL(+) RNA was recruited to the membrane non-specifically at low

levels and was unaffected by addition of different recombinant proteins (Figure 4.4. lanes 1-9, right panel). Together, these results indicate that LI to CT and R to A mutations in p92^{pol} may decrease the efficiency of RNA recruitment.

S1/S2 subdomains are required for efficient RNA binding of p33.

Since Q₂₄₅F p33 mutant was very strong in inhibiting the viral replication *in vitro*, and also because the effect was mainly restricted in the first 20 minutes of the replication (Figure 4.3B), I decided to test this protein's ability to bind to viral RNA, as without this accomplishment, the template can't be selected and recruited to replication. Prior results [32] showed that functional protein-protein interaction domain was critical for p33 to be able to bind specifically to viral RNA as deletion of the S1-S2 subdomains converted the p33 from a highly specific viral RNA binder to a non-specific promiscuous RNA binding protein. Importance of high specificity of RNA binding is also exemplified by the fact that a single mutation from C→G in RIISL(+) not only incapacitates its p33 binding ability but also destroys viral replication both in yeast and plants [71]. In keeping with these results I performed an electro mobility gel-shift assay (EMSA) with the purified p33, QF and IV proteins (in different concentrations) tested against wild type RII(+)SL or a C:G mutant hairpin. To increase the solubility of the above proteins and thus improving the EMSA, instead of full-length proteins I used the truncated versions [p33C (150-296 aa, devoid of the two transmembrane domains)]. Wt-p33C bound to the wt-RII(+)SL RNA whereas no shift was visualized with the C:G mutant RNA (Figure 4.5. compare lanes 5-8 vs 1-4). Q₂₄₅F-p33C was unable to shift both types of RNA tested (Figure 4.5. lanes 9-16). With I₂₄₃V I could see a full shift with wildtype RNA hairpin at the maximum concentration of 4 pmol whereas with the mutant hairpin, there was no shift (Figure 4.5 lane 24 and lanes 17-20). Thus, Q to F mutation at 245th aa position completely destroys the ability of p33 to bind to either wt or the mutant RNA; I₂₄₃V mutation just debilitates the capacity to bind to wt RNA while still maintaining the no binding phenotype to the mutant hairpin similar to wildtype p33.

Assembled and purified TCV or CNV RdRps are resistant to inhibitory effects of S1/S2 mutants.

Previous results of inhibition of *in vitro* replication by the dominant negative mutants might be due to the deranged protein-protein interaction or protein-RNA interaction, resulting in incompetent replication complex formation. In keeping with these results, I wanted to see if these mutants could wield their inhibitory effect on an already assembled, purified and functionally active RdRp complex. To achieve this, I utilized C-terminal truncation of p88, a very active RdRp from TCV (Figure 4.6.A) and CNV replicase purified from yeast co-expressing p33, p92 and repRNA (Figure 4.6.B). 1 and 2 pmol of purified recombinant proteins (p33, p92 and their mutant versions) were added in parallel to the RdRp reaction set up with p88C and DI72(-) as a template or CNV replicase and RI/III(-) as template. I failed to find any significant changes in the accumulation of RdRp product(s) in both p88C and CNV replicase containing reactions. Thus, I conclude that once the RdRp is activated, these mutants can't exert their effect. Also, previously observed deleterious effect on replication was not because of any modification to the RNA or its polymerized products during replication.

Q₂₄₅F doesn't alter the localization or the structures formed by wt-p33 in yeast cells.

CNV and TBSV replicate on the membranes of peroxisomes or ER when peroxisomes are absent [30, 80, 106]. p33 alone is able to form punctate structures on these organellar membranes when visualized under confocal microscope [30, 152] and special spherular structures when analyzed with an electron microscope [7]. Moreover, in the yeast cells where HSP70 protein's functions are knocked down, instead of punctuates structures p33 gets diffused in cytoplasm at the same time replication is undetectable in such cells [154]. To get a deeper insight of the mechanism by which, QF was inhibiting I wanted to check the localization pattern of wildtype p33 in the presence of QF. For this purpose, I transformed BY4741 wt yeast cells with GAL1 driven NH₂-terminal YFP tagged p33 and constitutively expressed Q₂₄₅F mutant. To track

peroxisomal membranes I used constitutively expressed pex13-CFP and to visualize ER membranes, pho86-CFP was employed. Expressing QF had no significant affect on p33 peroxisomal localization pattern when compared to an empty vector control [Compare (-) vs QF in Figure 4.7.A]. I also didn't notice localization of wt-p33 with ER marker in cells expressing either empty vector or QF (Figure 4.7.B).

S1/S2 sub-domain determines the quality of replication complex.

I previously showed that mutations in S1/S2 subdomains of p33 or p92 abolish or compromise RNA replication. In conjunction with such inhibition previous results also showed that a lack of RNA binding and thus very poor replicase complex assembly possibly reduced the RNA replication. To more accurately and precisely comprehend this process, I tested the efficiency of replicase complex assembly using the above mutants in parallel. For this purpose, p33 and S1/S2 mutants were dually tagged with MBP and 6X His residues. Amylose column purified proteins were used in an *in vitro* replicase assembly reaction (see materials and methods). The assembled replicases on yeast membranes were pelleted and solubilized with non-ionic detergents and the RdRp was purified by Ni⁺⁺ column chromatography. Finally, equal amounts of RdRps were tested for complementary RNA synthesis using a minus strand template (Figure 4.8.A). All mutants except IV and CF were less than 15% active in replicase assembly when compared to wtp33/p92 (Fig 3.8.B. lanes 2,3,4,5,7 vs 8). In agreement to the *in vitro* CFE replication data, IV and CF were 52% and 23% active to assemble replicases (Figure 4.8.B. lanes 1,6 vs 8). Thus, the loss or decrement of *in vitro* replication by S1/S2 mutants was closely linked with their ability to assemble an active replication complex.

DISCUSSION

Positive-strand viruses of plants utilize their replication auxiliary proteins to accomplish different processes during replication. These proteins play a major role in: RNA template selection, targeting specific membranes, recruitment of viral and cellular factors and replication complex assembly. These multifunctional proteins rely heavily on their ability to directly interact with other copies to execute different steps of replication. Thus, the mechanisms by which viral replication proteins interact with themselves and others are crucial to have deeper understanding of the entire viral replication process. In the case of CNV, the versatile replication protein p33 plays crucial roles in binding to the viral RNA and recruiting it and other p33 and p92 molecule to the site of replication i.e. peroxisome [30, 152]. p33 is membrane targeted via two of its transmembrane domains and by ability to interact with cellular proteins pex19p and ssa1p [80, 85]. Apart from being able to ubiquitinated and hijack the host ESCRT pathway for replicase assembly [95, 153] recently p33 has been shown to possess RNA chaperone activity [96]. Previously, I mapped two subdomains S1 (241-252 aa) and S2 (271-283 aa) crucial for p33-p33 interaction [26, 32]. The domain was important not only for interaction but also for viral replication. Additionally, S1-S2 was needed for the specific recognition of viral RNA. p33 molecules containing RPR sequence but without S1/S2 subdomains bound even to minus stranded DI72-RIII(-) sequences [26, 32], which was in contrast to the finding of complete lack of binding by wt-p33 to DI72(+) containing a C:G mutation on a RII stem loop [71, 72].

Role of S1/S2 in p33:p33/p92 interaction.

Previously, using yeast two hybrid and surface plasmon resonance assays it was shown that S1/S2 domains are critical for p33/p92 to directly bind to p33/p92. Utilizing CFE *in vitro* replication assay this report shows that mutations in the above mentioned domains had drastic affect on DI72(+) replication (Figure 4.1). Q to F, C to F in p33 and R to A, LI to CT changes in p92 abolished the replication whereas I to V, C to T in p33 and C to F mutations affected the replication albeit to a lesser extent. Interaction data from previous work and replication results from this report are well correlated. In other words, the interaction strength of different mutants is directly proportional to the accumulation of replicon RNA *in vitro*. Interestingly, the same amino

acid change from C to F on p33 and p92 had different phenotypes in the CFE assay, the mutation being not as deleterious on p92 as on p33. It's interesting to note that NH₂-terminal third of p92 that contains p33 sequence in entirety has been previously shown to possess extra functions during viral replication [30]. Using different truncations on p92 from NH₂-terminal I had found that the p92 molecules lacking trans-membrane domains but possessing S1/S2 still could be targeted to the peroxisomal membranes probably via "piggy-backing" on p33[30]. Also, p92 alone is not able to support RNA replication *in vitro* unlike the purified C terminal half of TCV polymerase p88 devoid of p28 portion analogous to p33. This suggests that p33 portion of p92 or p33 in trans provides extra-function related to replication. It might help to activate the polymerase, or load it properly on to the RNA. S1 deletion p33 molecules have been shown to partially localize to ER and form less punctate structures [30]. I envisaged that proper protein-protein interaction is important to efficiently assemble functional replication complex and spherules on peroxisomal membranes. Figure 4.2 suggests that even though the S1/S2 mutants might form inefficient replication complexes but those structures are not easily accessible to wild-type replication proteins therefore I could not see any rescue of diminished replication in spite of providing active proteins exogenously. To rule out that the lack of stimulus from wt p33/p92 is because of undersupply of Heat shock protein 70 (Ssa1p) that is known to be critical for membrane targeting and function of replication proteins [73], I added supernatant from yeast extract containing soluble cellular proteins including Ssa1p. Thus, these results indicate that either the structures formed by the assembled replicase is too close/inaccessible to exogenously added biomolecules; or once the replicase is assembled it can't change its structure or makeup. There are evidences for the prior model: as I have found that the *in vitro* assembled (approximately one hour after *in vitro* reconstitution) replicase complex is accessible to neither proteinase K nor RNase 1 [55, 73]. In contrast, the RdRp preparation obtained from purification of assembled replicase complex was influenced by the addition of auxiliary protein p33 could stimulate the TCV polymerase p88 activity on minus strand template [96]. Although this stimulation of plus strand synthesis might be via RNA chaperonic activity instead of protein-protein interaction, as it is known that p33 is unable to interact to p88 [26].

The main process during replication that is hurt by mutating S1/S2 domains seems to be the selection of RNA template as revealed in Figure 4.5. Q to F mutation in p33 completely abolishes binding ability of p33 to the viral RNA. This step of RNA binding is critical for replication as it has been shown that DI72(+) RNA containing C→G mutation in RII stem loop that makes it non-binder to p33, cannot replicate in yeast or plants. *In vitro* RNA replication activity is well correlated to the binding ability to wild type RNA, as I to V mutation, which can still bind to the RNA albeit with lower efficiency had a mild negative effect on RNA replication in Figure 4.4 The drastic affect of S1/S2 mutation on RNA binding ability is in contrast with the previous data from our lab where a polypeptide devoid of S1/S2 domains but still possessing RPR domain efficiently bound cooperatively to the viral RNA. In previous studies the protein carried major deletion of S1/S2 deletion and thus could have opened the juxtaposed RPR domain structure making it accessible to any kind of viral RNA with loss of specific binding.

Novel replication inhibitory dominant negative mutants.

The ability of S1 mutant Q₂₄₅F to prohibit the replication launched by using wild type p33 and p92 (Figure 4.3) reveals significant insights into the pathways by which TBSV RNA replication complexes assemble. CFE based replication assay indicated that the even at the equimolar ratio, QF could inhibit p33 based replication. This inhibition was profound when mutant was used in increasing amounts. Previous results showed that S1 deletions in p33 molecule changed the localization from peroxisome to ER [30]; the inability of QF to alter either the localization or pattern of punctate structures made by p33 on peroxisomal membranes indicated an alternative mechanism of this dominant negative phenotype. Fig 4.5 showed complete absence of RNA binding by QF, which indicated the inhibitory mechanism towards

template selection process. In congruence, when I tested a p33 devoid of a highly conserved RPR domain (critical for RNA binding) in CFE based *in vitro* replication assays, I found that this mutant also greatly reduced RNA replication and the pattern of inhibition observed was similar to that of the QF (Figure 4.3). The inability of both the mutants to act after the assembly of replicase complex was also similar.

All the S1/S2 mutants and even the wildtype p33/p92 proteins failed to impart any effect when were used with the purified RdRp preparations of CNV or TCV p88C (Figure 4.6). From previous experiments it is known that p33 and p88C don't interact, thus the neutral behavior of the added proteins in p88C based RdRp assay also indicates that protein-protein interaction is needed for any effect on the replication; or once the RdRp is active, then protein-protein interaction plays minor role(s) in replication thereby, above mentioned mutants or wild type proteins had little effect. Lack of previously demonstrated positive effect of p33 on p88C based RdRp reaction [96] might be due to a minus stranded template used in this study instead of a plus strand RNA.

These results suggest that QF and Δ RPR mutants inhibit the replication earlier than RNA synthesis steps, probably during template selection and recruitment and replicase assembly. The mechanism behind the dominant negative phenotype may lie in QF's ability to weakly interact with the wild-type p33 molecules but then rendering these protein-protein complexes unable to bind to the viral RNA, thus inhibiting the entire cascade of replication events in accordance with the prior results that suggest that for specific recognition of plus strand TBSV DI72(+) RNA, p33-p33 dimerization is needed.

In summary, I find that protein-protein interaction subdomains S1 and S2 play critical roles in TBSV RNA replication. They regulate the essential p33/p92 functions contingent upon protein-protein interaction like RNA template selection and its recruitment and replication complex assembly. In addition, they might play a role in inducing proper spherule formation via multimerization. I also discovered dominant negative mutants abolishing viral replication highlighting the potential of these mutants as an antiviral approach. Protein-protein interaction among many viral proteins plays crucial roles in replication. Dominant negative mutants have also been reported for viruses. Using ubiquitin-mimicking p33 chimeras, earlier work has demonstrated that high level of p33 ubiquitination is inhibitory for TBSV replication. A mutant of the two-exon HIV-1 Tat protein (Nullbasic) was described to potently inhibit multiple steps of the HIV-1 replication cycle [155]. Another HIV-1 protein (the capsid-spacer peptide 1 Gag) also is a dominant-negative inhibitor of virion maturation [156]. Glycoprotein D based dominant-negative recombinant of herpes simplex virus 2 was used to make viral vaccines [157]. Such similitude suggest that protein-protein interaction is used by viruses to increase the functionality of their proteins and also that it can exploited by virologist to add one strategy to fight against viruses.

MATERIALS AND METHODS

Yeast and E. coli strains

BY4741 , Top10, Codon plus described in chapters 2 and 3.

Plasmids:

pMAL-CNV-33, pMAL-CNV-92, pMAL-CNV-mutants, pMAL-CNV-33C, pMAL-CNV-33C(Mutants), Desired ORFs were amplified and cloned into pMAL vector digested with the same pair of enzymes.

Site directed mutagenesis.

A full-length cDNA clone of CNV, was used to generate the RPR motif mutants of p33/p92 listed in Figure 4.1. Mutagenesis was performed by PCR using the QuickChange XL Site-Directed Mutagenesis Kit (Stratagene). The PCR reactions included the *Pfu* Turbo DNA polymerase, different sets of primer pairs designed for each mutant and 40 ng of DNA as a template. PCR products were digested with *DpnI* before transformation into *E. coli* (DH5 α). The

presence of the desired mutations was confirmed by sequencing with primer (5'-GTATTTACACCAAGGGAC-3').

Cell free extract based in vitro replication assay.

The cell-free extract was prepared from yeast strain BY4741, untransformed as described [55, 73]. Briefly, the CFE (1 μ l) was pre-incubated on ice for 10 min in 10 μ l cell-free replication buffer containing 50 mM HEPES-KOH, pH 7.4, 150 mM potassium acetate, 5 mM magnesium acetate, 0.2 M sorbitol, and 0.4 μ l actinomycin D (5 mg/ml). Then, the reaction volume was adjusted to 20 μ l with 1x cell-free replication buffer also containing 2 μ l of 150 mM creatine phosphate; 2 μ l of 10 mM ATP, CTP, and GTP and 0.25 mM UTP; 0.3 μ l of [³²P]UTP, 0.2 μ l of 10-mg/ml creatine kinase, 0.2 μ l of RNase inhibitor, 0.2 μ l of 1 M dithiothreitol, and 0.5 μ g RNA transcript. The reaction mixture also contained 4 pmol MBP tagged CNV p33 and 1 pmol MBP-p92 purified from *E. coli* cells. This reaction mixture was incubated at 25°C for 3 h. The reaction was terminated by adding 110 μ l stop buffer (1% sodium dodecyl sulfate [SDS] and 0.05 M EDTA, pH 8.0), followed by phenol-chloroform extraction, isopropanol-ammonium acetate precipitation, and a washing step with 70% ethanol as described earlier. The RNA samples were electrophoresed under denaturing conditions (5% PAGE containing 8 M urea) and analyzed by phospho-imaging using a Typhoon (GE) instrument as described [75].

Purification of the recombinant tombusvirus replicase from yeast.

Yeast cells transformed with pGBK-His33, pGAD-His92 and pYC-DI72 were pre-grown in SC-ULH⁻ medium containing 2% glucose for 15 h at 29 °C with shaking at 250 rpm. The affinity-purification of the solubilized tombusvirus replicase was performed using ProBond resin (Invitrogen) as described [82]. The obtained template-dependent replicase was then used in a standard replicase reaction using either DI-72(-) or RI/RIII(-) exogenous templates and [³²P]UTP [75, 82].

In vitro RNA recruitment assay.

The recruitment assay was performed as described [76]. Briefly, recruitment assay based on yeast CFE and recombinant p33/p92 is similar to the replication assay, except for the following changes: [³²P]-labeled RNAs (2 pmol) were added to the CFE. In addition, only rATP and rGTP were used, while [³²P]UTP was omitted. The assay was performed at room temperature for 1 h. Then, the mixture was suspended in 980 μ l of pre-chilled Buffer A and centrifuged at 35,000g for 30 min at 4°C. Supernatant was discarded and the washing of the pellet was repeated twice. After final washing, the pellet was dissolved in 120 μ l of stop buffer (1% sodium dodecyl sulfate [SDS] and 0.05 M EDTA, pH 8.0). Afterwards standard RNA extraction and purification was performed followed by autoradiography of the electrophoresed RNA samples as described [75].

In vitro assembly and purification of replicase complex.

The cell free replication assay was conducted at 20°C for 1 h as described above except for following changes: The reaction volume was increased to 200 μ l, while the final concentration of DTT was reduced from 10 mM to 2.5 mM. In addition, only rATP and rGTP were used, while [³²P]UTP was omitted. The recombinant p33 was dually tagged with both MBP and 6xHis. After incubation, the assay mixture was diluted with 800 μ l chilled solubilization buffer and affinity-purification was done exactly as described [75, 82].

In vitro RdRp assay.

I used affinity-purified recombinant TCV p88C or affinity-purified CNV replicase from yeast in an RdRp assay as described [82, 110]. Briefly, the RdRp reaction was performed in 100 μ l volume containing RdRp buffer [40 mM Tris pH 8.0, 10 mM MgCl₂, 10 mM DTT, 0.2 μ l RNase inhibitor, 1 mM ATP, CTP, GTP, 0.1 μ l radioactive [³²P]UTP and 50 μ l RdRp fraction. As an external template, 300 ng of DI-72(-) RNA or RI/RIII(-) RNA were added. Samples were incubated at 25 °C for 2 h. The reaction was terminated by adding 70 μ l SDS/EDTA (1% SDS,

50 mM EDTA pH 8.0) and 100 μ l phenol-chloroform (1:1). The analysis of RdRp products was as described [82, 110].

Electromobility gel shift assay.

The affinity-purified recombinant proteins in twofold dilution series were incubated with 1 ng of radioactively labeled probe (see above) in a binding buffer (50 mM Tris-HCl [pH 8.2], 10 mM MgCl₂, 10 mM dithiothreitol, 10% glycerol, 100 ng of yeast tRNA [Sigma], and 2 U of RNase inhibitor [Ambion]) at 25°C for 15 min [28]. After the binding reaction, the samples were analyzed by 4 or 5% nondenaturing PAGE in Tris-acetate-EDTA buffer at 200 V in a cold room [28]. The gels were dried, exposed, and analyzed in a phosphorimager and quantified by using ImageQuant version 1.2 (Amersham).

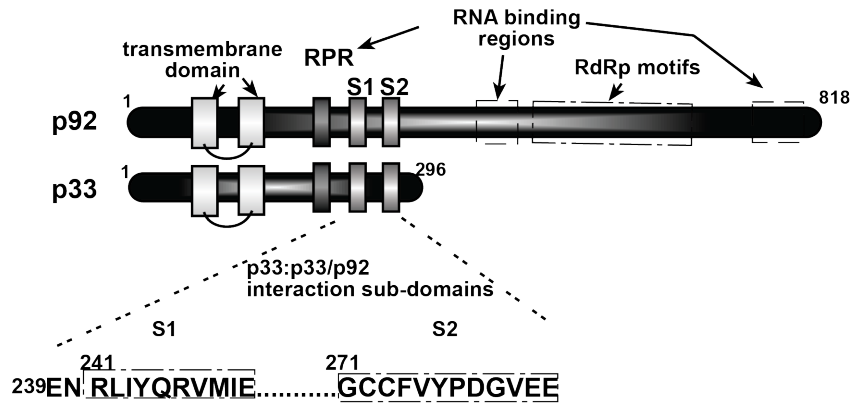
Protein purification from E. coli.

The MBP-tagged p33, p92, p33/p92 mutants and *Turnip crinkle virus* p88C were purified from *E. coli* as described by [28, 110]. Briefly, expression of the MBP tagged proteins was induced by isopropyl-d-thiogalactopyranoside (IPTG) in Epicurion BL21-codon-plus (DE3)-RIL cells (Stratagene). Cells were suspended in the column buffer (10 mM Tris-HCl [pH 7.4], 1 mM EDTA, 25 mM NaCl, 10 mM β -mercaptoethanol) and were broken by sonication, and then the cell lysate was passed through the equilibrated amylose columns to bind MBP tagged proteins. After passing the cell lysate, the columns were washed three times with ice-cold column buffer and eluted with column buffer containing 10 mM maltose and stored at -80°C until further use.

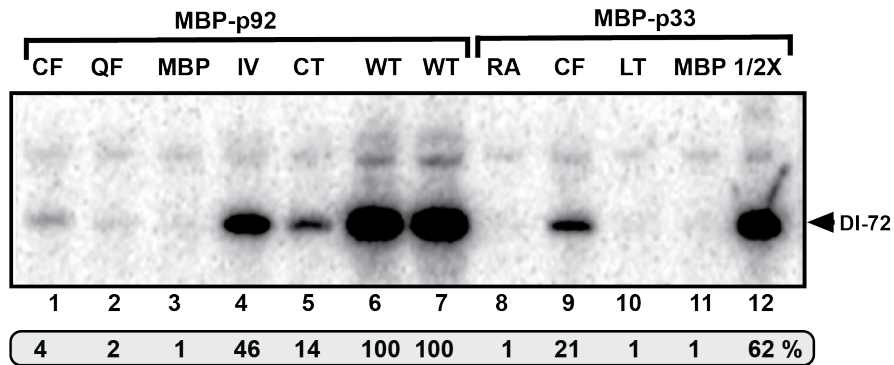
Confocal microscopy.

Confocal laser scanning micrographs were acquired on a Olympus FV1000 microscope (Olympus America Inc., Melville, New York) as described earlier [106]. ECFP was excited using 440 nm laser light, attenuated to 4.5-11.0% of the maximum laser power, while EYFP was excited using 515 nm laser line (3.5-8.0% of the maximum laser power). The images were acquired using sequential line-by-line mode in order to reduce excitation and emission cross-talk. The primary objective used was a water-immersion PLAPO60XWLSM (Olympus). Image acquisition was conducted at a resolution of 512x512 pixels and a scan-rate of 10 ms/pixel. Image acquisition and exportation of TIFF files were controlled by using Olympus Fluoview software version 1.5. Figures of micrographs were assembled using Photoshop 9.0 (Adobe Systems Incorporated, San Jose, CA).

A.



B. Yeast Cell free extract (CFE) replication assay:



C. Coomassie:

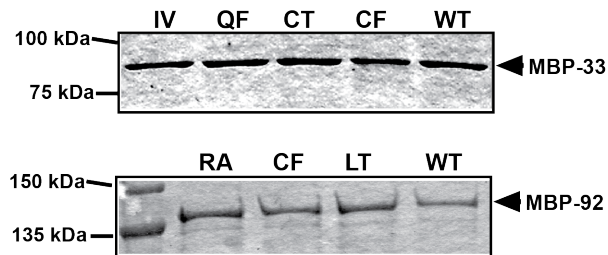
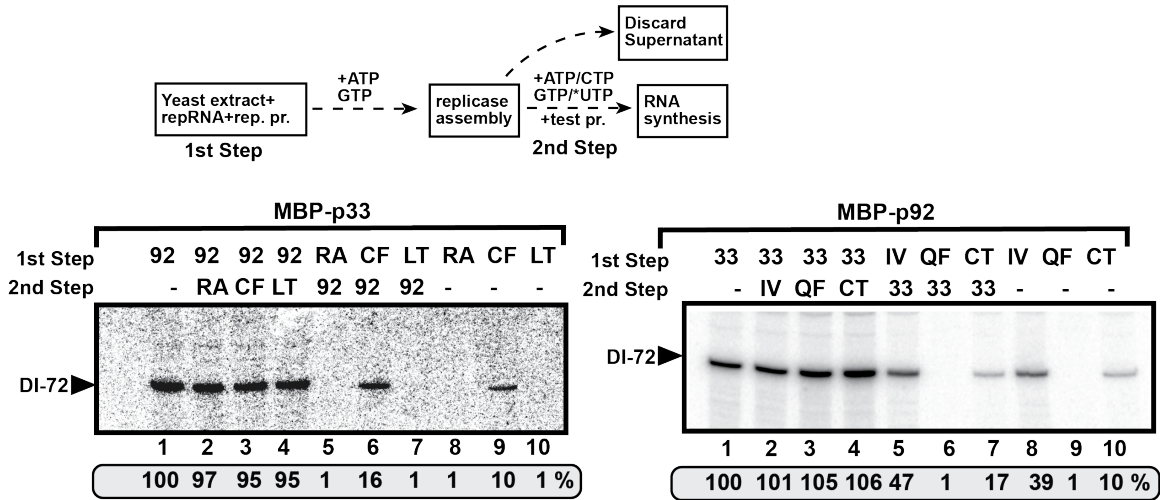


Figure 4.1. Mutations in S1/S2 domains of p33/p92 inhibits viral replication *in vitro*.

(A) Cartoons of p33 (positions 1-296 aa) and p92 (positions 1-818 aa). A read through product depicting protein-protein interactions sub-domains S1, S2 in context of other functional domains like RNA binding (RPR) and two trans-membrane domains. S1 domain (positions 241-251 aa) and S2 domain (positions 271-283 aa) are zoomed to show their amino acid sequences. Quick-change™ site-specific mutagenesis approach was used to introduce specific mutations (see *Materials and methods*) in the S1/S2 domains followed by fusing the MBP tag on NH₂-terminal end of mutant p33/p92. The two-letters names show respective amino acid changes and WT represents wild-type proteins. (B) A representative denaturing PAGE gel of newly synthesized ³²P-labeled repRNA in an *in vitro* CFE replication assay (shown as a flowchart) using purified recombinant proteins (rec.pr.) with equal amounts of DI72(+) as a repRNA. The full-length product is shown with arrowhead. Experiments were repeated three times and quantified using Imagequant®. (C) Coomassie blue staining after SDS-PAGE shows similar amounts of the amylose column purified recombinant MBP-p33 proteins (top panel) or MBP-p92 (bottom panel) used in the above CFE replication assays.

Cell free extract (CFE) replicase assay

A Scheme of *in vitro* replication assay in CFE:



B Scheme of *in vitro* replication assay in CFE:

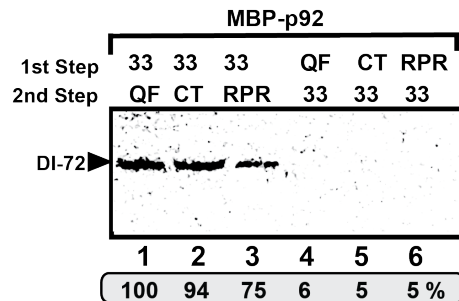
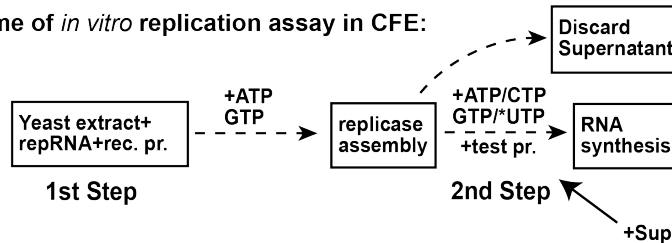
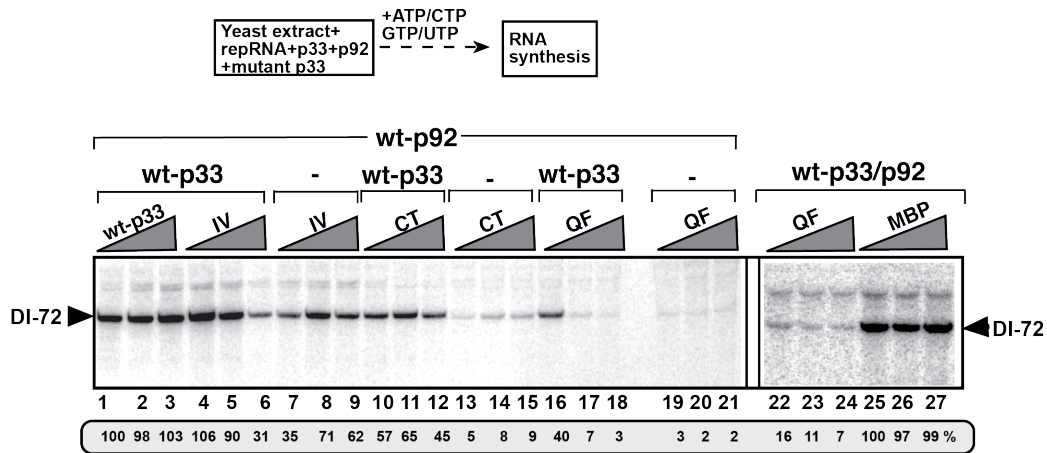


Figure 4.2. Mutant replication proteins' activity can't be rescued by wild-type p33/p92.

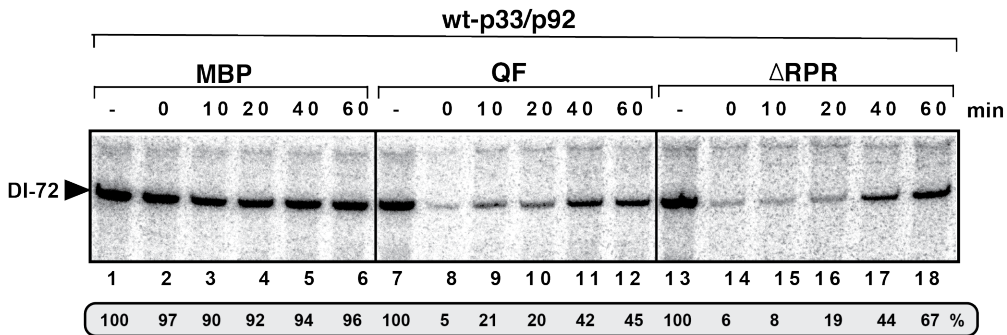
(A) Denaturing PAGE analysis of the CFE-based replication assay for wild type p92 and its mutants on left-hand side and for p33 and its mutants on right-hand panel. The ability of wild type or mutant replication proteins to affect the *in vitro* replication assay was tested after the first step (see scheme) of replication assay that was started using yeast CFE, repRNA and affinity

purified recombinant TBSV wild type or mutant p33 and p92^{pol} (as shown) and only two ribonucleotides (rATP and rGTP) so that the replication process could be arrested just after assembly of the replicase complex. Thereafter, the assembled replicase was centrifuged, supernatant discarded and the replication assay was continued with all four nucleotides including radiolabeled rUTP and the additional recombinant replication proteins. The authentic replication product is depicted with arrowheads on the left. (B) The CFE replication assay was performed as in (A) with only difference being that supernatant (+Sup) obtained after centrifuging yeast extract at 35000 g (containing soluble host factors) was added at the second step (see scheme) to help membrane insertion of the added wild-type p33 (lanes 4-6) or the p33 mutants (lanes 1-3). The replication product is shown with an arrowhead on a representative RNA-PAGE denaturing gel.

A. CFE replication assay:



B. Time-course CFE replication assay:



C. Time-course CFE replication assay:

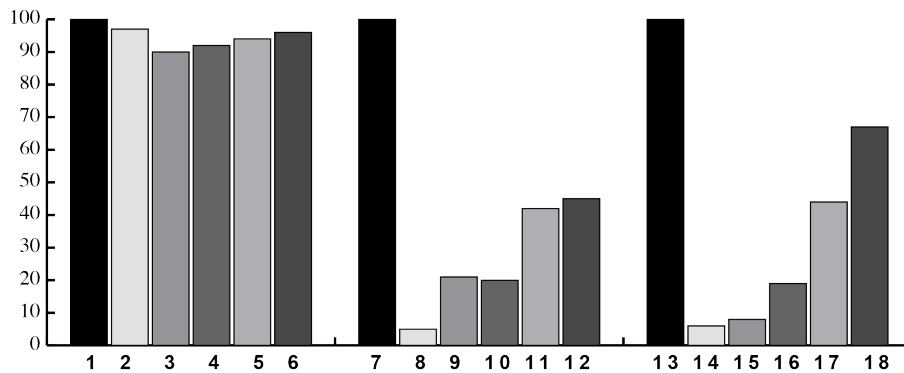
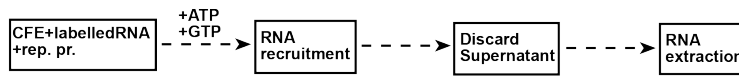


Figure 4.3 Dominant negative effect of p33-Q₂₄₅F mutant during *in vitro* CFE replication.

The replication assay was performed as shown in the scheme at the top. (A) Increasing amounts of test proteins (MBP and MBP-p33 as controls or p33 mutants) were added simultaneously with wild type p33, p92, repRNA, CFE and ribonucleotides to see their effect on replication. DI-72 sized product is depicted with arrowheads on both panels. (B) The maximum dominant negative effect of the mutants is exerted early during replication assembly. The *in vitro* replicase assay in

CFE was done using two different p33 mutants as shown. I provided the recombinant proteins at the 0, 10, 20, 40 or 60 min time points followed by continuation of the *in vitro* replicase assay up to 2 hours. The denaturing PAGE analysis of the ³²P-labeled repRNA products obtained is shown. (C) Graphical representation of the data from (B). The experiments were repeated and mock treated samples were arbitrarily assigned 100% value.

Scheme of *in vitro* RNA recruitment assay:



***In vitro* RNA recruitment assay:**

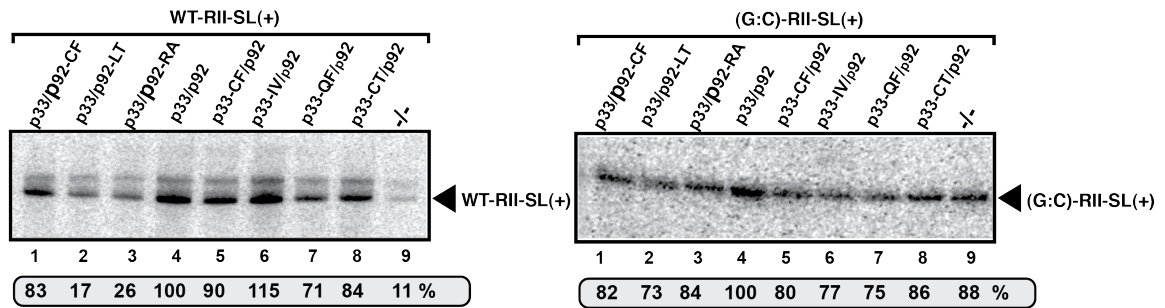
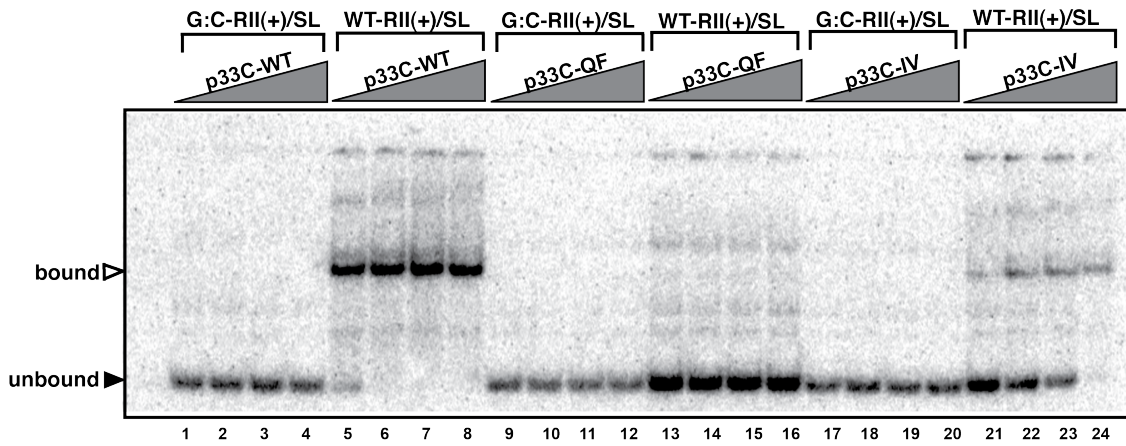


Figure 4.4 *In vitro* RNA recruitment to membranes affected by p92 mutants.

As depicted in the top scheme, the CFE was programmed with recombinant proteins, and radiolabeled wt-RII-SL(+) on the left-side panel and C→G mutation containing RNA shown on the right-hand panel. Retention of RNA to the membranes was checked by centrifuging the CFE and collecting the membranes followed by PAGE and autoradiography of phenol-chloroform extracted RNA samples. Please note that only rATP and rGTP were provided so that recruitment of the respective RNAs may not be carried to replication.

A. *In vitro* RNA binding electro mobility gel shift assay



B. *In vitro* RNA binding electro mobility gel shift assay

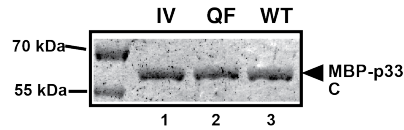
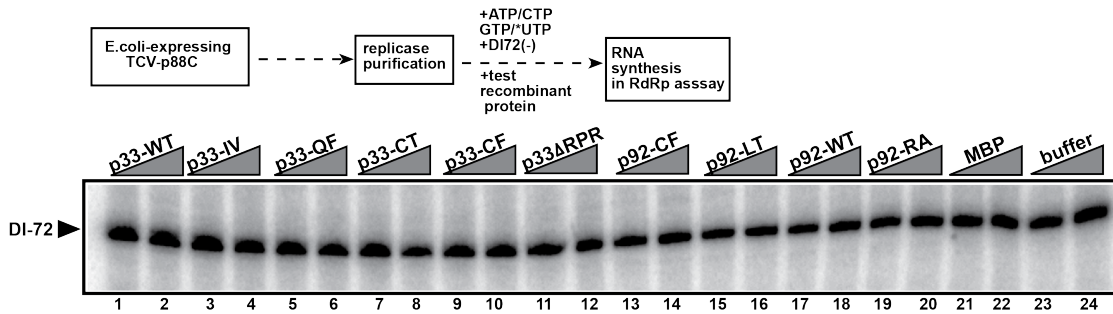


Figure 4.5. p33-Q₂₄₅F mutant is inefficient in binding viral RNA.

(A) EMSA was performed with 2, 4, 8 or 16 pmol purified MBP tagged wt or mutant p33C (150-296 aa) [shown with grey triangles]. 10 nM of Wt-RII(+)/SL RNA or C→G mutation containing RII(+)/SL RNA were used. Solid arrowhead depicts the unbound RNA probe whereas bound RNA-protein complexes are depicted by empty arrowhead. (B) SDS-PAGE followed by Coomassie blue staining of the proteins used in (A).

A. In vitro RdRp assay with TCV-p88C

Scheme of *in vitro* TCV p88c RdRp assay:



B. In vitro RdRp assay with CNV replicase purified from yeast

Scheme of *in vitro* RdRp assay from yeast:

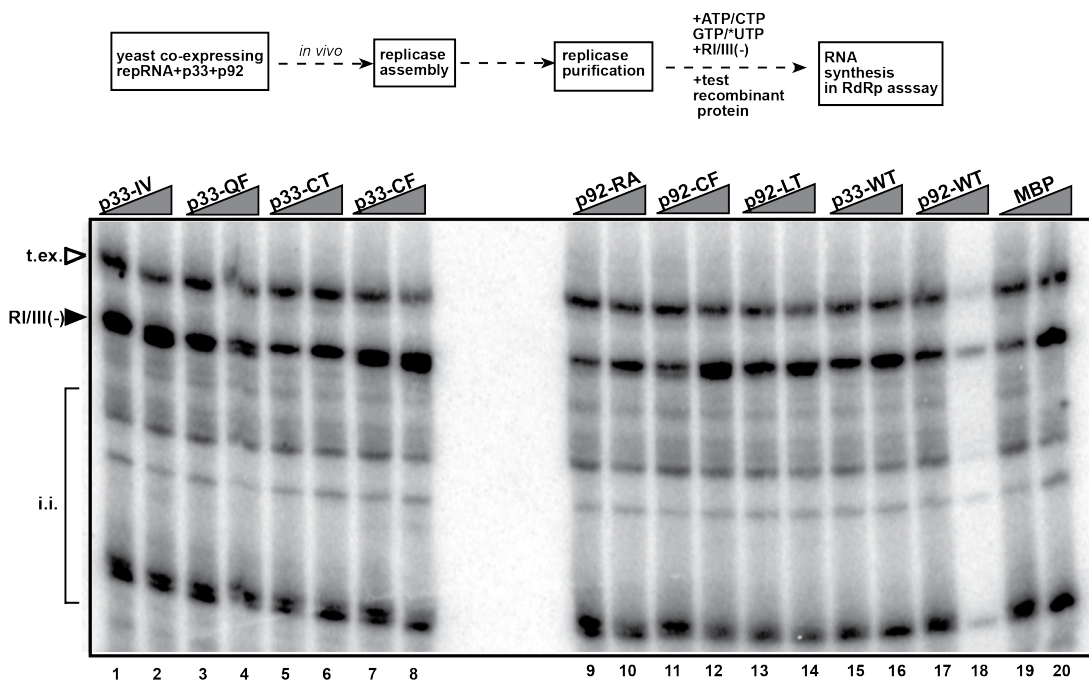
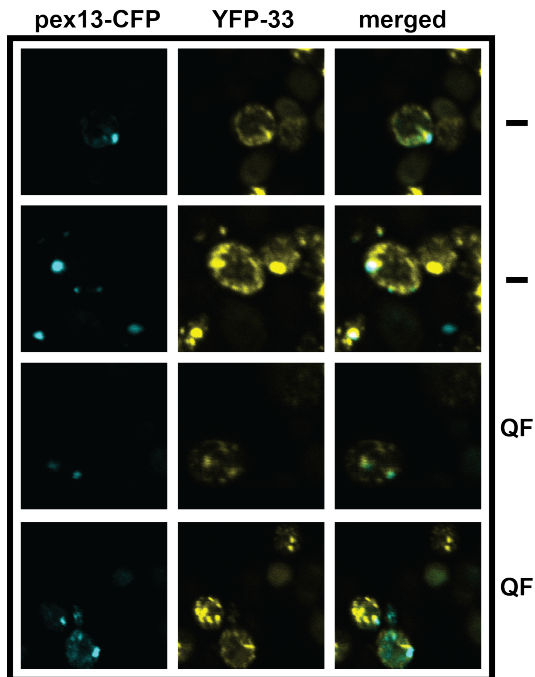


Figure 4.6 p33 mutants do not exert dominant negative effect on the RdRp activity of purified replicase complexes.

(A) Increasing amounts (2, 4 pmol) of wt p33 or wt p92 or different mutants were added to the *E. coli* purified and highly active RdRp (p88C) from TCV into the *in vitro* RdRp assay together with ribonucleotides including radiolabeled rUTP and template RNA DI72(-). Full-length *de novo* RNA product is shown with an arrowhead on left. (B) As shown in the scheme, effect of the mutant or wild type recombinant proteins (2, 4 pmol) were tested on the RdRp activity of CNV replicase, affinity purified from yeast co-expressing p33, p92 and DI72(+). RI/III(-) RNA was used as a template. Empty arrowhead depicts terminal extension product (tex), the solid arrowhead shows the *de novo* product RI/III(-) and the bracket represents internal initiation (ii) RdRp products.

A. Colocalization of p33 with peroxisome



B. Colocalization of p33 with ER

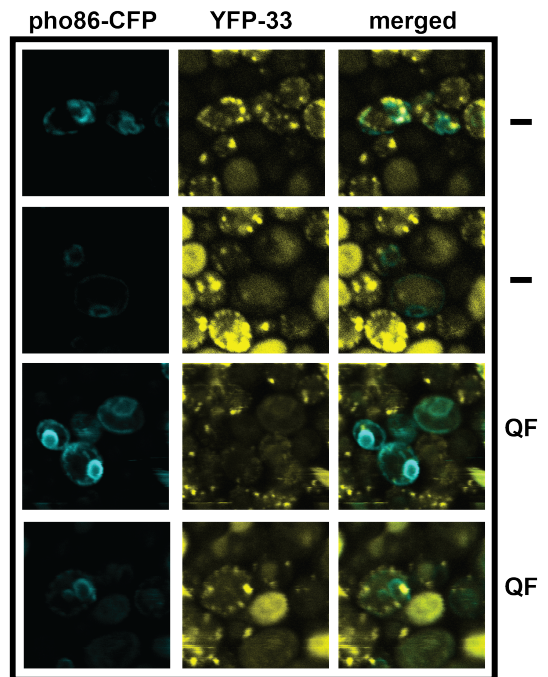


Figure 4.7. Peroxisomal localization and punctate pattern of wt-p33 is not affected by expression of Q₂₄₅F-p33 mutant in yeast.

Confocal laser microscopy analysis of subcellular localization [tracked for peroxisomes by pex13-CFP in (A) or ER by pho86-CFP in (B)] of NH₂-terminally YFP tagged wt-p33 in the presence Q₂₄₅F-p33 mutant (QF) or an empty vector (-). The images were taken 24 h post-induction. QF, pex13-CFP and pho86-CFP were expressed under constitutive *ADHI* promoter and p33-YFP was expressed from the *GALI* promoter, in wt BY4741 yeast cells.

In vitro replicase assembly assay

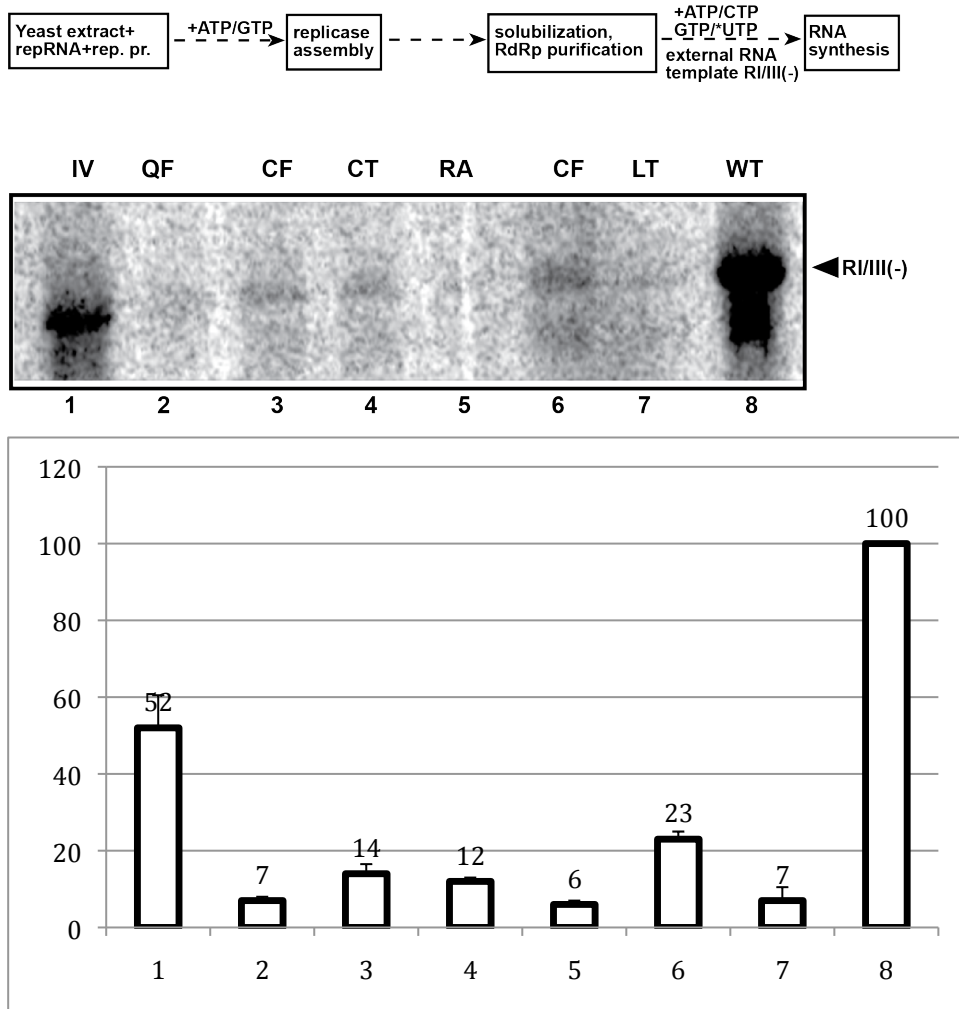


Figure 4.8. Denaturing PAGE analysis of the CFE-based replication assay.

The *in vitro* reconstitution assay contained yeast CFE, affinity purified recombinant CNV p33 and p92^{pol} or the p33 mutants with wild type p92 or the p92 mutants with wild type p33, and the same amount of various TBSV repRNA templates (as shown). After the *in vitro* reconstitution, the assembled replication complexes were purified (see scheme) by affinity chromatography and then the activity was tested using RI/RIII(-) template. The full-length RNA product is depicted with an arrowhead on the right. Note that the repRNAs (see scheme) serve only as assembly factor in this assay. (B) Graphical representation of the data obtained in panel (A) after three repeats. Wild type was arbitrarily assigned a value of 100%. Abscissa denotes the different mutants (lanes 1-7) and wild type control (lane 8) and ordinate represents the percentage activity on the external template RI/RIII(-).

Chapter 5. Summary

Two of the vital replication proteins p33 and p92 of tombusvirus a model positive strand RNA virus also directly interact with themselves via protein-protein interaction sub-domains S1 and S2. To dissect the different steps during RNA replication where this interaction plays essential role(s) I tested selected p33 and p92 interaction mutants in the replicase assay based on cell free extract from yeast that can support authentic replication of TBSV RNA *in vitro* utilizing purified replication proteins and host factors. This assay demonstrated that some of the S1 or S2 mutants were completely defunct for replication. Further RNA binding analyses revealed that Glutamine to Phenylalanine mutation at 245 aa position in p33 (Q₂₄₅F) completely abolished its ability to bind to viral RNA. I also found strong dominant negative effect of Q₂₄₅F on the replication started by wild type replication proteins. Using *in vitro* replicase assembly assay, I found close correlation between interaction and the ability to assemble active replication complex. In addition, I show that the interaction defective mutants are not able to modify RNA dependent RNA polymerase (RdRp) activity of purified *Turnip crinckle virus* (TCV) polymerase p88 and CNV replicase preparations suggesting that already assembled replicases are not prone to modification through protein-protein interaction domain. The results provide new insights into the replication proteins RNA template selection and subsequently in replicase complex assembly. Also I discovered a novel dominant negative replication protein mutant that can abolish viral replication.

Replication of *Tomato bushy stunt virus* (TBSV) RNA takes place on the cytosolic membrane surface of peroxisomes in plants and in yeast, a model host. To identify the host proteins involved in assisting the peroxisomal localization of the tombusvirus p33 replication protein, I tested if p33 could bind directly to yeast proteins involved in peroxisomal transport *in vitro*. This work led to the demonstration of Pex19p-p33 interaction via pull-down and co-purification experiments. Pex19p was also detected in the tombusvirus replicase after protein cross-linking, suggesting that Pex19p transiently binds to the replicase as could be expected from a transporter. To validate the importance of Pex19p - p33 interaction in TBSV replication in yeast, I re-targeted Pex19p to the mitochondria, which resulted in the re-distribution of a large fraction of p33 to the mitochondria. The expression of the mitochondrial-targeted Pex19p inhibited TBSV RNA accumulation by 2-4-fold *in vivo* and reduced the *in vitro* activity of the tombusvirus replicase by 80%. These data support the model that Pex19p is the cellular transporter for localization of p33 replication protein to the host peroxisomal membranes.

The studies presented in Chapter two revealed the critical role of viral genome in its replication beyond its usage as a genetic carrier. In addition to its central role as a template for replication and translation, the viral (+)RNA genome also has non-template functions, such as recruitment to the site of replication and assembly of the viral replicase; activities that are mediated by cis-acting RNA elements within viral genomes. Two non-contiguous RNA elements, RII(+)-SL, located internally in the tombusvirus genome and RIV, located at the 3'-terminus, are involved in template recruitment into replication and replicase assembly. However, the importance of each of these RNA elements for these two distinct functions is unknown. I used an *in vitro* replicase assembly assay based on yeast cell-free extract and purified recombinant tombusvirus replication proteins to show that RII(+)-SL, in addition to its known requirement for recruitment of the (+)RNA into replication, is also necessary for assembly of an active viral replicase complex. Additional studies using a novel two-component RNA system revealed that the recruitment function of RII(+)-SL can be provided *in trans* by a separate RNA and that the replication silencer element, located within RIV, defines the template that is used for initiation of minus strand synthesis. Collectively, this work has revealed new functions for tombusvirus cis-acting RNA elements and provided insights into the pioneering round of minus strand synthesis.

These findings put the viral RNA into the central stage of its own replication where it orchestrates the entire series of events starting from disassembly, template selection/recruitment, formation of replication complex and transcription of the complementary strands and in the ensuing steps. Different viruses positive strand RNA viruses share some common principles like, viral RNA codes for a specific region in order to bind to the early replication proteins and it also contains some other secondary structures that are subsequently needed in order to form active replicase complexes utilizing viral proteins, host factors and host membranes. Contemporarily, many essential questions remain or have become apparent from these works. Among these unsettled queries are the thorough molecular mechanisms by which the RNA helps to assemble the replication complexes. It is evident that RNA doesn't play a major role in targeting of the proteins to the organellar membranes for formation of specialized replication structures. Discovery of many viral RNA binding proteins affecting replication indicates that RNAs might coordinate the usurping of critical host factors for assembly of replication complex. Related issues would be how the viruses temporally and spatially regulate the replication processes using just its RNA. Clues may lie in the dynamics of the secondary structures and long-range interactions occurring on the RNA molecule. It can be imagined that the structural studies will become even more complex because of discoveries of more host-factors binding to the RNA and heavily modifying its structure to achieve a different secondary/tertiary structure. It is also possible that positive strand RNA viruses use their RNAs upon entry into the cells to monitor the conduciveness of their hosts for replication by sensing protein(s) via binding. Making an analogy of viral RNA role during replicase assembly to the rRNA role in ribosomal assembly is also not far-fetched. As during both, ribosome assembly and replicase complex assembly, RNAs provide necessary factors as well as an assembly platform. The viral RNA is already known to play a critical role during assembly of virion particles, henceforth extending their ability to assemble a complex using proteins onto the membranous compartments for replication.

The novel roles of viral RNA, viral proteins and host factor should enrich the understanding of viral replication at the same time provide new challenges and opportunities to virologists to help improve antiviral strategies. In this regards, one crucial area to work on will be to disrupt the viral RNA:viral/host-protein or viral protein:viral/host-protein interaction through chemicals or RNA biology tools. Undoubtedly, the emerging picture is complicated but will provide important insights in the area of viral biology.

REFERENCES

1. Ray D, White KA. An internally located RNA hairpin enhances replication of Tomato bushy stunt virus RNAs. *J Virol* 2003,**77**:245-257.
2. Lai M, Liaw YF. Chronic hepatitis B: past, present, and future. *Clinics in liver disease* 2010,**14**:531-546.
3. Ahlquist P, Noueir AO, Lee W-M, Kushner DB, Dye BT. Host Factors in Positive-Strand RNA Virus Genome Replication. *J. Virol.* 2003,**77**:8181-8186.
4. Li Z, Nagy PD. Diverse roles of host RNA binding proteins in RNA virus replication. *RNA Biol* 2011,**8**:305-315.
5. Nagy PD. Yeast as a model host to explore plant virus-host interactions. *Annu Rev Phytopathol* 2008,**46**:217-242.
6. Nagy PD, Pogany J. Yeast as a model host to dissect functions of viral and host factors in tombusvirus replication. *Virology* 2006,**344**:211-220.
7. Nagy PD, Pogany J. Global genomics and proteomics approaches to identify host factors as targets to induce resistance against tomato bushy stunt virus. *Adv Virus Res* 2010,**76**:123-177.
8. Birn AE. Small(pox) success? *Ciencia & saude coletiva* 2011,**16**:591-597.
9. Wommack KE, Colwell RR. Virioplankton: viruses in aquatic ecosystems. *Microbiology and molecular biology reviews : MMBR* 2000,**64**:69-114.
10. Lu TK, Koeris MS. The next generation of bacteriophage therapy. *Current opinion in microbiology* 2011.
11. Herzog RW, Cao O, Srivastava A. Two decades of clinical gene therapy--success is finally mounting. *Discovery medicine* 2010,**9**:105-111.
12. Tarascon JM. Nanomaterials: Viruses electrify battery research. *Nature nanotechnology* 2009,**4**:341-342.
13. Panavas T, Nagy PD. Yeast as a model host to study replication and recombination of defective interfering RNA of Tomato bushy stunt virus. *Virology* 2003,**314**:315-325.
14. Panavas T, Serviene E, Pogany J, Nagy PD. Genome-wide screens for identification of host factors in viral replication. *Methods Mol Biol* 2008,**451**:615-624.
15. Panavas T, Serviene E, Brasher J, Nagy PD. Yeast genome-wide screen reveals dissimilar sets of host genes affecting replication of RNA viruses. *Proc Natl Acad Sci U S A* 2005,**102**:7326-7331.
16. Jiang Y, Serviene E, Gal J, Panavas T, Nagy PD. Identification of essential host factors affecting tombusvirus RNA replication based on the yeast Tet promoters Hughes Collection. *J Virol* 2006,**80**:7394-7404.
17. Serva S, Nagy PD. Proteomics analysis of the tombusvirus replicase: Hsp70 molecular chaperone is associated with the replicase and enhances viral RNA replication. *J Virol* 2006,**80**:2162-2169.
18. Li Z, Pogany J, Panavas T, Xu K, Esposito AM, Kinzy TG, *et al.* Translation elongation factor 1A is a component of the tombusvirus replicase complex and affects the stability of the p33 replication co-factor. *Virology* 2009,**385**:245-260.
19. Mendu V, Chiu M, Barajas D, Li Z, Nagy PD. Cpr1 cyclophilin and Ess1 parvulin prolyl isomerases interact with the tombusvirus replication protein and inhibit viral replication in yeast model host. *Virology* 2010,**406**:342-351.
20. Serviene E, Shapka N, Cheng CP, Panavas T, Phuangrat B, Baker J, *et al.* Genome-wide screen identifies host genes affecting viral RNA recombination. *Proc Natl Acad Sci U S A* 2005,**102**:10545-10550.

21. Serviene E, Jiang Y, Cheng CP, Baker J, Nagy PD. Screening of the yeast yTHC collection identifies essential host factors affecting tombusvirus RNA recombination. *J Virol* 2006,**80**:1231-1241.
22. Friedel CC, Haas J. Virus-host interactomes and global models of virus-infected cells. *Trends in microbiology* 2011.
23. Scholthof KB, Scholthof HB, Jackson AO. The tomato bushy stunt virus replicase proteins are coordinately expressed and membrane associated. *Virology* 1995,**208**:365-369.
24. Oster SK, Wu B, White KA. Uncoupled expression of p33 and p92 permits amplification of tomato bushy stunt virus RNAs. *Journal of virology* 1998,**72**:5845-5851.
25. Panaviene Z, Baker JM, Nagy PD. The overlapping RNA-binding domains of p33 and p92 replicase proteins are essential for tombusvirus replication. *Virology* 2003,**308**:191-205.
26. Rajendran KS, Nagy PD. Interaction between the replicase proteins of Tomato bushy stunt virus *in vitro* and *in vivo*. *Virology* 2004,**326**:250-261.
27. White KA, Nagy PD. Advances in the molecular biology of tombusviruses: gene expression, genome replication, and recombination. *Prog Nucleic Acid Res Mol Biol* 2004,**78**:187-226.
28. Rajendran KS, Nagy PD. Characterization of the RNA-binding domains in the replicase proteins of tomato bushy stunt virus. *J Virol* 2003,**77**:9244-9258.
29. Panavas T, Panaviene Z, Pogany J, Nagy PD. Enhancement of RNA synthesis by promoter duplication in tombusviruses. *Virology* 2003,**310**:118-129.
30. Panavas T, Hawkins CM, Panaviene Z, Nagy PD. The role of the p33:p33/p92 interaction domain in RNA replication and intracellular localization of p33 and p92 proteins of Cucumber necrosis tombusvirus. *Virology* 2005,**338**:81-95.
31. Navarro B, Rubino L, Russo M. Expression of the Cymbidium ringspot virus 33-kilodalton protein in *Saccharomyces cerevisiae* and molecular dissection of the peroxisomal targeting signal. *Journal of virology* 2004,**78**:4744-4752.
32. Rajendran KS, Nagy PD. Kinetics and functional studies on interaction between the replicase proteins of Tomato Bushy Stunt Virus: requirement of p33:p92 interaction for replicase assembly. *Virology* 2006,**345**:270-279.
33. Huang AS. Defective interfering viruses. *Annu Rev Microbiol* 1973,**27**:101-117.
34. Simon AE, Roossinck MJ, Havelda Z. Plant virus satellite and defective interfering RNAs: new paradigms for a new century. *Annu Rev Phytopathol* 2004,**42**:415-437.
35. Perrault J. Origin and replication of defective interfering particles. *Curr Top Microbiol Immunol* 1981,**93**:151-207.
36. Qiu W, Scholthof KB. Defective interfering RNAs of a satellite virus. *J Virol* 2001,**75**:5429-5432.
37. Luytjes W, Gerritsma H, Spaan WJ. Replication of synthetic defective interfering RNAs derived from coronavirus mouse hepatitis virus-A59. *Virology* 1996,**216**:174-183.
38. White KA, Morris TJ. Nonhomologous RNA recombination in tombusviruses: generation and evolution of defective interfering RNAs by stepwise deletions. *J Virol* 1994,**68**:14-24.
39. Rochon DM. Rapid de novo generation of defective interfering RNA by cucumber necrosis virus mutants that do not express the 20-kDa nonstructural protein. *Proc Natl Acad Sci U S A* 1991,**88**:11153-11157.
40. Rubino L, Burgyan J, Grieco F, Russo M. Sequence analysis of cymbidium ringspot virus satellite and defective interfering RNAs. *J Gen Virol* 1990,**71** (Pt 8):1655-1660.
41. Pogany J, Romero J, Huang Q, Sgro JY, Shang H, Bujarski JJ. De novo generation of defective interfering-like RNAs in broad bean mottle bromovirus. *Virology* 1995,**212**:574-586.

42. Li XH, Heaton LA, Morris TJ, Simon AE. Turnip crinkle virus defective interfering RNAs intensify viral symptoms and are generated de novo. *Proc Natl Acad Sci U S A* 1989,**86**:9173-9177.
43. Hillman BI, Carrington JC, Morris TJ. A defective interfering RNA that contains a mosaic of a plant virus genome. *Cell* 1987,**51**:427-433.
44. Hernandez C, Carette JE, Brown DJ, Bol JF. Serial passage of tobacco rattle virus under different selection conditions results in deletion of structural and nonstructural genes in RNA 2. *J Virol* 1996,**70**:4933-4940.
45. Eliasco E, Livieratos IC, Muller G, Guzman M, Salazar LF, Coutts RH. Sequences of defective RNAs associated with potato yellow vein virus. *Arch Virol* 2006,**151**:201-204.
46. Desvoyes B, Scholthof HB. Host-dependent recombination of a Tomato bushy stunt virus coat protein mutant yields truncated capsid subunits that form virus-like complexes which benefit systemic spread. *Virology* 2002,**304**:434-442.
47. Ayllon MA, Lopez C, Navas-Castillo J, Mawassi M, Dawson WO, Guerri J, *et al.* New defective RNAs from citrus tristeza virus: evidence for a replicase-driven template switching mechanism in their generation. *J Gen Virol* 1999,**80** (Pt 3):817-821.
48. White KA, Morris TJ. Defective and defective interfering RNAs of monopartite plus-strand RNA plant viruses. *Curr Top Microbiol Immunol* 1999,**239**:1-17.
49. Nagy PD, Simon AE. New insights into the mechanisms of RNA recombination. *Virology* 1997,**235**:1-9.
50. Kim MJ, Kao C. Factors regulating template switch *in vitro* by viral RNA-dependent RNA polymerases: implications for RNA-RNA recombination. *Proc Natl Acad Sci U S A* 2001,**98**:4972-4977.
51. Cheng CP, Nagy PD. Mechanism of RNA recombination in carmo- and tombusviruses: evidence for template switching by the RNA-dependent RNA polymerase *in vitro*. *J Virol* 2003,**77**:12033-12047.
52. Cheng CP, Pogany J, Nagy PD. Mechanism of DI RNA formation in tombusviruses: dissecting the requirement for primer extension by the tombusvirus RNA dependent RNA polymerase *in vitro*. *Virology* 2002,**304**:460-473.
53. Wierzoslawski R, Bujarski JJ. Efficient *in vitro* system of homologous recombination in brome mosaic bromovirus. *J Virol* 2006,**80**:6182-6187.
54. Wierzoslawski R, Dzionot A, Kunimalayan S, Bujarski JJ. A transcriptionally active subgenomic promoter supports homologous crossovers in a plus-strand RNA virus. *J Virol* 2003,**77**:6769-6776.
55. Pogany J, Nagy PD. Authentic replication and recombination of Tomato bushy stunt virus RNA in a cell-free extract from yeast. *J Virol* 2008,**82**:5967-5980.
56. Cheng CP, Panavas T, Luo G, Nagy PD. Heterologous RNA replication enhancer stimulates *in vitro* RNA synthesis and template-switching by the carmovirus, but not by the tombusvirus, RNA-dependent RNA polymerase: implication for modular evolution of RNA viruses. *Virology* 2005,**341**:107-121.
57. Nagy PD, Simon AE. *In vitro* characterization of late steps of RNA recombination in turnip crinkle virus. I. Role of motif1-hairpin structure. *Virology* 1998,**249**:379-392.
58. Nagy PD, Simon AE. *In vitro* characterization of late steps of RNA recombination in turnip crinkle virus.II. The role of the priming stem and flanking sequences. *Virology* 1998,**249**:393-405.
59. Bujarski JJ, Nagy PD, Flasiniski S. Molecular studies of genetic RNA-RNA recombination in brome mosaic virus. *Adv Virus Res* 1994,**43**:275-302.
60. Havelda Z, Szittyá G, Burgyan J. Characterization of the molecular mechanism of defective interfering RNA-mediated symptom attenuation in tombusvirus-infected plants. *J Virol* 1998,**72**:6251-6256.

61. Chetverin AB, Chetverina HV, Demidenko AA, Ugarov VI. Nonhomologous RNA recombination in a cell-free system: evidence for a transesterification mechanism guided by secondary structure. *Cell* 1997,**88**:503-513.
62. Gmyl AP, Korshenko SA, Belousov EV, Khitrina EV, Agol VI. Nonreplicative homologous RNA recombination: promiscuous joining of RNA pieces? *Rna* 2003,**9**:1221-1231.
63. Nagy PD, Dziafott A, Ahlquist P, Bujarski JJ. Mutations in the helicase-like domain of protein 1a alter the sites of RNA-RNA recombination in brome mosaic virus. *J Virol* 1995,**69**:2547-2556.
64. Figlerowicz M, Nagy PD, Bujarski JJ. A mutation in the putative RNA polymerase gene inhibits nonhomologous, but not homologous, genetic recombination in an RNA virus. *Proc Natl Acad Sci U S A* 1997,**94**:2073-2078.
65. Fodor E, Mingay LJ, Crow M, Deng T, Brownlee GG. A single amino acid mutation in the PA subunit of the influenza virus RNA polymerase promotes the generation of defective interfering RNAs. *J Virol* 2003,**77**:5017-5020.
66. Panaviene Z, Nagy PD. Mutations in the RNA-binding domains of tombusvirus replicase proteins affect RNA recombination in vivo. *Virology* 2003,**317**:359-372.
67. Jaag HM, Stork J, Nagy PD. Host transcription factor Rpb11p affects tombusvirus replication and recombination via regulating the accumulation of viral replication proteins. *Virology* 2007,**368**:388-404.
68. Nagy PD, Pogany J. Multiple roles of viral replication proteins in plant RNA virus replication. *Methods Mol Biol* 2008,**451**:55-68.
69. Pantaleo V, Rubino L, Russo M. Replication of Carnation Italian ringspot virus defective interfering RNA in *Saccharomyces cerevisiae*. *J Virol* 2003,**77**:2116-2123.
70. Li Z, Barajas D, Panavas T, Herbst DA, Nagy PD. Cdc34p ubiquitin-conjugating enzyme is a component of the tombusvirus replicase complex and ubiquitinates p33 replication protein. *J Virol* 2008,**82**:6911-6926.
71. Pogany J, White KA, Nagy PD. Specific binding of tombusvirus replication protein p33 to an internal replication element in the viral RNA is essential for replication. *J Virol* 2005,**79**:4859-4869.
72. Monkewich S, Lin HX, Fabian MR, Xu W, Na H, Ray D, *et al.* The p92 polymerase coding region contains an internal RNA element required at an early step in Tombusvirus genome replication. *J Virol* 2005,**79**:4848-4858.
73. Pogany J, Stork J, Li Z, Nagy PD. *In vitro* assembly of the Tomato bushy stunt virus replicase requires the host Heat shock protein 70. *Proc Natl Acad Sci U S A* 2008,**105**:19956-19961.
74. Pogany J, Fabian MR, White KA, Nagy PD. A replication silencer element in a plus-strand RNA virus. *EMBO J* 2003,**22**:5602-5611.
75. Panaviene Z, Panavas T, Nagy PD. Role of an internal and two 3'-terminal RNA elements in assembly of tombusvirus replicase. *J Virol* 2005,**79**:10608-10618.
76. Li Z, Pogany J, Tupman S, Esposito AM, Kinzy TG, Nagy PD. Translation elongation factor 1A facilitates the assembly of the tombusvirus replicase and stimulates minus-strand synthesis. *PLoS Pathog* 2010,**6**:e1001175.
77. Jiang Y, Li Z, Nagy PD. Nucleolin/Nsr1p binds to the 3' noncoding region of the tombusvirus RNA and inhibits replication. *Virology* 2010,**396**:10-20.
78. McCartney AW, Greenwood JS, Fabian MR, White KA, Mullen RT. Localization of the Tomato Bushy Stunt Virus Replication Protein p33 Reveals a Peroxisome-to-Endoplasmic Reticulum Sorting Pathway. *Plant Cell* 2005,**17**:3513-3531.
79. Russo M, Di Franco A, Martelli GP. Cytopathology in the identification and classification of tombusviruses. *Intervirology* 1987,**28**:134-143.

80. Pathak KB, Sasvari Z, Nagy PD. The host Pex19p plays a role in peroxisomal localization of tombusvirus replication proteins. *Virology* 2008,**379**:294-305.
81. Wang RY, Stork J, Pogany J, Nagy PD. A temperature sensitive mutant of heat shock protein 70 reveals an essential role during the early steps of tombusvirus replication. *Virology* 2009.
82. Panaviene Z, Panavas T, Serva S, Nagy PD. Purification of the cucumber necrosis virus replicase from yeast cells: role of coexpressed viral RNA in stimulation of replicase activity. *J Virol* 2004,**78**:8254-8263.
83. Gursinsky T, Schulz B, Behrens SE. Replication of Tomato bushy stunt virus RNA in a plant *in vitro* system. *Virology* 2009,**390**:250-260.
84. Wu B, Pogany J, Na H, Nicholson BL, Nagy PD, White KA. A discontinuous RNA platform mediates RNA virus replication: building an integrated model for RNA-based regulation of viral processes. *PLoS Pathog* 2009,**5**:e1000323.
85. Wang RY, Stork J, Nagy PD. A key role for heat shock protein 70 in the localization and insertion of tombusvirus replication proteins to intracellular membranes. *J Virol* 2009,**83**:3276-3287.
86. Panavas T, Pogany J, Nagy PD. Analysis of minimal promoter sequences for plus-strand synthesis by the Cucumber necrosis virus RNA-dependent RNA polymerase. *Virology* 2002,**296**:263-274.
87. Panavas T, Nagy PD. The RNA replication enhancer element of tombusviruses contains two interchangeable hairpins that are functional during plus-strand synthesis. *J Virol* 2003,**77**:258-269.
88. Panavas T, Nagy PD. Mechanism of stimulation of plus-strand synthesis by an RNA replication enhancer in a tombusvirus. *J Virol* 2005,**79**:9777-9785.
89. Wang RY, Nagy PD. Tomato bushy stunt virus co-opts the RNA-binding function of a host metabolic enzyme for viral genomic RNA synthesis. *Cell Host Microbe* 2008,**3**:178-187.
90. Stork J, Panaviene Z, Nagy PD. Inhibition of *in vitro* RNA binding and replicase activity by phosphorylation of the p33 replication protein of Cucumber necrosis tombusvirus. *Virology* 2005,**343**:79-92.
91. Shapka N, Stork J, Nagy PD. Phosphorylation of the p33 replication protein of Cucumber necrosis tombusvirus adjacent to the RNA binding site affects viral RNA replication. *Virology* 2005,**343**:65-78.
92. Barajas D, Li Z, Nagy PD. The Nedd4-type Rsp5p ubiquitin ligase inhibits tombusvirus replication via regulating degradation of the p92 replication protein and decreasing the activity of the tombusvirus replicase. *J Virol* 2009.
93. Na H, White KA. Structure and prevalence of replication silencer-3' terminus RNA interactions in Tombusviridae. *Virology* 2006,**345**:305-316.
94. Novoa RR, Calderita G, Arranz R, Fontana J, Granzow H, Risco C. Virus factories: associations of cell organelles for viral replication and morphogenesis. *Biol Cell* 2005,**97**:147-172.
95. Barajas D, Jiang Y, Nagy PD. A unique role for the host ESCRT proteins in replication of Tomato bushy stunt virus. *PLoS Pathog* 2009,**5**:e1000705.
96. Stork J, Kovalev N, Sasvari Z, Nagy PD. RNA chaperone activity of the tombusviral p33 replication protein facilitates initiation of RNA synthesis by the viral RdRp *in vitro*. *Virology* 2011,**409**:338-347.
97. den Boon JA, Ahlquist P. Organelle-Like Membrane Compartmentalization of Positive-Strand RNA Virus Replication Factories. *Annual Review of Microbiology* 2010,**64**:241-256.
98. Pathak KB, Nagy PD. Defective Interfering RNAs: Foes of Viruses and Friends of Virologists. *Viruses-Basel* 2009,**1**:895-919.

99. Goregaoker SP, Culver JN. Oligomerization and activity of the helicase domain of the tobacco mosaic virus 126- and 183-kilodalton replicase proteins. *J Virol* 2003,**77**:3549-3556.
100. Osman TA, Buck KW. Identification of a region of the tobacco mosaic virus 126- and 183-kilodalton replication proteins which binds specifically to the viral 3'-terminal tRNA-like structure. *J Virol* 2003,**77**:8669-8675.
101. Sullivan ML, Ahlquist P. A brome mosaic virus intergenic RNA3 replication signal functions with viral replication protein 1a to dramatically stabilize RNA in vivo. *J Virol* 1999,**73**:2622-2632.
102. Wang X, Lee WM, Watanabe T, Schwartz M, Janda M, Ahlquist P. Brome mosaic virus 1a nucleoside triphosphatase/helicase domain plays crucial roles in recruiting RNA replication templates. *J Virol* 2005,**79**:13747-13758.
103. Iwakawa HO, Mine A, Hyodo K, An M, Kaido M, Mise K, *et al.* Template recognition mechanisms by replicase proteins differ between bipartite positive-strand genomic RNAs of a plant virus. *J Virol* 2011,**85**:497-509.
104. An M, Iwakawa HO, Mine A, Kaido M, Mise K, Okuno T. A Y-shaped RNA structure in the 3' untranslated region together with the trans-activator and core promoter of Red clover necrotic mosaic virus RNA2 is required for its negative-strand RNA synthesis. *Virology* 2010,**405**:100-109.
105. Ray D, Na H, White KA. Structural properties of a multifunctional T-shaped RNA domain that mediate efficient tomato bushy stunt virus RNA replication. *J Virol* 2004,**78**:10490-10500.
106. Jonczyk M, Pathak KB, Sharma M, Nagy PD. Exploiting alternative subcellular location for replication: tombusvirus replication switches to the endoplasmic reticulum in the absence of peroxisomes. *Virology* 2007,**362**:320-330.
107. Bertrand E, Chartrand P, Schaefer M, Shenoy SM, Singer RH, Long RM. Localization of ASH1 mRNA particles in living yeast. *Mol Cell* 1998,**2**:437-445.
108. Spear A, Sharma N, Flanagan JB. Protein-RNA tethering: the role of poly(C) binding protein 2 in poliovirus RNA replication. *Virology* 2008,**374**:280-291.
109. Panavas T, Pogany J, Nagy PD. Internal initiation by the cucumber necrosis virus RNA-dependent RNA polymerase is facilitated by promoter-like sequences. *Virology* 2002,**296**:275-287.
110. Rajendran KS, Pogany J, Nagy PD. Comparison of turnip crinkle virus RNA-dependent RNA polymerase preparations expressed in *Escherichia coli* or derived from infected plants. *J Virol* 2002,**76**:1707-1717.
111. Salonen A, Ahola T, Kaariainen L. Viral RNA replication in association with cellular membranes. *Curr Top Microbiol Immunol* 2005,**285**:139-173.
112. Snijder EJ, van der Meer Y, Zevenhoven-Dobbe J, Onderwater JJ, van der Meulen J, Koerten HK, *et al.* Ultrastructure and origin of membrane vesicles associated with the severe acute respiratory syndrome coronavirus replication complex. *J Virol* 2006,**80**:5927-5940.
113. Ahlquist P, Noueir AO, Lee WM, Kushner DB, Dye BT. Host factors in positive-strand RNA virus genome replication. *J Virol* 2003,**77**:8181-8186.
114. Miller S, Krijnse-Locker J. Modification of intracellular membrane structures for virus replication. *Nat Rev Microbiol* 2008,**6**:363-374.
115. Schwartz M, Chen J, Janda M, Sullivan M, den Boon J, Ahlquist P. A positive-strand RNA virus replication complex parallels form and function of retrovirus capsids. *Mol Cell* 2002,**9**:505-514.
116. Koppek BG, Perkins G, Miller DJ, Ellisman MH, Ahlquist P. Three-dimensional analysis of a viral RNA replication complex reveals a virus-induced mini-organelle. *PLoS Biol* 2007,**5**:e220.

117. Hagiwara Y, Komoda K, Yamanaka T, Tamai A, Meshi T, Funada R, *et al.* Subcellular localization of host and viral proteins associated with tobamovirus RNA replication. *Embo J* 2003,**22**:344-353.
118. Beckham CJ, Light HR, Nissan TA, Ahlquist P, Parker R, Noueir A. Interactions between brome mosaic virus RNAs and cytoplasmic processing bodies. *J Virol* 2007,**81**:9759-9768.
119. Lazarow PB. Viruses exploiting peroxisomes. *Current opinion in microbiology* 2011,**14**:458-469.
120. Mohan KV, Som I, Atreya CD. Identification of a type 1 peroxisomal targeting signal in a viral protein and demonstration of its targeting to the organelle. *Journal of virology* 2002,**76**:2543-2547.
121. Liu LX, Margottin F, Le Gall S, Schwartz O, Selig L, Benarous R, *et al.* Binding of HIV-1 Nef to a novel thioesterase enzyme correlates with Nef-mediated CD4 down-regulation. *The Journal of biological chemistry* 1997,**272**:13779-13785.
122. Wolff T, O'Neill RE, Palese P. Interaction cloning of NS1-I, a human protein that binds to the nonstructural NS1 proteins of influenza A and B viruses. *Journal of virology* 1996,**70**:5363-5372.
123. Tu H, Gao L, Shi ST, Taylor DR, Yang T, Mircheff AK, *et al.* Hepatitis C virus RNA polymerase and NS5A complex with a SNARE-like protein. *Virology* 1999,**263**:30-41.
124. Wang C, Gale M, Jr., Keller BC, Huang H, Brown MS, Goldstein JL, *et al.* Identification of FBL2 as a geranylgeranylated cellular protein required for hepatitis C virus RNA replication. *Mol Cell* 2005,**18**:425-434.
125. Oster SK, Wu B, White KA. Uncoupled expression of p33 and p92 permits amplification of tomato bushy stunt virus RNAs. *J Virol* 1998,**72**:5845-5851.
126. Rubino L, Navarro B, Russo M. Cymbidium ringspot virus defective interfering RNA replication in yeast cells occurs on endoplasmic reticulum-derived membranes in the absence of peroxisomes. *J Gen Virol* 2007,**88**:1634-1642.
127. Matsuzono Y, Matsuzaki T, Fujiki Y. Functional domain mapping of peroxin Pex19p: interaction with Pex3p is essential for function and translocation. *J Cell Sci* 2006,**119**:3539-3550.
128. Hoepfner D, Schildknegt D, Braakman I, Philippsen P, Tabak HF. Contribution of the endoplasmic reticulum to peroxisome formation. *Cell* 2005,**122**:85-95.
129. Kragt A, Voorn-Brouwer T, van den Berg M, Distel B. Endoplasmic reticulum-directed Pex3p routes to peroxisomes and restores peroxisome formation in a *Saccharomyces cerevisiae* pex3Delta strain. *J Biol Chem* 2005,**280**:34350-34357.
130. Lazarow PB. Peroxisome biogenesis: advances and conundrums. *Curr Opin Cell Biol* 2003,**15**:489-497.
131. Tam YY, Fagarasanu A, Fagarasanu M, Rachubinski RA. Pex3p initiates the formation of a preperoxisomal compartment from a subdomain of the endoplasmic reticulum in *Saccharomyces cerevisiae*. *J Biol Chem* 2005,**280**:34933-34939.
132. Rottensteiner H, Kramer A, Lorenzen S, Stein K, Landgraf C, Volkmer-Engert R, *et al.* Peroxisomal membrane proteins contain common Pex19p-binding sites that are an integral part of their targeting signals. *Mol Biol Cell* 2004,**15**:3406-3417.
133. Hettema EH, Girzalsky W, van Den Berg M, Erdmann R, Distel B. *Saccharomyces cerevisiae* pex3p and pex19p are required for proper localization and stability of peroxisomal membrane proteins. *Embo J* 2000,**19**:223-233.
134. Weber-Lotfi F, Dietrich A, Russo M, Rubino L. Mitochondrial targeting and membrane anchoring of a viral replicase in plant and yeast cells. *J Virol* 2002,**76**:10485-10496.
135. Mackenzie J. Wrapping things up about virus RNA replication. *Traffic* 2005,**6**:967-977.
136. Fang Y, Morrell JC, Jones JM, Gould SJ. PEX3 functions as a PEX19 docking factor in the import of class I peroxisomal membrane proteins. *J Cell Biol* 2004,**164**:863-875.

137. Burgyan J, Rubino L, Russo M. The 5'-terminal region of a tombusvirus genome determines the origin of multivesicular bodies. *J Gen Virol* 1996,**77 (Pt 8)**:1967-1974.
138. Rubino L, Russo M. Membrane targeting sequences in tombusvirus infections. *Virology* 1998,**252**:431-437.
139. Sopko R, Papp B, Oliver SG, Andrews BJ. Phenotypic activation to discover biological pathways and kinase substrates. *Cell Cycle* 2006,**5**:1397-1402.
140. Dreher TW, Miller WA. Translational control in positive strand RNA plant viruses. *Virology* 2006,**344**:185-197.
141. Loregian A, Marsden HS, Palu G. Protein-protein interactions as targets for antiviral chemotherapy. *Reviews in medical virology* 2002,**12**:239-262.
142. O'Reilly EK, Kao CC. Analysis of RNA-dependent RNA polymerase structure and function as guided by known polymerase structures and computer predictions of secondary structure. *Virology* 1998,**252**:287-303.
143. Kao CC, Quadt R, Hershberger RP, Ahlquist P. Brome mosaic virus RNA replication proteins 1a and 2a from a complex *in vitro*. *Journal of virology* 1992,**66**:6322-6329.
144. Watanabe T, Honda A, Iwata A, Ueda S, Hibi T, Ishihama A. Isolation from tobacco mosaic virus-infected tobacco of a solubilized template-specific RNA-dependent RNA polymerase containing a 126K/183K protein heterodimer. *Journal of virology* 1999,**73**:2633-2640.
145. Goregaoker SP, Lewandowski DJ, Culver JN. Identification and functional analysis of an interaction between domains of the 126/183-kDa replicase-associated proteins of tobacco mosaic virus. *Virology* 2001,**282**:320-328.
146. Agol VI, Paul AV, Wimmer E. Paradoxes of the replication of picornaviral genomes. *Virus research* 1999,**62**:129-147.
147. Hope DA, Diamond SE, Kirkegaard K. Genetic dissection of interaction between poliovirus 3D polymerase and viral protein 3AB. *Journal of virology* 1997,**71**:9490-9498.
148. Lyle JM, Bullitt E, Bienz K, Kirkegaard K. Visualization and functional analysis of RNA-dependent RNA polymerase lattices. *Science* 2002,**296**:2218-2222.
149. Tellinghuisen TL, Rice CM. Interaction between hepatitis C virus proteins and host cell factors. *Current opinion in microbiology* 2002,**5**:419-427.
150. Suzuki M, Yoshida M, Yoshinuma T, Hibi T. Interaction of replicase components between Cucumber mosaic virus and Peanut stunt virus. *The Journal of general virology* 2003,**84**:1931-1939.
151. Schaad MC, Jensen PE, Carrington JC. Formation of plant RNA virus replication complexes on membranes: role of an endoplasmic reticulum-targeted viral protein. *The EMBO journal* 1997,**16**:4049-4059.
152. McCartney AW, Greenwood JS, Fabian MR, White KA, Mullen RT. Localization of the tomato bushy stunt virus replication protein p33 reveals a peroxisome-to-endoplasmic reticulum sorting pathway. *The Plant cell* 2005,**17**:3513-3531.
153. Barajas D, Nagy PD. Ubiquitination of tombusvirus p33 replication protein plays a role in virus replication and binding to the host Vps23p ESCRT protein. *Virology* 2010,**397**:358-368.
154. Wang RY, Stork J, Pogany J, Nagy PD. A temperature sensitive mutant of heat shock protein 70 reveals an essential role during the early steps of tombusvirus replication. *Virology* 2009,**394**:28-38.
155. Meredith LW, Sivakumaran H, Major L, Suhrbier A, Harrich D. Potent inhibition of HIV-1 replication by a Tat mutant. *PLoS One* 2009,**4**:e7769.
156. Checkley MA, Luttge BG, Soheilian F, Nagashima K, Freed EO. The capsid-spacer peptide 1 Gag processing intermediate is a dominant-negative inhibitor of HIV-1 maturation. *Virology* 2010,**400**:137-144.

157. Akhrameyeva NV, Zhang P, Sugiyama N, Behar SM, Yao F. Development of a glycoprotein D-expressing dominant-negative and replication-defective herpes simplex virus 2 (HSV-2) recombinant viral vaccine against HSV-2 infection in mice. *Journal of virology* 2011,**85**:5036-5047.

VITA

Author's Name: Kunj Bihari Pathak

Date of Birth: April 8, 1978

Place of Birth: Dhanbad, India

Education

- M.V.Sc. 9/2002-8/2004, Veterinary Virology; Indian Veterinary Research Institute, Mukteswar, India. Thesis: Prokaryotic expression and characterization of blue tongue virus serotype-23 VP7 protein.
- B.V.Sc. & A.H. 8/1997-7/2002, Veterinary Medicine, Govind Ballabh Pant University of Agriculture & Technology, Pantnagar, India.

Publications and Presentations

- 1) Pathak KB, Pogany J, Xu K, White KA and Nagy PD (2011). Critical role of RNA in assembly of tombusviral replicase complex. *J. Virol.* Oct 19 [Epub ahead of print].
- 2) Pathak KB, Pogany J and Nagy PD (2011). Non-template functions of viral RNA in plant virus replication. *Current Opinions in Virology* (In press).
- 3) Pathak KB and Nagy PD (2009). Defective interfering RNAs: Foes of viruses and friends of virologists. *Viruses* 1:895-919.
- 4) Pathak KB, Sasvari Z and Nagy PD (2008). The host Pex19p plays a role in peroxisomal localization of tombusvirus replication proteins. *Virology* 379:294-305.
- 5) Jonczyk M, Pathak KB, Sharma M and Nagy PD (2007). Exploiting alternative subcellular location for replication: tombusvirus replication switches to the endoplasmic reticulum. *Virology* 362:320-30.
- 6) Tembhumne, PA, Mondal B, Pathak KB, Biswas SK, Sanyal A, Yadav MP, Bandyopadhyay SK and Singh RK (2009). Segment-2 sequence analyses and crossneutralization studies on some Indian bluetongue viruses suggest isolates are VP2-variants of serotype 23. *Archives of Virology.* 155:89-95.
- 7) Pathak KB, Biswas SK, Tembhumne PA, Hosamani M, Bhanuprakash V, Prasad G, Singh RK, Rasool TJ and Mondal B (2008). Prokaryotic expression of truncated VP7 of bluetongue virus (BTV) and reactivity of the purified recombinant protein with all BTV type-specific sera. *Journal of Virological Methods* 152:6-12.
- 8) Pathak KB and Nagy PD (2010) Critical role of RNA in assembly of tombusviral replicase complex. *American Society of Virology*, July 17-21. Oral presentation, Montana State University, Bozeman, MT.
- 9) Pathak KB, Sasvari Z and Nagy PD (2008) Role of host pex19p in transportation of tombusviral replication proteins. *American Society of Virology*, July 14-18. Oral presentation, Cornell University, Ithaca, NY.
- 10) Pathak KB, Pogany J and Nagy PD (2006) Role of viral RNA in assembly of tombusvirus replicase complex. *American Society of Virology*, July 13-17. Oral presentation, University of Wisconsin, Madison, WI.
- 11) Nagy PD, Pogany J and Pathak KB (2006) Role of viral RNA as an assembly platform for the tombusvirus replicase complex. *Rustbelt RNA Meeting*, October 20-21. Mt. Sterling, OH.
- 12) Pathak KB, Bhanuprakash V, Hosamani M, Singh RK, Singh N and Mondal B (2004) Potential of recombinant VP7 as an antigen for detection of bluetongue antibody in sera, Presented in XI Annual Convention of Indian Society for Veterinary Immunology and

Biotechnology and “National on Alternate Strategies for Livestock Production and Protection: Role of Biotechnology and Immunology.” November 3-4, at Indian Veterinary Research Institute, Mukteswar, India.Symposium

Honors And Awards

- 1) Philip Morris, USA, Graduate Fellowship to support Ph.D. program, 2004-2009.
- 2) Student Travel Award by American Society for Virology (ASV) to attend annual meeting at Bozeman, MT. July, 2010.
- 3) Student Travel Support Award by Graduate School, University of Kentucky, to attend ASV annual meeting at Bozeman, MT. July, 2010.
- 4) Student Travel Award by ASV to attend annual meeting at Ithaca, NY. July, 2008.
- 5) Student Travel Support Award by Graduate School, University of Kentucky, to attend ASV annual meeting at Ithaca, NY. July, 2008.
- 6) Student Travel Award by ASV to attend annual meeting at Madison, WI. July, 2006.
- 7) Student Travel Support Award by Graduate School, University of Kentucky, to attend ASV annual meeting at Madison, WI. July, 2006.
- 8) Indian Council of Agricultural Research National Talent Search (ICAR-NTS) scholarship to support undergraduate studies from 1997-2002.
- 9) ICAR award for winning team participant in All India Agricultural University Cultural Festival (2000) held in Assam Agricultural University, Jorhat, Assam, India. 10) Junior Research Fellowship during Masters program after gaining an all India First rank in joint entrance examination conducted by ICAR New Delhi, 2002-2004.